Doctoral Thesis

Mathematical Modeling of Disease Transmission Dynamics with Data Generating Processes

(データ生成過程を伴う疾病伝播ダイナミクスの数理モデリング)

Keisuke Ejima
(江島　啓介)

Supervisor:　Professor Kazuyuki Aihara (合原一幸　教授)

December 6, 2013

Department of Mathematical Informatics
Graduate School of Information Science and Technology
the University of Tokyo

Abstract

In history, fight against infectious diseases has never ended since the dawn of human being, and infectious diseases acted as the leading cause of death. To overcome the diseases, pharmaceutical approaches have been invented. However, even at the present moment emerging infectious diseases such as HIV/AIDS, Middle East respiratory syndrome coronavirus (MERS-CoV), Severe Acute Respiratory Syndrome (SARS), influenza continuously cause epidemics across the world. Accordingly, we confront with the needs to evaluate the efficacy and effectiveness of pharmaceutical or non-pharmaceutical interventions (e.g. school closure during influenza epidemic) in quantitative and qualitative manners. Despite the importance of modeling approaches to infectious disease control, the methodology has not been straightforward. The most popular and classical model that describes an infectious disease epidemic was developed by Kermac and McKendrick (hereafter I call the model as SIR (Susceptible-Infectious-Recovered) model), and the SIR model has been extended to practical problems in many ways. Apart from these progresses, a lot of quantitative questions have remained in public health. To answer the questions, this thesis has focused on the data generating process of epidemics in order to fit models to limited data that is empirically observed. Moreover, the infectious disease modelling framework has been further extended to other health related problems that are known to be contagious.

The main contributions of this thesis are summarized as follows; (1) I constructed a transmission model of influenza during the early phase of an epidemic, investigating the required length of time to reliably estimate case fatality ratio (CFR) of influenza. The study suggested that 2-3 month would be required to reliably compare the estimated CFR with the pre-specified CFR value such as those defined by US Pandemic Severity Index. (2) I proposed a modeling method to estimate the vaccine efficacy against measles, jointly quantifying parameters governing the temporal dynamics of measles (e.g. R_0). The study suggested that population aged from 5-19 year should be (re-) vaccinated to prevent further epidemic in Japan. (3) I discussed the use of chance-adjusted agreement coefficients to measure the assortativity of both contact and transmission of an infectious disease. I have demonstrated that the proportion of contacts that are reserved for within group mixing, p in the preferential mixing assumption has excellently corresponded to the Newman's assortativity coefficient (or the so-called Cohen's kappa). Subsequently, I have explicitly distinguished the transmission assortativity from contact assortativity, because the former captures not only the contact heterogeneity but also many other intrinsic and

extrinsic factors characterizing the frequency of within- and between- group transmission. (4) I have emphasized that an appropriate model would be essential to answer public health question including vaccination problems. Examining the validity of incorporation of vaccine effect against clinical disease in epidemic models, I have shown that an explicit formulation would also help to clarify underlying assumptions that tend to be hidden in common model structures. (5) I investigated epidemiological model that describes an obesity epidemic which is known to spread via social contact and can also be acquired in a non-contagious manner. I compared the effectiveness of different types of intervention programs against obesity, identifying associated data gaps in empirical observation.

Through these five original studies, I have shown that appropriate model building approaches that explicitly account for data generating process would be essential not only for modeling researchers but also for public health practitioners. The needs for sound model building approaches have been emphasized.

Declaration of previous publications

This thesis includes the following previously published material:

Thesis chapter	**Publication title**
Chapter 2	Ejima K, Omori R, Cowling BJ, Aihara K, Nishiura H. The time required to estimate the case fatality ratio of influenza using only the tip of an iceberg: Joint estimation of the virulence and the transmission potential. Computational and Mathematical Methods in Medicine. 978901 2012.
Chapter 3	Ejima K, Omori R, Aihara K, Nishiura H. Real-time investigation of measles epidemics with estimate of vaccine efficacy. International Journal of Biological Sciences. 8:620-629 2012.
Chapter 4	Ejima K, Aihara K, Nishiura H. On the use of chance-adjusted agreement statistic to measure the assortative transmission of infectious diseases. Computational & Applied Mathematics. 32(2):303-313 2013.
Chapter 5	Ejima K, Aihara K, Nishiura H. The impact of model building on the transmission dynamics under vaccination: Observable (symptom-based) versus unobservable (contagiousness-dependent) approaches. PLoS ONE. 8:4:e62062 2013.
Chapter 6	Ejima K, Aihara K, Nishiura H. Modeling the obesity epidemic: Social contagion and its implications for control. Theoretical Biology and Medical Modelling. 10:17 2013.

Contents

Chapter 1

Introduction

1.1 Preface

The fight against infectious disease, which only until recently represented the leading cause of death globally, has been ongoing since the dawn of human civilization. The plague pandemic which occurred in 14th century Europe was responsible for the deaths of an estimated 30% of the population at the time. In response, human society has developed a number of pharmaceutical approaches to cope with infectious disease. For instance, in 1798, Edward Jenner developed the first vaccine for smallpox, and in 1929, Alexander Fleming discovered penicillin—the first antibiotic. In recent years, however, new emerging infectious diseases such as HIV/AIDS, Middle East respiratory syndrome coronavirus (MERS-CoV), Severe Acute Respiratory Syndrome (SARS) and new strains of influenza, for which the majority of the worldwide population has no resistance, are precipitating both local epidemics and global pandemics. Given the delays inherent in developing new vaccines or antibiotics against these new health threats, and the lack of access for those living in poverty once they are developed, it is therefore critical to evaluate the efficacy and effectiveness of both pharmaceutical and non-pharmaceutical approaches (i.e. school closures during influenza epidemics) in both a quantitative and qualitative manner.

Despite the importance of such an approach, this type of evaluation is rarely straightforward. Additionally, infectious disease modeling must account for the "dependency of the risks".

Figure 1.1 illustrates the difference between the infectious disease and other non-communicable diseases such as cancer, asthma and diabetes. In the case of a non-communicable disease, the risk of morbidity should be the same for both of these two individuals with four contacts each. However, in the case of an infectious disease, the risk of infection is dependent on the status of one's contacts. The susceptible individual on the right is surrounded by three infected contacts while the one on the left has only one infected contact. The individual on the right is therefore more vulnerable to infection. As the risk of infection is dependent on the risk of others, it is necessary to construct

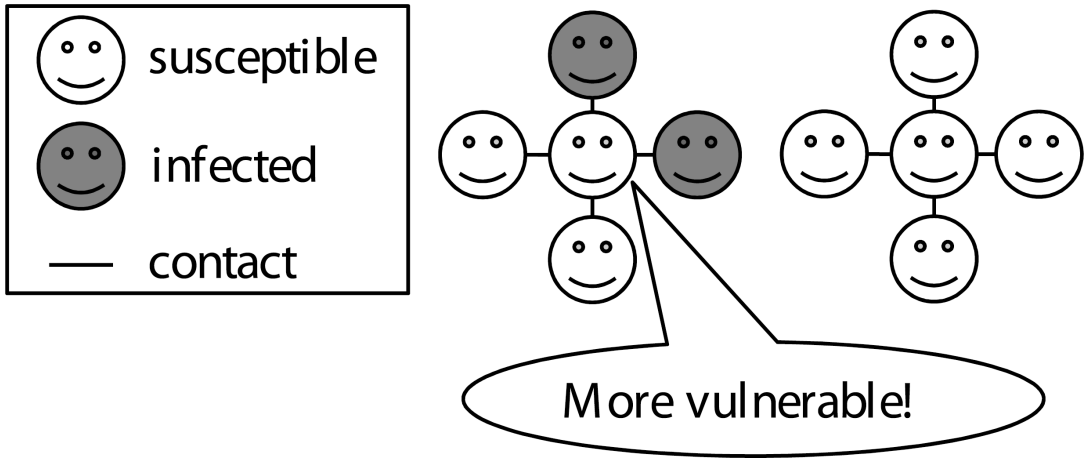

Figure 1.1. The risk of infection of individuals with same number of contacts and the different status of contactees.

mathematical and statistical models to reflect this dependency. Furthermore, these models should account for the biological characteristics of the infectious disease in question, such as its mode of reproduction, and the social contacts patterns. The classical model to describe an infectious disease epidemic, which is still the most popular among epidemiologists and hereafter referred to as the SIR (susceptible-infectious-recovered) model [68], was developed by Kermack and McKendrick in the 1920s and 1930s. Although its original version was described using partial differential equations, this model is shown below in terms of ordinary differential equations for illustration:

$$\begin{aligned} \frac{\mathbf{d}S(t)}{\mathbf{d}t} &= -\lambda S(t), \\ \frac{\mathbf{d}I(t)}{\mathbf{d}t} &= \lambda S(t) - \gamma I(t), \\ \frac{\mathbf{d}R(t)}{\mathbf{d}t} &= \gamma I(t), \\ \lambda &= \beta I, \end{aligned} \tag{1.1}$$

where $S(t)$, $I(t)$ and $R(t)$ are the sizes of the susceptible, infectious and recovered populations at time t. The susceptible individuals are infected at the rate of $\lambda(t) = \beta I(t)$, also known as the "force of infection", and move from the susceptible to the infectious population, $I(t)$. As shown, the force of infection is proportional to $I(t)$, which implies that individuals come into contact with one other at the same rate (i.e. a homogeneous mixing assumption). Infected individuals recover at a constant rate, γ , and move to the recovered population, $R(t)$. Although this ODE model cannot be solved analytically, it can be solved numerically.

Figure 1.2 shows an example of the solution. The dashed line corresponds to the temporal distribution of the infected population. Although this model is relatively simple and based on a number of unrealistic assumptions, such as homogeneous mixing and a single

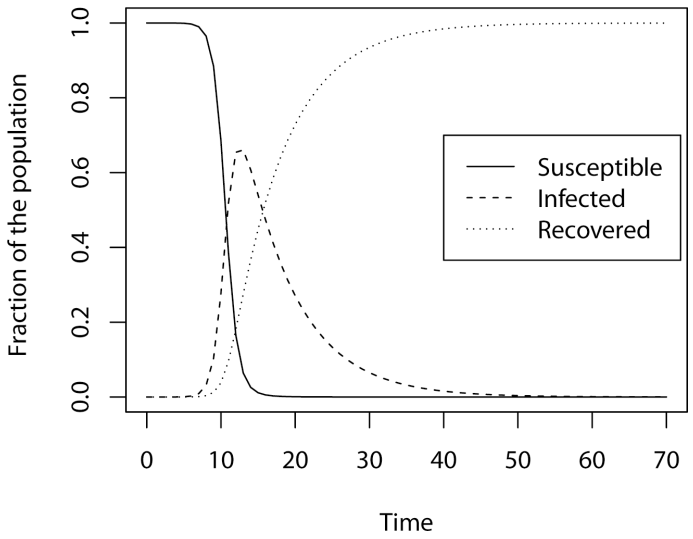

Figure 1.2. The example of numerical solution of SIR model. The parameter settings are as follows; $\beta = 1.4247$, $\gamma = 0.14286$. The initial settings are as follows; $(S(0), I(0), R(0)) = (0.999999, 0.000001, 0.0)$.

host type (i.e. susceptibility and infectivity are both the same in the host population), it can capture the typical features of epidemic curves which are frequently observed in nature; the infected population increases exponentially in the early phase of the epidemic in an almost fully susceptible population and then begin to decrease due to the depletion of the susceptible population. While this model is not only able to represent the progress of the epidemic, it is also useful in a public health context. For instance, it could be used to calculate the target vaccination coverage needed to prevent a similar outbreak. In equations 1.1, the total population, $N(t) = S(t) + I(t) + R(t)$, is constant over time, so that $N(t) = N$. If almost all of the population is susceptible to the disease, or $S(0) = N$, and a substantial number of cases enter this population, so that $I(0) > 0$, $R(t) = 0$, then we can linearize the system (1.1) and describe the dynamics of the infected population as follows:

$$\frac{dI(t)}{dt} = (\beta N - \gamma)I(t). \tag{1.2}$$

Therefore, in the early phase of the epidemic, the infected population increases exponentially,

$$I(t) = e^{(\beta N - \gamma)t} I(0), \tag{1.3}$$

$\beta N - \gamma$ is the growth rate in the early phase, and the condition in which the epidemic occurs is expressed as $\beta N - \gamma > 0$. This can be rewritten as:

$$\frac{\beta N}{\gamma} > 0. \tag{1.4}$$

The left hand side of this equation corresponds to the basic reproduction number, R_0, which can be interpreted as the average number of secondary cases generated by a given primary case over the course of its infectious period in a fully susceptible population. In other words, if $R_0 > 1$, then an epidemic can occur. Now, if p is the vaccination coverage before the epidemic, then the initial susceptible population decreases to $N(1-p)$. The effective reproduction number, which is the reproduction number in cases where the population is not fully susceptible, is $R^* = \frac{\beta N(1-p)}{\gamma}$. As the condition that the epidemic occurs is $R^* > 1$, the target vaccination coverage is defined as $p > 1 - \frac{1}{R_0}$.

After Kermack and McKendrick proposed the SIR model, little further progress in infectious disease modeling was made until the 1970s. From the 1970s to the present day, thanks to the progress in mathematical demography [60, 61, 85, 132], the SIR model has been extended in several ways. Further innovations include Hethcote's [56] consideration of the impact of births and deaths in the population, and the age structured model proposed by Diekmann [26].

One reason why infectious disease modeling has attracted the attention of so many researchers is the nonlinearity of the model (i.e. dependency of the risks), which makes the analysis complex and produces unintuitive results. Despite the progress made by these studies, there remain many unanswered quantitative questions in public health. Although the topics are broad and methods vary widely according to the disease studied, I have focused on two issues: (a) the evaluation of the interventions, such as vaccination, prophylaxis, and countermeasures to prevent the spread of pathogens, and (b) the estimation of parameters to determine disease dynamics, such as the basic reproduction number, the next generation matrix and the case fatality ratio (CFR). In practice, both of these issues are of relevance to public health policy-making. For instance, while the evaluation of the vaccine efficacy is of use in determining the target vaccination coverage (Chapter 3), the case fatality ratio (CFR) can be used to decide which interventions are appropriate during an influenza pandemic (Chapter 2). To address these issues, I have focused on the data generating process which explains the limited data normally available in public health practice. The data generating process can roughly be divided into two parts: the transmission process and the observation process. The transmission process is the process by which the pathogen is transferred from infected cases to susceptible individuals. To describe this process, we must consider the route of infection. In the case of a direct infection (by physical contact), the pattern of contacts (the frequency and nature of both infected and susceptible individuals), is of significant importance. During the 2009 influenza pandemic in Japan, assortativity of contacts between different age groups meant that the majority of patients in the early phase were children and that only later did the outbreak gradually shift to adults. Assortativity is defined as a preference for an individual node in a network to connect with others that have similar characteristics.

Mossong et.al. conducted the serveillance about the age dependent frequency of contact [90]. From this, we can infer that contacts between individuals of the same age group are

more frequent than between individuals from different age groups. Additionally, viral reproduction in vivo, and the relationship between the viral load and infectivity are also important factors [63, 115].

The observation process is also important, given that we cannot directly observe infections as they occur. In practice, it is impossible to report all infected cases because of the delay between the infection and appearance of symptoms. Furthermore, some cases may remain asymptomatic during the entire course of infection. Subsequently, only a fraction of the symptomatic cases attend hospital. If the cases that attended hospitals were diagnosed using a polymerase chain reaction (PCR) test and surely reported, the cases were counted in the data. As we cannot count all the cases, these disease processes should be considered when we fit models to observed data.

1.2 Structure of the Thesis

As mentioned above, I have aimed to address a number of public health issues by focusing on the data generating process. Furthermore, I have applied an infectious disease modeling framework to other health-related topics.

In Chapters 2 and 3, I attempt to address these public health issues using limited passive data. In Chapter 2, I propose a method for jointly estimating the CFR and the exponential growth rate in the early phase of an influenza epidemic. In the early phase of the epidemic, when the available data is limited, we can only determine the number of confirmed cases and deaths at most. I go on to construct realistic epidemic and observational models, and then assess the minimum number of days required to compare the estimated CFR with the pre-specified CFR value, as defined by the US Pandemic Severity Index. In Chapter 3, I propose a modeling approach to estimate vaccine efficacy against measles by jointly quantifying parameters governing the temporal dynamics of a measles outbreak such as R_0. This method is based solely on epidemiological surveillance data with partial information on vaccination history. Furthermore, this is possible using only readily available data, and is not as costly as conducting a specialized field study, which would be required, for example, to observe household transmission.

In Chapters 4 and 5, I show the importance of model building for describing the data generating process. In Chapter 4, I focus on several factors influencing the transmission process; assortativity in particular. I discuss the use of chance-adjusted agreement coefficients to measure the assortativity of contacts and transmission of infectious diseases. I go on to demonstrate that p, as expressed in the preferential mixing formulation, closely corresponds with Newman's assortativity coefficient (or Cohen's kappa). Subsequently, I explicitly distinguish transmission assortativity from contact assortativity, given that the former captures not only the heterogeneity of contacts but also many other intrinsic and extrinsic factors characterizing the frequency of within- and between-group transmission. In Chapter 5, I emphasize that it is essential to adapt model formulation for each specific

scientific or public health question. As shown, an explicit formulation would also aid in clarifying the underlying assumptions that tend to be hidden in commonly encountered model structures.

Finally, I apply the infectious disease model to other communicable diseases. Recent work has revealed that not only infectious diseases, but also health behaviors and conditions such as smoking and obesity, which have previously been categorized as non-communicable diseases, can also be described as contagious. In Chapter 6, I investigate epidemiological models to describe the obesity epidemic, which can be considered as spreading via social contacts and also acquired non-communicably. I then undertake a comparative assessment of the effectiveness of different types of intervention programs to reduce the risk of obesity.

Lastly, I conclude the thesis in Chapter 7.

Chapter 2

The Time Required to Estimate the Case Fatality Ratio of Influenza

2.1 Introduction

When a new infectious disease emerges, the case fatality ratio (CFR) informs how lethal the infection or the disease is, measuring the virulence of the novel infection as the conditional probability of death given infection or disease [81, 98]. To understand the severity of infection, assess the impact of clinical and public health interventions, and anticipate the likely number of deaths in the population given the total number of infected individuals, quantifying the CFR during the early stage of an epidemic is of utmost importance.

Among various uses of the CFR, the present study focuses on influenza, and in particular, the epidemiological determination of the severity in relation to epidemiological indices, such as the Pandemic Severity Index (PSI) in the United States [25]. As a process of public health policy-making, this index is used as a scientific criterion in the decision-making processes about implementation of public health countermeasures, and thus, the CFR is regarded as key information for policy making [78]. For instance, if the estimated CFR exceeds a pre-specified reference value of 2.0%, which is sometimes quoted as the estimate of the CFR for the H1N1-1918 pandemic [96], the PSI suggests that the government should recommend and implement all the non-pharmaceutical interventions listed, including voluntary isolation of clinically ill individuals at home, quarantine of household contacts and social distancing [25].

However, while the CFR is theoretically calculated as a proportion of deaths to infected individuals, the actual calculation practice involves several technical problems owing to a few epidemiological features. First, one cannot directly count all infected individuals during the course of an epidemic due to unobservable nature of infection, and commonly available datasets may be only confirmed cases through surveillance efforts. Moreover, the mild nature of influenza involves multiple steps of bias including ignorance of asymptomatic and subclinical infections, case ascertainment bias, imperfectness of a diagnostic

testing method, and reporting bias. In fact, approximately 10% of confirmed infections with influenza (H1N1-2009) in households were shown to be fully asymptomatic [23, 114]. To partly address the issue of under-ascertainment, a technical advancement in synthesizing epidemiological evidences enabled us to estimate the symptomatic case fatality ratio (sCFR), the proportion of deaths to all symptomatic cases [116], although the denominator data are frequently based on non-specific disease information such as influenza-like illness. As an alternative, a real-time serological study could potentially offer the denominator based on all infected individuals [139], but the seroepidemiological survey is costly and the diagnostic performance of serological testing in relation to the estimation of the CFR has yet to be fully clarified. While specific CFRs using confirmed cases and symptomatic cases as the denominator have been expressed as cCFR and sCFR, respectively, among studies of H1N1-2009 [98], the present study consistently uses the simplest notation "CFR", intending it to represent the risk of death among all infected individuals (and so may be abbreviated as iCFR when necessary).

Second, the real-time estimation of the CFR has to take into account the time delay from illness onset to death, and thus, requires us to employ an appropriate statistical method to address censoring. This point must be addressed, because all the cases are not fully exposed to the risk of death at a point in time during the course of an epidemic, and a simple ratio of the cumulative numbers of deaths to cases can yield biased (mostly, underestimated) CFR [45, 46, 65, 107]. Third, it is critical to always keep in mind that the risk of death is heterogeneous. In particular, the higher risk of influenza death than healthy adults is seen among those with underlying health conditions [101], including chronic obstructive pulmonary disease, asthma, pregnancy, chronic kidney failure, diabetes and so on. Perhaps reflecting this feature, the CFR clearly differs by age with the highest estimate among elderly and infants and the lowest among school-age children and young adults [30, 140]. Fourth, during an early stage of a pandemic, the number of deaths still remains very small, and so the estimation of CFR suffers from broad uncertainty. Given that the CFR of influenza is likely to be small, and suffers from wide uncertainty, it is fruitful to clarify the minimum number of cases that are required to determine if the estimated CFR in real-time is significantly below a pre-specified cut-off value such as 2.0%.

While directly addressing clinically mild features and case ascertainment bias calls for synthesizing epidemiological evidences, for example by employing hierarchical modeling approach [116], it is also important to clarify what can be done with readily available epidemiological information, such as confirmed cases and confirmed deaths. In the present study, we aim to propose a method to estimate the CFR based on the limited epidemiological data during the early stage of an epidemic. Through this investigation, we also aim to clarify the minimum number of days that are required to explicitly compare the estimated CFR to pre-determined cut-off values of the CFR.

2.2 Materials and Methods

2.2.1 Assumptions

For clarity, here we describe the underlying epidemiological assumptions and settings. First, we focus on the early stage of a pandemic and ignore the depletion of susceptible individuals during this particular time period in which the number of newly infected individuals $i(t)$ increases exponentially. That is, we focus on the log-linear phase alone for simplicity. Second, in realistic settings, $i(t)$ cannot be directly counted as a function of time, and it is possible to observe only the confirmed cases, $c(t)$. Third, during the early epidemic phase, a constant factor, k which scales the ratio of confirmed cases to all infected individuals is assumed to remain a constant. In other words, we assume that the frequency of confirmed diagnosis among infected individuals does not vary over time. Fourth, we assume that the time delay from infection to death is independently and identically distributed and denote the probability density function as $f(s)$ of length s days since infection. Moreover, among the confirmed cases, we assume that all death counts are recorded over time through surveillance system. Except for being reflected in the generation time distribution and the reproduction number, the event of death is assumed to be independent of the process of renewal. Finally, we consider a public health setting in which the time of emergence (or the time to initiate exponential growth), t_0 is known (even approximately) as was the case in a specific epidemic study in which the starting time point of an epidemic was estimated [83]. In the next sub-section, we describe the estimation procedure of only a homogeneous population. However, the estimation problem of a population with heterogeneous risks of infection and death is discussed in Results section.

2.2.2 Model Structure

We first describe the model structure deterministically. Throughout the manuscript, we ignore demographic stochasticity in infection process (see Discussion). Let $i(t)$ be the incidence of infection at calendar time t. Also, let t_0 be the time at which an epidemic starts with a single index case. Then $i(t)$ increase exponentially as follows:

$$i(t) = \exp\left\{r(t - t_0)\right\}, \tag{2.1}$$

where r is the exponential growth rate of incidence. Let p be the CFR among all infected individuals. Assuming that the conditional probability density function of the time from infection to death, $f(s)$ is known, the number of deaths, $d(t)$ is modeled as

$$d(t) = p \int_0^\infty i(t - s) f(s) ds, \tag{2.2}$$

which can be rewritten as

$$\begin{aligned} d(t) &= p \exp\{r(t-t_0)\} \int_0^\infty \exp(-rs) f(s) ds \\ &= p \exp\{r(t-t_0)\} M(-r), \end{aligned} \tag{2.3}$$

where $M(-r)$ represents the moment-generating function of the time from infection to death given the exponential growth rate r. One may integrate both sides and use the cumulative number of deaths by day t, $D(t)$ for the estimation of CFR. The estimator of the CFR is then given by

$$\hat{p} = \frac{D(t)}{[\exp(r(t-t_0)) - \exp(-rt_0)] \frac{M(-r)}{r}}. \tag{2.4}$$

Other than parameters for $f(s)$, which we will assume as known, the estimator (2.4) indicates that, to estimate the CFR, an unknown parameter r has to be estimated from an additional series of data other than the death process, e.g. from the confirmed case series. The exponential growth rate r quantifies the denominator of the above mentioned estimator. To estimate r, we analyze the incidence of confirmed cases, $c(t)$. Let l denote the proportion of confirmed cases to the total of infected individuals, the data generating process of $c(t)$ is described by

$$\begin{aligned} c(t) &= l \int_0^t i(t-s) h(s) ds \\ &= lQ(-r) i(t) \\ &= ki(t), \end{aligned} \tag{2.5}$$

where $h(s)$ is the density function of the time from infection to confirmatory diagnosis and $Q(-r)$ represents the moment-generating function given the exponential growth rate r. We refer to the parameter k as the confirmed coefficient (i.e. $k = lQ(-r)$) which acts as a constant factor to translate $i(t)$ into $c(t)$.

Let us consider an adjusted calendar time based on known t_0 (i.e., $t + t_0$), we simplify all the following equations by eliminating t_0 (and hereafter we consistently use t as the adjusted time in which t_0 is equated to be zero). In addition to this adjustment, we discretize both the series of confirmed cases and deaths, because the observed dataset is given with discrete-time (i.e. daily data), that is,

$$\begin{aligned} c_t &= \int_{t-1}^t c(x) dx \\ &= \frac{k}{r} \left[\exp(rt) - \exp\{r(t-1)\}\right], \end{aligned} \tag{2.6}$$

and

$$\begin{aligned} d_t &= \int_{t-1}^{t} d(x)dx \\ &= p\left[\exp(rt) - \exp\left\{r(t-1)\right\}\right]\frac{M(-r)}{r}, \end{aligned} \tag{2.7}$$

The proposed estimation method based on these linear approximations would work even when the exponential growth rate varies with time (e.g., varies as a step function) as was considered when evaluating the effectiveness of public health interventions such as school closure [Nishiura2010g, Wu2010a]. The number of parameters would have to increase to capture the time variation (e.g., from a single r alone to r_0 and r_1 for two consecutive epidemic phases), and thus the required sample size for estimation would also increase. However, all we have to do to cope with the time dependence is to update (2.1) and (2.2) using multiple growth rates and, thus, revise (2.6), accordingly.

2.2.3 Maximum Likelihood Estimation

Assuming that the observed number of confirmed cases on day t results from Poisson sampling process with mean $c_t = k[\exp(rt) - \exp r(t-1)]/r$ where r and k are parameters, the likelihood function is given as follows:

$$L_1(r,k;m_t) = \prod_{t=1}^{T} \frac{\left(\frac{k}{r}\right)^{m_t}\left[\exp(rt) - \exp r(t-1)\right]^{m_t}\exp\left[-\frac{k}{r}\left[\exp(rt) - \exp r(t-1)\right]\right]}{m_t!}, \tag{2.8}$$

where m_t is the observed daily number of confirmed cases on day t and T represents the latest time of observation.

Let π_t be a random variable which yields an estimator of the CFR on day t since the start of an epidemic and is the realized value in the particular epidemic. Assuming that the realized CFR is the result of binomial sampling process of death with sample size $[\exp(rT) - 1]M(-r)/r$, the likelihood to estimate the CFR based on the total number of deaths up to the latest time of observation T is

$$L_2(\pi_T; D(T), r) = \binom{(\exp(rT) - 1)\frac{M(-r)}{r}}{D(T)} \pi_T^{D(T)}(1-\pi_T)^{(\exp(rT)-1)\frac{M(-r)}{r} - D(T)}. \tag{2.9}$$

Because of an assumption of conditional independence between the renewal process and death, the total likelihood L is given by

$$L = L_1 L_2. \tag{2.10}$$

Minimizing the negative logarithm of the total likelihood L, we jointly estimate three parameters, π_T, r and k. The 95% confidence intervals are derived from the profile likelihood.

2.2.4 Simulations

Whereas the above mentioned estimation procedure enables us to estimate the CFR based only on the confirmed cases and deaths, the estimation rests on limited epidemiological information as compared to other methods involving additional symptomatic case data or serological dataset. Thus, it is important to examine if we can overcome uncertainty and realistically employ the proposed method during an early phase of a pandemic. Specifically, we explore the time required to confidently suggest the range of the CFR and compare the CFR against a pre-specified cut-off value during the early stage. We assess the reliability and validity by means of random simulations.

As a plausible parameter range, we examine three different exponential growth rates, r, of 0.05, 0.15 and 0.25 per day. These are chosen as plausible, because, assuming that the mean generation time of influenza is 3 days and exponentially distributed, the basic reproduction number ranges from 1.15 to 1.75. If the generation time is a constant 3 days, the reproduction number ranges from 1.16 to 2.11. These are in line with published estimates of the reproduction number for H1N1-2009 [10]. In fact, the growth rate of influenza A (H1N1-2009) is estimated as 0.08 [103] and 0.10 per day [43] in Japan and Mexico, respectively. The reference values of CFR, p, are set at 0.1%, 0.5% and 2.0% that are in line with the PSI in the United States. The CFR of Spanish influenza is sometimes thought to be approximately 2.0% [96, 123] and those of Asian and Hong Kong influenza pandemics are thought to be up to 0.5% [76]. The CFR of seasonal influenza is thought to be below 0.1% [123]. Although the CFR of the H1N1-2009 pandemic among all infected individuals is estimated to be smaller than 0.1% [120], we do not examine smaller estimates of the CFR, because 0.1% may be most reasonably defined as the lowest cut-off value in practical setting to distinguish a mild influenza strain from severe ones, and it is likely to be infeasible to robustly estimate a CFR below 0.1% during the early epidemic phase due to sampling errors. Since the empirically estimated proportion of confirmed cases among all infected individuals is 5% [140], we fix k at 0.05 assuming that the time delay from infection to confirmed diagnosis is sufficiently short. Ignoring small delay from infection to illness onset (as it doesn't influence the above mentioned estimation framework), the conditional probability density function of the time from infection to death of influenza A (H1N1-2009), $f(s)$ is assumed to be gamma distribution with the mean and standard deviation being 9.5 and 4.7 days, respectively [100]. As for simulation-based assessment, we first perform Monte Carlo simulations for 1000 times for each specified combination of parameter values, calculating the coverage probability of including the assigned CFR value within the 95% confidence intervals. Second, we assess the time at which the estimated CFR is confidently said as smaller than the pre-specified CFR value. Again, the model is randomly simulated for 1000 times per each parameters setting, calculating the number of simulation runs in which the upper 95% confidence interval is below the reference CFR value.

2.2.5 Heterogeneous Population

The proposed method can be extended to a heterogeneous population with differential risks of infection and death, perhaps by age- and risk-groups. We present the extended model analytically and demonstrate that the above mentioned approach is directly applicable to a multi-host population, and thus, the age-stratified epidemiological data.

2.3 Results

2.3.1 Reliability

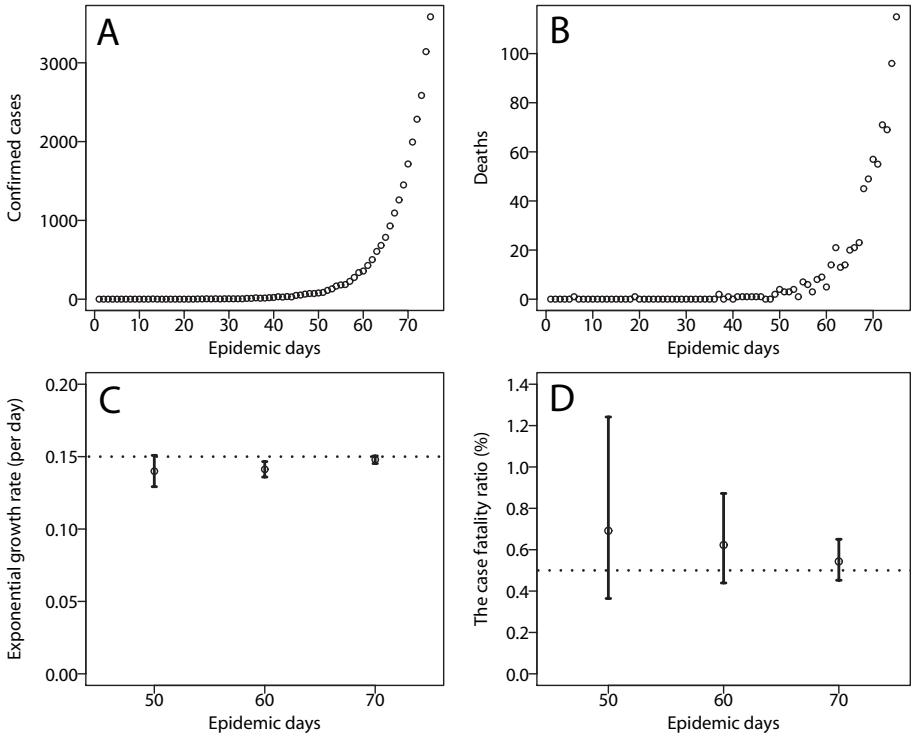

Figure 2.1. A single simulation run and the joint estimation results of the case fatality ratio and the exponential growth rate. The assigned CFR value is 0.5%, and the exponential growth rate, r is set at 0.15 per day. (A & B) Incidence of confirmed cases and deaths as a function of epidemic days. The epidemic day 0 is the date on which an index case is infected. The numbers of confirmed cases and deaths increase exponentially. (C & D) The maximum likelihood estimates of (C) the exponential growth rate r and (D) the case fatality ratio with the 95% confidence intervals. The 95% confidence intervals were computed by employing the profile likelihood. Unfilled circles are the maximum likelihood estimates accompanied by the whiskers extending to lower and upper 95% confidence intervals. The dotted horizontal line shows the assigned parameter value.

Figure 2.1 illustrates a single simulation run and the resulting maximum likelihood estimates with the 95% confidence intervals with the assigned parameters, the CFR of

0.5% and r=0.15 per day. As one can imagine, the confidence intervals for each parameter is gradually narrowed down as the epidemic progresses due to reduced sampling errors. During the very early stage of the pandemic (e.g. for the first 40 days given the assumed parameters), it is not feasible to expect the narrow confidence interval for the CFR, and thus, one may fail to assess the reliability using only the very limited early epidemiological data.

		T (epidemic day to estimate the CFR; days)							
CFR	r	30	40	50	60	70	80	90	100
0.10 %	0.05	1.50 %	1.80 %	7.80 %	19.10 %	34.20 %	49.10 %	66.00 %	82.60 %
	0.15	13.20 %	52.40 %	93.80 %	94.60 %	95.00 %	94.90 %	95.00 %	*
	0.25	62.10 %	94.40 %	95.30 %	*	*	*	*	*
0.50 %	0.05	4.40 %	8.00 %	25.10 %	57.30 %	82.60 %	91.90 %	94.80 %	95.70 %
	0.15	55.30 %	93.60 %	95.20 %	95.00 %	95.90 %	93.80 %	94.20 %	*
	0.25	94.40 %	95.40 %	95.30 %	*	*	*	*	*
2.00 %	0.05	15.20 %	26.90 %	51.80 %	86.40 %	94.40 %	95.20 %	95.10 %	96.20 %
	0.15	90.90 %	95.30 %	96.00 %	96.40 %	96.20 %	95.90 %	95.00 %	*
	0.25	95.50 %	95.80 %	95.00 %	*	*	*	*	*

Table 2.1. Coverage probability of the case fatality ratio (CFR) for each set of parameter values. CFR: case fatality ratio (assigned value). All the values were calculated as the proportion of successful simulation runs with the 95% confidence intervals that include the assigned CFR value among the total of 1000 simulation runs. The parameter r is the exponential growth rate of infection (per day). T is the date on which the estimation is performed. Those exceeding the coverage probability of 90% are highlighted in grey, while the cells with $*$ mark represent combinations of parameter values which generate too large numbers of cases and for which we refrained from estimation.

Table 2.1 shows the coverage probability of the CFR for each set of parameters. When estimating the CFR based on early epidemic data, the exponential growth rate appears to play a critical role in determining reliability. To attain the coverage probability greater than 90% with r=0.05, 0.15 and 0.25 per day, respectively, the latest times of observation, T, should be at least 80, 40 and 30 days with the reference CFR value of 0.5%. This indicates that the smaller the transmission potential is, the longer time it would take to obtain a reproducible estimate of the CFR. Of course, the coverage probability converges to 95% with longer observation times. Given a larger CFR, the coverage probability converges earlier due to smaller sampling errors. However, the coverage probability appears to be more sensitive to variation in r than that in the CFR value.

2.3.2 Validity

The validity of comparing the CFR against pre-specified cut-off values is summarized in Table 2.2. The overall qualitative patterns are similar to those of the coverage probability in Table 2.1. The minimum number of days that is required to declare that the CFR is below cut-off values is very sensitive to the exponential growth rate of cases. In other

words, smaller transmission potential requires us to wait for longer time to compare the estimated CFR against the cut-off values. In addition, the validity is also sensitive to the estimated CFR relative to the cut-off value. When the relative ratio of the CFR to the cut-off value gets smaller, the difficulty in differentiating the CFR is magnified. Given identical transmission potential and an identical assigned value of CFR, there was approximately a 20-day lag in the minimum numbers of days for differentiation between the relative case fatality ratios of 50% and 80%. With the smallest growth rate of r=0.05 per day, the estimation framework failed to yield any successful differentiation of CFR, even observing the epidemic for T=100 days. Of course, the estimated CFR also influences the feasibility, but the successful differentiation appears to be most sensitive to the exponential growth rate.

			T (epidemic day to estimate the CFR; days)							
relative CFR	CFR	r	30	40	50	60	70	80	90	100
80 %	0.10 %	0.05	0.00 %	0.10 %	0.30 %	0.10 %	0.00 %	0.00 %	0.00 %	0.00 %
		0.15	0.00 %	0.00 %	1.50 %	10.50 %	31.30 %	86.10 %	100.00 %	*
		0.25	0.00 %	11.10 %	67.50 %	*	*	*	*	*
	0.50 %	0.05	0.40 %	1.00 %	1.70 %	0.30 %	0.70 %	1.90 %	5.90 %	8.20 %
		0.15	0.00 %	3.20 %	11.50 %	23.30 %	64.80 %	99.30 %	100.00 %	*
		0.25	6.60 %	26.30 %	98.10 %	*	*	*	*	*
	2.00 %	0.05	2.50 %	6.20 %	6.60 %	5.00 %	6.90 %	6.50 %	7.20 %	8.80 %
		0.15	2.10 %	7.10 %	13.20 %	34.80 %	80.40 %	99.90 %	100.00 %	*
		0.25	10.00 %	41.90 %	99.60 %	*	*	*	*	*
50 %	0.10 %	0.05	0.00 %	0.10 %	0.10 %	0.00 %	0.00 %	0.00 %	0.00 %	0.10 %
		0.15	0.00 %	0.00 %	3.30 %	54.00 %	99.20 %	100.00 %	100.00 %	*
		0.25	0.00 %	49.10 %	100.00 %	*	*	*	*	*
	0.50 %	0.05	0.20 %	0.60 %	0.60 %	0.60 %	0.20 %	3.40 %	15.50 %	27.80 %
		0.15	0.00 %	7.80 %	45.30 %	95.80 %	99.90 %	100.00 %	100.00 %	*
		0.25	17.70 %	95.60 %	100.00 %	*	*	*	*	*
	2.00 %	0.05	2.70 %	5.10 %	5.00 %	8.10 %	21.10 %	28.70 %	38.10 %	48.70 %
		0.15	3.70 %	33.00 %	74.00 %	99.80 %	100.00 %	100.00 %	100.00 %	*
		0.25	44.80 %	99.90 %	100.00 %	*	*	*	*	*
30 %	0.10 %	0.05	0.00 %	0.00 %	0.20 %	0.00 %	0.00 %	0.00 %	0.00 %	0.00 %
		0.15	0.00 %	0.00 %	2.70 %	91.10 %	100.00 %	100.00 %	100.00 %	*
		0.25	0.00 %	86.70 %	100.00 %	*	*	*	*	*
	0.50 %	0.05	0.30 %	0.40 %	0.40 %	0.30 %	0.40 %	5.50 %	24.50 %	49.50 %
		0.15	0.00 %	8.30 %	84.70 %	100.00 %	100.00 %	100.00 %	100.00 %	*
		0.25	29.60 %	100.00 %	100.00 %	*	*	*	*	*
	2.00 %	0.05	1.40 %	3.30 %	4.20 %	10.40 %	33.90 %	55.00 %	72.80 %	86.40 %
		0.15	4.30 %	64.90 %	98.70 %	99.90 %	100.00 %	100.00 %	100.00 %	*
		0.25	86.10 %	100.00 %	100.00 %	*	*	*	*	*

Table 2.2. Proportion of simulation runs in which the upper 95% confidential interval of CFR (p) falls below specified cut-off values. CFR: case fatality ratio (assigned value). relative CFR: the ratio of assigned CFR value relative to the cut-off value. The proportion of successful simulation runs with the upper 95% confidence interval below the pre-specified cut-off value is shown. The parameter r is the exponential growth rate of infection (per day). T is the date on which the comparison is performed. Those exceeding the proportion of 90% are highlighted in dark grey, while the cells with $*$ mark represent combinations of parameter values which generate too large numbers of cases and for which we refrained from estimation.

2.3.3 Heterogeneous Population

The proposed method is not directly applicable to realistic setting in which we observe substantial heterogeneities in the risks of infection and death. Accordingly, here we show the modeling approach to heterogeneous populations analytically. Specifically, we consider age-dependent dynamics: while the risk of infection may be higher among children than among elderly in the case of influenza, the conditional risk of death given infection is likely to be higher among elderly than school age children, perhaps reflecting higher proportion of elderly with the underlying co-morbidities.

Let $i_s(t)$ be the incidence of infection among sub-group s at calendar time t. Also, let R_{qs} be the average number of secondary cases in sub-group q generated by a single primary case in sub-group s, which would act as a single entry of the age-dependent next-generation matrix [28]. Assuming that the density function of the generation time, $g(\tau)$ of length τ days is shared among sub-groups, the multivariate renewal process is described by

$$i_s(t) = \sum_q R_{sq} \int_0^\infty i_q(t-s)g(s)ds. \tag{2.11}$$

Let p_s be the group-specific CFR (e.g. age-specific CFR) among all infected individuals of sub-group s. As was shown with application to the homogeneous population, we employ the confirmed coefficient k_s, reflecting both the proportion of confirmed cases to all infected individuals of sub-group s and the time delay from infection to confirmatory diagnosis. Then the confirmed cases among sub-group s, $c_s(t)$ is

$$c_s(t) = k_s i_s(t). \tag{2.12}$$

Since the observed dataset is discrete time series, i.e. daily data, we integrate the confirmed cases as follows:

$$c_{s,t} = \int_{t-1}^{t} c_s(x)dx. \tag{2.13}$$

Assuming that the conditional probability density function of the time from infection to death, $f(s)$ is known and is shared among sub-groups, the number of new deaths of sug-group s at time t, $d_s(t)$ is described as

$$d_s(t) = p_s \int_0^\infty i_s(t-s)f(s)ds, \tag{2.14}$$

which is rewritten as

$$d_s(t) = p_s \int_0^\infty \sum_q \int_0^\infty i_q(t-\tau-s)g(\tau)d\tau f(s)ds. \tag{2.15}$$

As was integrated in the homogeneous case, one may focus on the cumulative number of deaths, $D_s(T)$ by the latest time of observation T. The estimator of the group-specific CFR is given by

$$\hat{p_s} = \frac{D_s(T)}{\int_0^T \int_0^\infty \sum_q R_{sq} \int_0^\infty i_q(t-\tau-s)g(\tau)d\tau f(s)dsdt}. \tag{2.16}$$

The likelihood function to estimate the next generation matrix may partially account for stochastic dependence structure of the transmission dynamics, and thus, conditions for every future expectation on the past history of the epidemic. Let $Z(t)$ represent the history of age-specific confirmed cases from time 0 up to time $t-1$. Given the series up to $t-1$, and assuming that the incidence of confirmed cases on day t is sufficiently characterized by Poisson distribution, the conditional likelihood is written as

$$L_1(R_{ij}, k; Z(t)) = \prod_s \prod_{i=1}^n \frac{\exp\left(-\sum_q R_{sq} \int_0^\infty c_q(t-s)g(s)ds\right)\left(\sum_q R_{sq} \int_0^\infty c_q(t-sg(s)ds)\right)^{m_{t,s}}}{m_{t,s}!}, \tag{2.17}$$

where $m_{t,s}$ represents the observed number of confirmed cases in sub-group s on day t. This likelihood function is useful to describe the underlying epidemic dynamics of the heterogeneous population. Let $\pi_{t,s}$ be a random variable which yields an estimator of the CFR of sub-group s at day t since the start of an epidemic. The other likelihood to estimate $\pi_{t,s}$ is assumed to be given by binomial sampling process as follows:

$$\begin{aligned} L_{2,s}(\pi_{s,T}; D_s(T), R_{ij}, k) = &\binom{\int_0^T \int_0^\infty \sum_q R_{sq} \int_0^\infty i_q(t-\tau-s)g(\tau)d\tau f(s)dsdt}{D_s(T)} \\ &\times \pi_{s,T}^{D_s(T)} (1-\pi_{s,T})^{\int_0^T \int_0^\infty \sum_q R_{sq} \int_0^\infty i_q(t-\tau-s)g(\tau)d\tau f(s)dsdt - D_s(T)}. \end{aligned} \tag{2.18}$$

Therefore, the total likelihood is calculated as the following product:

$$L = L_1 \prod_s L_{2,s}. \tag{2.19}$$

Although the estimation framework can thus be very similar to that for the homogeneous population, it should be noted that the validity and reliability of estimation procedure for the heterogeneous population are likely to be influenced by way of parameterizing the next-generation matrix. For example, if the quantification of the matrix requires us to estimate only a small number of parameters (e.g. one parameter for each age-group), we expect that the validity and reliability are not too much different from those we examined for the homogeneous population. However, when more parameters should be estimated to describe more detailed underlying heterogeneous transmission dynamics, the proposed method has to face greater uncertainty.

2.4 Discussion

We proposed an estimation method to jointly infer the CFR and the exponential growth rate using only the confirmed case and death data. By means of Monte Carlo simulations, we assessed the minimum length of days required to compare the estimated CFR with the pre-specified CFR value such as those in the US Pandemic Severity Index. To do so, it appeared that the validity and reliability were very sensitive to the exponential growth rate, and thus, to the transmission potential of a novel pandemic strain. To be confident that the method included the CFR estimate within the 95% confidence interval, it appears that we have to wait at least for a month, and perhaps in general for about a few months given that the growth rate is equal to or smaller than 0.15 per day. The successful differentiation of CFR from cut-off values also takes about a few months. More importantly, the differentiation may not be feasible, if the growth rate is 0.05 per day or smaller. The growth rate was thus shown to play the most critical role in determining the feasibility of the proposed method than the CFR value to be estimated. This finding is attributable to the fact that the number of deaths is the result of binominal sampling of cases. In general, as the sample size (or the number of binomial trials) increased, the standard error of binomial probability decreased, and the number of binomial trials in the proposed model substantially increased as the exponential growth rate increased. The validity and reliability were more sensitive to the growth rate than the binomial probability: the influence of variation in binomial probability on its confidence interval was small for the assumed range of CFR values, which can be understood from the approximate standard error of the binomial probability derived from the normal approximation to binomial.

Already, there have been multiple epidemiological methods to estimate the CFR using different datasets. Presanis et al. [116] proposed a Bayesian evidence synthesis approach using various different types of data that describe a pyramid structure, explaining that confirmed cases represent the tip of an iceberg of infected individuals and emphasizing a need to observe milder fraction of cases such as those attended medical service. The useful datasets for that method included medically attended symptomatic cases and those required hospitalization and those admitted to intensive care unit. Comparing our proposed method with the evidence synthesis approach, the proposed method has two important advantages: (i) the proposed method can comply with a need to offer the CFR estimate in real-time and (ii) we use the time series data of the confirmed cases and deaths which are readily available and accessible. The two different methods may thus be combined and used in practical setting: while the proposed method is used for the real-time assessment using widely available data, the sCFR estimate employing the evidence synthesis approach may be subsequently offered based on datasets of well-defined cohort populations. On the other hand, Wu et al. [140] used real-time sero-prevalence data during the course of an epidemic. This approach enables us to estimate the background denominator of incidence

of infections directly. In fact, a seroepidemiological study may be the only method to explicitly and directly quantify the underlying transmission dynamics. However, seroepidemiological surveys are costly and explicit interpretations of seroconversion and changes in antibody titers have yet to be offered. As a method to supplement the explicit estimation approaches, we believe that the proposed method based on readily available data would be a useful real-time assessment tool.

There are a few important future tasks for improvement. First, we used no prior information of parameters in the present study, but some information may be retrieved from earlier data, other datasets or from literature including historical epidemic records (e.g. the exponential growth rate of the same epidemic before conducting the estimation). In fact, it is frequently the case that the transmission potential or the growth rate of cases is estimated earlier than the CFR in practical setting, and one may know a plausible value of r in advance of CFR estimation. If the prior knowledge could compensate unknown information of the proposed method, it will help to greatly reduce the associated uncertainty of the CFR, thereby improving the validity of estimation. Second, we did not take into account demographic stochasticity in the present study, but the stochasticity may not be negligible during the early epidemic phase [102,119]. The uncertainty that we quantified in the present study is likely to have been underestimated, although the qualitative findings are expected not to be different from those when we explicitly account for stochasticity using appropriate models (e.g. [12, 102]), especially for highly transmissible virus. Third, the proposed method as well as two earlier estimation studies based on evidence synthesis and serological study relied on the observed number of deaths as the numerator of the CFR. If there are many undiagnosed deaths, the direct estimation of the CFR is not feasible, and so, the virulence may also have to be assessed by indirect measurement such as that using excess mortality [15,75]. Of course, constant k over time is also an unsupported assumption for epidemics with time-varying ascertainment efforts.

For a heterogeneous population we have shown that the proposed estimation framework for the homogeneous population can be easily extended to the heterogeneous setting. However, we have also discussed that the limited degrees of freedom might increase the relevant uncertainty. That is, when we consider n different sub-groups, we have to deal with the next generation matrix with n^2 entries in addition to n unknown parameters for the group-specific CFR, p_s. Thus, the minimum length of days, T that is required to estimate the CFR would increase, and T would depend on the way we parameterize the next generation matrix. Thus, we failed to offer simulation results with general conclusions with respect to the validity and reliability for the heterogeneous population. Given that the transmission of H1N1-2009 has been highly dependent on age [43, 102, 119, 141], one will have to balance the detailed descriptions of dynamics involving many sub-populations with the uncertainty surrounding the joint estimation of the CFR and the transmission potential.

If policy-making and public health response have to be made based on the real-time estimate of the CFR, the proposed method can be employed using only the readily available epidemiological datasets. However, as long as the estimation of the CFR relies on the proposed method, it should be noted that it may take longer than a few months to derive the CFR with sound uncertainty bounds, and thus, the very early response may not be able to base the policy decision on the CFR. Moreover, when the transmission potential is small, the number of infected individuals (or cases) may better be estimated directly from serological data (or medical attendance), because the proposed method is prone to uncertainties arising from low frequency of infection. While such limitation exists, we believe that the proposed method can be coupled with or supplement existing estimation frameworks which have to use additional epidemiological and serological data, especially for diseases with high transmission potential.

Chapter 3

Real-time Investigation of Measles Epidemics

3.1 Introduction

Although the World Health Organization (WHO) and its member states across the world have aimed to eliminate measles, the elimination has been so far fully successful only in the North American region. As the transmission potential of measles is extremely high with the estimated basic reproduction number of the order of 6-45 [31,91,129,133], i.e. the average number of secondary cases generated by a single primary case in a fully susceptible population being 6-45, it is necessary to maintain very high vaccination coverage to eliminate the infection by means of mass vaccination. In industrialized countries, all children are subject to routine immunization mostly by the age of 18 months using either MR (measles and rubella) or MMR (measles, mumps and rubella) vaccine. Moreover, to boost the vaccine-induced immunity, children aged from 4-5 years receive the second dose, and depending on each individual country's policy, additional revaccinations are scheduled.

Understanding the vaccine efficacy at an individual level is essential to assess the vaccination program. Although the vaccine efficacy against measles is believed to be high (e.g. $> 95\%$) [135], in practice even vaccinated individuals may be susceptible if the vaccination failure occurred or if their immunity was lost [113]. If the evaluation can be made based on readily available epidemiological dataset in real-time, disease control policy making will be able to reflect the results of such analysis. For instance, if we can detect the signature of a potential major epidemic in near future [38] or if we can identify specific sub-population which is less protected than others [32], the epidemiological modeling study could inform real-time policy making, e.g. identifying an essential part of the population to be (re-)vaccinated.

To estimate the vaccine efficacy, three distinct study approaches have been taken. First, laboratory measurement (e.g. seroconversion) has been used as a surrogate marker of successful immunization, allowing us to judge the vaccine-induced immunity in a biologically well-defined manner. However, such measurement requires laboratory test samples

as well as testing capacity, and perhaps more importantly, makes it difficult to directly attribute the result to actual vaccine-induced protection (e.g. actual causal impact of vaccination against infection) at an individual level. Other two approaches thus tackle the issue of assessment using epidemiological data. Since the epidemiological data of directly transmitted infectious diseases involve the technical problem of dependent risk of infection between individuals (i.e. the so-called "dependent happening"), the empirically observed datasets are greatly influenced by the indirect effect of vaccination [54]. Therefore, as the second method, the conditional risks of infection (i.e. conditional on an exposure to an infected individual) in vaccinated and unvaccinated individuals are compared to estimate the conditional direct effect of vaccination while reasonably eliminating the influence of indirect effect. For instance, household secondary attack proportion (SAP) is conventionally used to estimate the efficacy using the conditional risk of infection given a primary case in households. However, collection of household transmission data requires substantial observational effort and moreover, such study needs to ensure uniform susceptibility among household contacts. As the third method, the population data may be analyzed by employing a mathematical model that can be believed to have captured the underlying transmission dynamics. In particular, the final size of an epidemic (i.e. the fraction of the total infected individuals in a population throughout the course of an epidemic) has been used to estimate the efficacy in a highly vaccinated population [91, 125, 128]. However, there has been little attempt to estimate the vaccine efficacy jointly with the epidemic dynamics in real-time (e.g. during the course of an epidemic).

The present study aims to propose an epidemiological method which we can employ to estimate the vaccine efficacy of measles while conducting real-time assessment of the epidemic based on readily available epidemiological surveillance dataset. While not requiring us to conduct field investigations to specifically assess the vaccine efficacy, we show that the assessment could be partly achieved by analyzing the counts of cases with vaccination history over time.

3.2 Materials and Methods

3.2.1 Epidemiological Data

The present study investigates empirical data from Aichi prefecture, around the middle of Japan in which children aged from 12-24 months had received a single-dose MMR vaccination from 1988 to 1993. MMR vaccine was replaced by MR vaccine in 1993 due to the reporting of the substantial number of bacterial meningitis cases that were attributed to MMR vaccination, lowering the overall vaccination coverage for a while. In 2006, the country initiated two-dose vaccination program in which first and second doses are given at the age of 12-24 months and before entering primary school (i.e. before the age of 6 years), respectively. Despite nationwide vaccination campaigns, the vaccination coverage remained insufficient to prevent the epidemic, and only in recent years, the vaccination

coverage of first dose clearly exceeded 95.0% which is the minimum coverage to eliminate a disease with the basic reproduction number of 20. Due to the presence of the various pockets of susceptible individuals, sporadic minor outbreaks have been seen continuously across Japan. To monitor the outbreaks and strengthen the measles control, the Ministry of Health, Labour and Welfare of Japan has enhanced the measles surveillance which enforced compulsory reporting of all measles case since 2008. Our study rests on the pilot data of the enhanced surveillance in Aichi prefecture in 2007 and 2008.

During the surveillance, the confirmed measles case was defined as follows: (i) the cases who reveal all three specific signs and symptoms (i.e. rash, fever and catarrh including coughing, nasal discharge and congestion of conjunctiva) with (ii) laboratory diagnosis based either on (a) isolation of the virus, (b) isolation of the virus RNA, or (c) serological diagnosis (i.e. seroconversion of IgM antibody using paired sera). Isolation of confirmed case and contact tracing of all known contacts have been made upon confirmatory diagnosis of each case.

The population size of Aichi prefecture in 2007 was approximately 7.3 million [122]. The enhanced surveillance data included the information regarding the date of illness onset (date of fever and date of rash), age and vaccination history. Hereafter, we consistently use only the date of fever to describe the temporal patterns. In 2007 and 2008, the totals of 212 and 198 confirmed measles cases were reported, respectively. Counting from 1st January in each year, the epidemic in these years revealed a single peak around Days 150 and 100, respectively. A part of the confirmed cases did not remember their own vaccination history in the past against measles. In 2007, there were 57 vaccinated and 87 unvaccinated cases that clearly remembered the vaccination history, while 68 cases did not remember vaccination history. In 2008, there were 50 vaccinated and 86 unvaccinated cases with 62 cases without known vaccination history.

3.2.2 Mathematical Model 1: Homogeneous Population

To develop a real-time estimation framework, we first consider a model to describe the transmission dynamics of measles in a homogeneously mixing population. Let p and α be the vaccination coverage and vaccine efficacy, respectively. Usually, the vaccination coverage is known, and in the case of Aichi prefecture, the baseline coverage of first dose has been estimated at 94.8% [29], while as sensitivity analysis we estimate the vaccine efficacy by varying the coverage from 90.0 to 99.5%. Let k and l represent the vaccination history of an exposed individual and the primary case, respectively, for which 1 stands for vaccinated and 0 otherwise. We consider the renewal process of measles in which the incidence (the number of new cases) of those with vaccination history k on calendar day t, $j_{k,t}$ is described as

$$j_{k,t} = \sum_{l} \sum_{t=0}^{\infty} A_{kl,t,\tau} j_{l,t-\tau}, \tag{3.1}$$

where $A_{kl,t,\tau}$ describes the rate of causing secondary transmissions per single primary case whose vaccine status is l among susceptible contacts of those with vaccination history k on day t at infection-age τ (i.e. the time since infection in each primary case). Let U_t represent the vaccine-unrelated frequency of secondary transmissions per single primary case on day t, which is influenced by all factors other than vaccination including intrinsic and extrinsic ones. We assume that the vaccine efficacy reduces susceptibility of vaccinated individuals by $(1-\alpha)$ as was adopted in an earlier study [125] and assume that $A_{kl,t,\tau}$ is separable into the functions of t and α as follows:

$$\begin{aligned} A_{0y,t,\tau} &= (1-p)U_t g_\tau, \\ A_{kl,t,\tau} &= p(1-\alpha)U_t g_\tau, \end{aligned} \tag{3.2}$$

where g_τ is the probability mass function of the generation time, i.e. the time from infection in a primary case to infection in the secondary case caused by the primary case, and $A_{kl,t,\tau}$ is thus assumed to be scaled by p, α and U_t. Based on a published statistical study [72], g_τ is assumed to be the discrete function that is derived from the continuous, lognormal distribution with the mean and the standard deviation of 12.0 and 3.5 days, respectively. The instantaneous reproduction number, i.e. the average number of secondary cases per single primary case at calendar time t, is calculated as

$$R_t = [(1-p) + p(1-\alpha)]U_t, \tag{3.3}$$

which is useful to objectively interpret the epidemic curve in real-time, because if the R_t exceeds 1, it clearly indicates increase in infections on day t. The renewal process in (1) is rewritten as

$$j_{0,t} = \frac{(1-p)R_t}{(1-p)+p(1-\alpha)} \sum_{t=0}^{\infty} g_\tau (j_{0,t-\tau} + j_{1,t-\tau}), \tag{3.4}$$

for unvaccinated cases and

$$j_{1,t} = \frac{p(1-\alpha)R_t}{(1-p)+p(1-\alpha)} \sum_{t=0}^{\infty} g_\tau (j_{0,t-\tau} + j_{1,t-\tau}), \tag{3.5}$$

for vaccinated cases.

Due to enhanced surveillance, and because measles rarely involves secondary transmissions arising from asymptomatic or subclinical cases, the number of infected cases is assumed to have been fully captured as a function of time. For mathematical convenience, we assume that the incubation period is a constant so that the epidemic curve can be theoretically shifted leftward for a constant day for the purpose of statistical analysis using the above mentioned model. In empirical observation, a part of cases did not remember vaccination history. Assuming that the past vaccination history is independent of possessing a memory of vaccination history, the probability of knowing vaccination status, q, is assumed to be governed by a binomial sampling process of the cumulative number of cases

with known vaccination history among the cumulative total of cases. Let $h_{0,t}$, $h_{1,t}$ and $h_{9,t}$ denote the observed numbers of unvaccinated cases, vaccinated cases and cases who did not remember vaccination status on day t, respectively. We assume that the observed incidence with vaccination history $h_{0,t}$ and $h_{1,t}$ are the results of Poisson sampling with expected values $qE(j_{0,t}; Z_{t-1})$ and $qE(j_{1,t}; Z_{t-1})$, respectively, where $E(j_{x,t}; Z_{t-1})$ denotes the conditional expected value of the incidence of cases with vaccination history x on day t given the history of observed data (i.e. $h_{0,t}$, $h_{1,t}$ and $h_{9,t}$) from time 0 up to $(t-1)$, denoted by Z_{t-1}.The likelihood function to estimate the reproduction number for each date, $\mathbf{R}$, and other parameters q and α is written as follows:

$$L(\mathbf{R}, q, \alpha; \mathbf{Z}) = \binom{\sum_s (h_{0,s} + h_{1,s} + h_{9,s})}{\sum_s h_{9,s}} (1-q)^{\sum_s h_{9,s}} q^{\sum_s (h_{0,s}+h_{1,s})}$$
$$\times \prod_s \frac{(qE(j_{0,s};Z_{s-1}))^{h_{0,s}} (qE(j_{1,s};Z_{s-1}))^{h_{1,s}} \exp\{-q[E(j_{0,s};Z_{s-1})+E(j_{1,s};Z_{s-1})]\}}{h_{0,s}! h_{1,s}!}. \quad (3.6)$$

The maximum likelihood estimates of R, q, and α are found by minimizing the negative logarithm of (3.6). The 95% confidence intervals are computed based on profile likelihood.

3.2.3 Mathematical Model 2: Heterogeneous Population

Although the above-mentioned model is kept simple, the empirical data suggest that the frequency of cases greatly differs by age (Figure 3.1). Differential frequency of cases by age may be attributable to (i) the differential population structure, (ii) the different contact patterns, (iii) the differential protection conferred by vaccination and so on. Thus we extend the above-mentioned model to age-dependent data so that the epidemiological dynamics are better captured. We take an approximate approach and divide the population into three discrete age-groups. Since the second-dose vaccination is scheduled by the age of 6 years with the available social contact data discretized at age 0-4 years, and because the adult infections may be separated from those in children to clarify the contribution of schools to the epidemic, the age groups are classified as 0-4 years, 5-19 years and 20 years and above, respectively. The relative population sizes of the age group i, n_i are 4.9%, 15.1% and 80.1% in 2007 and 4.8%, 14.8% and 80.4% in 2008, respectively. Let the age-specific incidence of vaccination status k and age group a as $j_{ka,t}$ on day t, the dynamics are described by the multivariate renewal process:

$$j_{0a,t} = (1-p_a) U_t n_a \sum_b \beta_{ab} \sum_{\tau=0}^{\infty} g_\tau (j_{0b,t-\tau} + j_{1b,t-\tau}). \quad (3.7)$$

for unvaccinated cases and

$$j_{1a,t} = p_a (1-\alpha_a) U_t n_a \sum_b \beta_{ab} \sum_{\tau=0}^{\infty} g_\tau (j_{0b,t-\tau} + j_{1b,t-\tau}), \quad (3.8)$$

for vaccinated cases. Here β_{ij} is the normalized contact matrix with the eigenvalue 1, describing the age-dependent contact frequency which we retrieve from the published result of social contact survey in the UK [90] and we assume that the age-dependent frequency with an adjustment of age-dependent population size in Japan is similar to that in the UK (Table 3.1). U_t represents the average number of secondary transmissions per single primary case at calendar time t, which is influenced by all factors other than vaccination including intrinsic and extrinsic ones. The age-dependent vaccination coverage p_a is assumed as known, i.e. 97.0, 93.4 and 99.0% for those aged 0-4 years, 5-19 years and 20 years and above, respectively. The average of those coverage estimates is greater than that for the base-line in the homogeneous setting, because the coverage for adults 99.0% is not realistically tractable due to past natural exposures and booster effect [92]. Namely, among adults we assume that the above mentioned coverage denotes the fraction immune or seropositive based on serological survey [1].

Year 2007			
Age	0-4	5-19	20 and above
0-4	0.139	0.113	0.440
5-19	0.037	0.633	0.532
20 and above	0.027	0.100	0.829
Year 2007			
0-4	0.145	0.118	0.460
5-19	0.038	0.600	0.561
20 and above	0.027	0.103	0.828

Table 3.1. The matrix describing the within and between age-group frequency of social contact. The age-groups in the first column represent those of contactee (i.e. those who are exposed to cases), while the age-groups in second and seventh rows represent those of contactor (i.e. the primary cases). The contact is expressed by per unit time (i.e. per day in case of this table), although each element is adjusted due to normalization.

Let h_{0a},t , $h_{1a,t}$ and $h_{9a,t}$ be the observed incidence of unvaccinated cases, vaccinated cases and the cases did not remember their own vaccination history in age group a on day t. As discussed in the homogeneous case, we assume that the vaccination status of the cases is independent of remembering their own vaccination history, and we also assume that the probability of having the memory, q is independent of age. To estimate U, q and α_a, we maximize the following likelihood:

$$L(\mathbf{U}, q, \alpha; \mathbf{Z}) = \binom{\sum_a \sum_s (h_{0,s} + h_{1,s} + h_{9,s})}{\sum_s h_{9a,s}} (1-q)^{\sum_a \sum_s h_{9a,s}} q^{\sum_s (h_{0a,s} + h_{1a,s})}$$
$$\times \prod_a \prod_s \frac{(qE(j_{0a,s}; Z_{s-1}))^{h_{0a,s}} (qE(j_{1a,s}; Z_{s-1}))^{h_{1a,s}} \exp\{-q[E(j_{0a,s}; Z_{s-1}) + E(j_{1a,s}; Z_{s-1})]\}}{h_{0a,s}! h_{1a,s}!}, \quad (3.9)$$

where $\mathbf{Z}$ represents the history of epidemic data across all age-groups.

3.3 Results

Figure 3.1 shows the temporal and age-specific distributions of measles cases stratified by vaccination history. The epidemic curves in 2007 and 2008 recorded the highest incidence in weeks 22 and 15, respectively. Since there have been very few cases nearby new-year and year-end days in both years, and due to epidemic in discrete geographic locations, we analyzed each epidemic year separately from the other, while we focused on the data which combined both years when we estimate the vaccine efficacy (because the vaccine efficacy is not expected to vary greatly by a single year). The mean (and the standard error, SD) and median age of cases (and inter-quartile range) were 18.9 (13.9) and 17.0 (10.0-26.0) years in 2007, respectively. Similarly, the mean and median were 14.2 (12.5) and 13.0 (2.0-24.0) years in 2008, respectively. In both years, the cases were aggregated among children and very few elderly cases were observed. The cases in 2008 appeared to be significantly younger than that in 2007 (p=0.0003, t-test). The proportion of cases who remember as vaccinated was 26.9% (95% confidence interval (CI): 20.9, 32.9) and 25.3% (95% CI: 19.2, 31.3), respectively, in 2007 and 2008, which did not significantly differ by year (p=0.76, x^2 test). The proportion of cases who remembered either as vaccinated or unvaccinated was 67.9% (95% CI: 61.6, 74.2) and 68.7% (95% CI: 62.2, 75.1) in 2007 and 2008, respectively, which was again not significantly different by year (p=0.99, x^2 test).

Figures 3.2 and 3.3 show the estimated instantaneous reproduction numbers using the homogeneous model in 2007 and 2008, respectively, along with the visual comparisons between the observed and predicted epidemic curves with known vaccination history. The estimated reproduction numbers in early and late epidemic phases were very high, reflecting mathematical property of the renewal process, i.e., in these time periods, the effective reproduction number tends to be very large due to small number of primary cases, and thus, we omitted in Figures. While the majority of the maximum likelihood estimates of R_t fell below unity, the upper 95% confidence interval continuously exceeded 1, reflecting small number of cases (i.e. sampling error) and high transmission potential of measles with limited vaccination coverage. Analyzing both years were analyzed jointly, the maximum likelihood estimates of the vaccine efficacy, α, was estimated at 96.7% (95% CI: 95.8, 97.4). The proportion of cases with known vaccination history, q, was estimated at 68.3% (95% CI: 65.1, 71.4). Even when we estimated a separately by 2007 and 2008, they were not significantly different: α in 2007 and 2008 were 96.5% (95% CI: 95.2, 97.5) and 96.8% (95% CI: 95.5, 97.8), respectively.

When we employed the age-heterogeneous model, the vaccine efficacy was separately estimated for each age-group. The maximum likelihood estimates of the vaccine efficacy α_1 and α_2 and α_3 for those aged 0-4 years, 5-19 years and 20 years and above were 97.9% (95% CI: 95.8, 99.0) and 93.4% (95% CI: 89.0, 96.1) and 99.6% (95% CI: 99.2, 99.8), respectively. The proportion of cases with known vaccination history, q, was estimated to be 68.1% (95% CI: 65.2, 70.9).

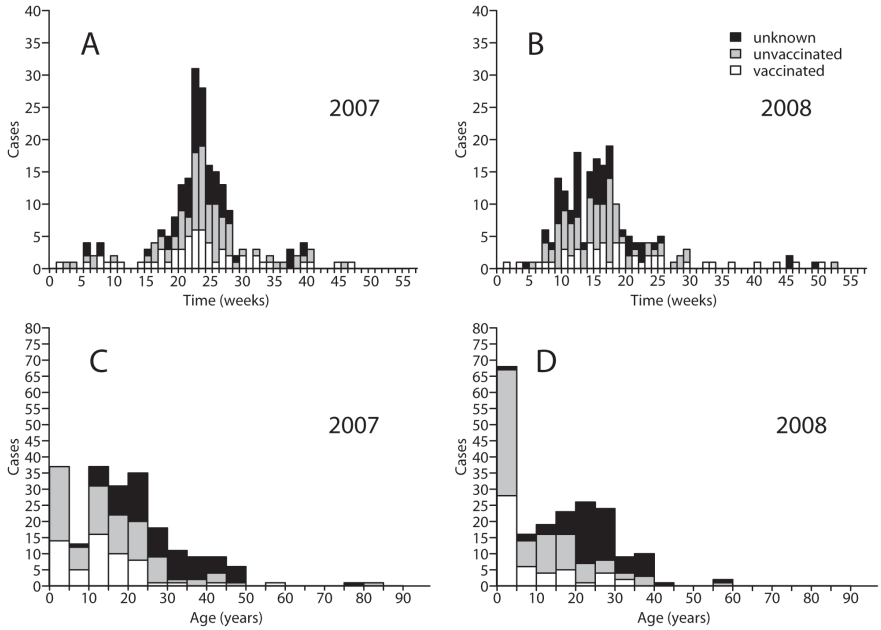

Figure 3.1. The time and age-specific distributions of the measles outbreak in Aichi prefecture, Japan, from 2007-08. A & B. The temporal distribution of measles cases. The week 1 corresponds to the week that includes 1st January. C & D. The age distribution of measles cases. In all panels, the vaccinated and unvaccinated correspond to the cases who clearly remembered as previously vaccinated and unvaccinated, respectively. Unknown represents the cases who did not remember vaccination history at the time of diagnosis of measles.

Since we cannot assess the exact vaccination coverage, the sensitivity analysis was conducted (Figure 3.4). The vaccine efficacy increased as the vaccination coverage increased. Within the assumed range of vaccination coverage (90.0%-99.5%), the maximum likelihood estimate of the vaccine efficacy ranged 93.3%-99.7%. The estimated vaccine efficacy increased as the vaccine coverage increased. The reason for positive relationship in Figure 3.4 is intuitively understood from equations (3.4) and (3.5). That is, if we take the ratio of the incidence of unvaccinated to vaccinated, we get

$$\frac{j_{0,t}}{j_{1,t}} = \frac{1-p}{p}\frac{1}{1-\alpha}. \tag{3.10}$$

The left-hand side of equation 3.10 corresponds to the observed data which is a constant on a single day (given empirical data). If we increase the vaccination coverage p, then $(1-p)/p$ decreases and this necessitates $1/(1-\alpha)$ to increase in equation (10) or forces the vaccine efficacy α to increase.

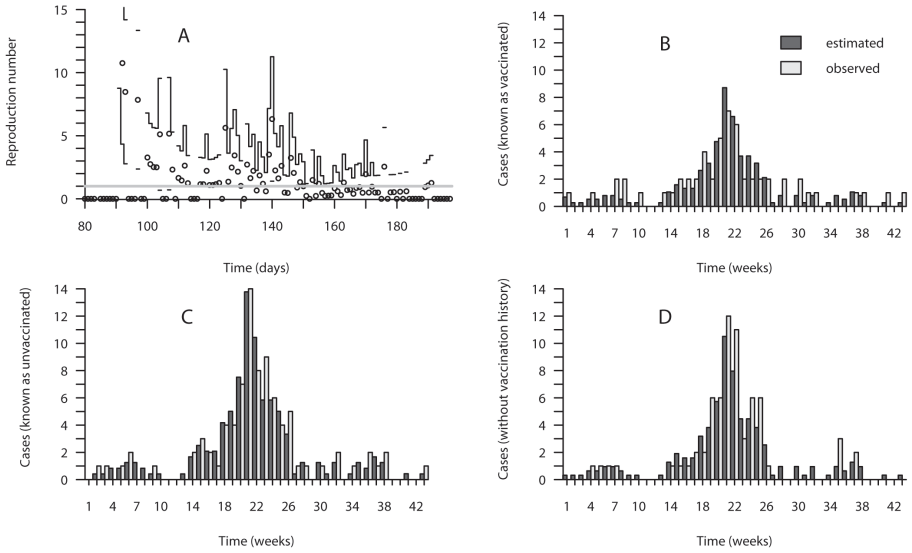

Figure 3.2. The estimated instantaneous reproduction numbers and visual comparisons between the observed and predicted temporal distributions by known vaccination history in 2007. A. The maximum likelihood estimates (circles) and the upper 95% confidence interval (steps) of the instantaneous reproduction number. The horizontal axis is expressed as the calendar date in which 1st January is set to be 0. The horizontal grey line shows the level at which $R_t = 1$. For mathematical reasons R_t is unrealistically high during the very early and late epidemic phases, and thus, the estimates are omitted from this panel. B, C and D. Comparisons between observed and predicted temporal distributions of cases. B and C compare cases who were known to be vaccinated and unvaccinated, respectively. D shows the cases who did not remember vaccination history at the time of diagnosis of measles. The week 1 corresponds the week that includes 1st January.

3.4 Discussion

The present study proposed a simple method to estimate the vaccine efficacy against measles, jointly quantifying the parameters governing the temporal dynamics of measles. The method uses only the epidemiological surveillance data with partial information of vaccination history, which can rest on readily available dataset and is not as costly as conducting specialized field study such as that observing household transmissions. To capture the realistic aspect of measles transmission, the extended model accounted for age-dependent heterogeneity. Although not significant, the vaccine efficacy among those aged 5-19 was shown to be clearly smaller than that in children aged below 5 years, which may perhaps reflect the waning immunity among school children [47]. The straightforward policy implication is that one may target school children aged 5-19 for (re-)vaccination to eliminate the pockets of susceptible individuals.

As the proposed method can rest on the readily available data (i.e. routinely collected surveillance data), we believe that the model has a potential to be integrated with

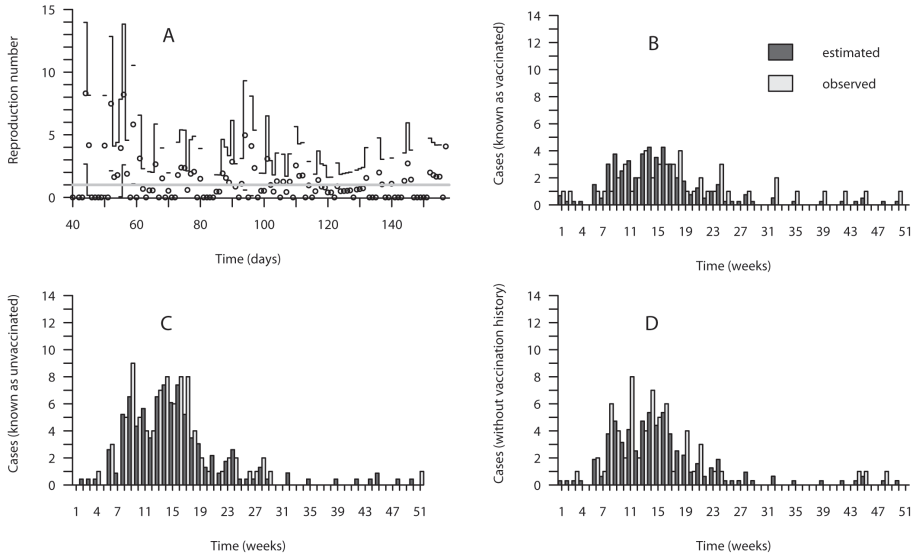

Figure 3.3. The estimated instantaneous reproduction numbers and visual comparisons between the observed and predicted temporal distributions by known vaccination in 2008. A. The maximum likelihood estimates (circles) and the upper 95% confidence interval (steps) of the instantaneous reproduction number. The horizontal axis is expressed as the calendar date in which 1st January is set to be 0. The horizontal grey line shows the level at which $R_t = 1$. For mathematical reasons R_t is unrealistically high during the very early and late epidemic phases, and thus, the estimates are omitted from this panel. B, C and D. Comparisons between observed and predicted temporal distributions of cases. B and C compare cases who were known to be vaccinated and unvaccinated, respectively. D shows the cases who did not remember vaccination history at the time of diagnosis of measles. The week 1 corresponds the week that includes 1st January.

the routine surveillance practice of measles across the world. While various mathematical approaches have been proposed to model the measles epidemic, the present study offered advancement in two different aspects. First, although many studies analyzed the temporal dynamics using mathematical models, the objectives of those studies have been different from the efficacy estimation, and they frequently focused on the estimation of time-dependent notification characteristics [42] or clarification of the kinetics of measles transmission using mathematical model [8]. The present study has shown that the vaccine efficacy is very conveniently estimated, assuming that the depletion of susceptible individuals is negligible. Second, whereas a few other studies estimated the vaccine efficacy, including that based on final size [91, 129] and an explicit modeling of temporal epidemic dynamics [130], the present study is the first to have jointly conducted the vaccine efficacy estimation and the real-time assessment of an epidemic, by estimating the effective reproduction number R_t along with the vaccine efficacy parameter. In other words, our proposed approach not only helps assess vaccine efficacy but permits us to interpret the temporal dynamics in an objective manner.

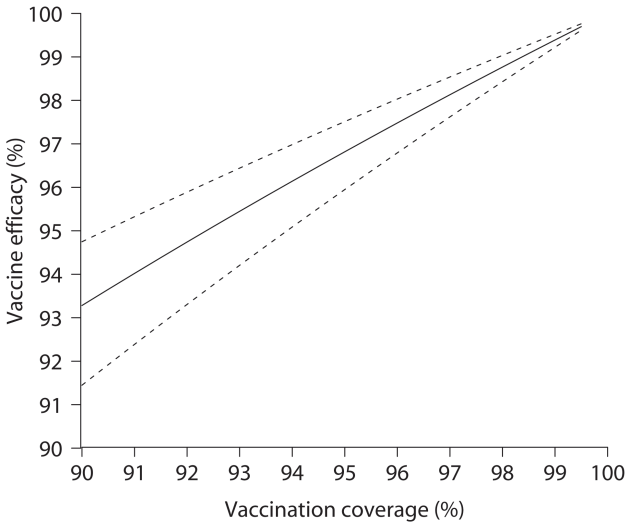

Figure 3.4. Sensitivity of vaccine efficacy to the vaccination coverage. Solid line represents the maximum likelihood estimate, while dashed lines are the upper and lower 95% confidence intervals of vaccine efficacy. The 95% confidence intervals were derived from profile likelihood. Although we show the results from homogeneous model, the qualitative patterns of age-heterogeneous model are not different.

However, three reservations should be noted as technical limitations. First, we successfully estimated the vaccine efficacy as well as R_t, but we did so assuming that the depletion of susceptible individuals is negligible. We believe that this assumption is reasonable because the number of cases in Aichi remained very small as compared to the population size of unvaccinated individuals who can be theoretically considered as fully susceptible, and also because the epidemic data in question were seen in a population which was large enough. However, the model cannot capture detailed heterogeneous transmission such as local depletion of susceptible individuals (e.g. due to formation of a cluster) and thus, may not be directly applicable to outbreaks in a small population. Second, we did not account for detailed revaccination schedules in Japan due to impossibility of precisely tracking the fraction of unvaccinated susceptible individuals as a function of age. The number of doses may have a profound impact on vaccine efficacy, but unfortunately we did not have access to the dose data for each confirmed case. Third, the proposed model assumes a closed population, i.e., without emigration and immigration. However, obviously the observed data must have involved imported cases. From modeling perspectives, the host migration has little impact on the estimate of vaccine efficacy, while it would influence the estimates of R_t. Given the individual case record for the entire country in the future, one can analyze the dynamics, explicitly accounting for the geographic spread of measles across Japan.

Despite such limitations, we believe that the real-time assessment of epidemic dynamics with (age-specific) estimates of vaccine efficacy based on readily available surveillance dataset would be the huge advantage for epidemiological monitoring of measles in any vaccination population. As was seen in age-dependent vaccine efficacy, the proposed method could inform useful vaccination policy to objectively curb the measles epidemic in real-time. At the very least, we believe that the proposed approach can supplement the existing evaluation methods of vaccine efficacy.

Chapter 4

Chance-adjusted Agreement Statistic for the Assortative Transmission

4.1 Introduction

Assortativity is defined as a preference for a network's node to attach to others that have similar characteristics or in some way different characteristics [95]. Adding the assortativity to a mathematical model often helps us to closely capture and approximate the dynamics in real world, which has been in particular demonstrated in the transmission dynamics of infectious diseases [64, 103]. Provided that an infectious disease (e.g. pandemic influenza A (H1N1-2009)) is frequently transmitted within a group of individuals that share similar characteristics (e.g. school children), the counter measures of the epidemic should ideally focus on those specific groups or their neighbors to effectively curb the epidemic (e.g. school closure) [73, 104].

The assortativity is not only applicable to individual-based datasets, but can also be incorporated into approximate modeling framework when we employ a population-based dynamic model, i.e. even when we use a model with discrete type space, the assortativity can be analytically devised into the model in order to approximately capture the realistic transmission dynamics [64, 111]. For instance, an epidemic model with the so-called "preferential mixing" assumption can be written by a set of ordinary differential equations [70], and the assortativity is eventually quantified as one of model parameters based on an epidemic data [43]. Of course, not only by fitting the mathematical model to the epidemiological data, but also by conducting a field survey of socially defined contact in a population, one can compute and quantify the assortative mixing of the heterogeneous transmission model [24, 90, 131].

Despite these theoretically useful characteristics, there have been only a few statistical measures to quantify the assortativeness. The most straightforward measure of assortativeness may be the correlation between the degrees of linked pairs of nodes [95], but the correlation coefficient only captures the extent of linear association, rather than the

propensity of assortative mixing. Farrington et al. [40] therefore proposed the use of mean-squared deviation from assortativeness as an index of absolute disassortativeness. However, the proposed measure has remained as applicable to assessing assortativeness in a population with continuous type space. Although discrete type space (e.g. mixing within and between age-groups rather than individual network with continuous age) is more relevant to analyzing widely available empirical data in practical setting (e.g. epidemiological surveillance data classified by discrete age groups), the measure of assortativity for the discrete data has yet to be discussed more than the original description by Newman [94].

In this study, we aim to discuss the applicability of two known chance-adjusted agreement statistics, kappa and AC1 to measure the assortativeness of infectious disease transmission. In particular, we aim to show that AC1 statistic can address known paradoxes of kappa, and thus, perhaps allows us to assess the assortativeness of transmission more appropriately than kappa. We first review the existing measures of assortativity in the next section, which is subsequently followed by a description of our motivations and computation of AC1.

4.2 Materials and Methods

4.2.1 Existing Measures of Assortativeness

In the following, we denote the contact rate between host groups i and j by c_{ij}. Let the sum of all the elements of the contact matrix $\{c_{ij}\}$ be C, we denote the normalized contact rate by e_{ij}. The sums over a single row and single column of the normalized contact matrix are respectively denoted by a_i and b_j, namely,

$$a_i = \sum_j e_{ij}, \tag{4.1}$$

$$b_j = \sum_i e_{ij}. \tag{4.2}$$

The assortativity coefficient, r, proposed by Newman [95], is written as:

$$r = \frac{\sum_i e_{ii} - \sum_i a_i b_i}{1 - \sum_i a_i b_i}, \tag{4.3}$$

where the trace of matrix $\{e_{ij}\}$ gives the observed fraction of within-group contacts, while the product of marginal sums is interpreted as the fraction of within-group contacts that occur by chance. The assortativity coefficient r typically takes the value from 0 to 1 with $r = 1$ indicating perfect assortative mixing, while $r = 0$ means random mixing. The measure is based on cross-classification of existing contacts. As the probability of within-group contact is calculated as the product of marginal sums of all columns and rows, it should be noted that the probability of assortative mixing is evaluated as if all observed contacts may result in within-group contact by chance.

Prior to the coefficient r, there was an earlier measure in epidemiology, proposed by Gupta et al. [51]. The earlier measure intended to quantify the impact of mixing patterns of sexual contacts on the spread of HIV epidemic. The Q statistic, a measure of the degree of within-group mixing, was proposed as:

$$Q = \frac{1}{m-1} \sum_i \frac{e_{ii} - a_i b_i}{a_i}, \tag{4.4}$$

where m is the number of node types. The measure captures assortativeness, varying between $-1/(m-1)$ (minimally disassortative) and 1 (maximally assortative). Q is regarded as an ad hoc measure of assortativeness, because the quantity is interpreted as the proportion of contacts that occur along the main diagonal of the contact matrix. However, Q was later shown to be vulnerable to grouping of hosts used to define the diagonal of the contact matrix and to be sensitive to different sub-population sizes between different types of host [51]. Accordingly, we focus on the assortative coefficient r in the following discussion.

An interesting property of r in (4.3) is that the measure is consistent with the classical preferential mixing formulation in an approximate modeling approach. Let p be the proportion of contact that is spent for within-group mixing among the total contacts. The contact rate c_{ij} is then modeled as a simple mixture of an assortative mixing component and a proportionate mixing component:

$$c_{ij} \propto \begin{cases} (1-p)n_i, & \text{if } i \neq j, \\ p + (1-p)n_i, & \text{if } i = j, \end{cases} \tag{4.5}$$

where n_i is the relative population size of host i. In order to calculate assortativity coefficient, we normalize c_{ij} as

$$e_{ij} \propto \begin{cases} \frac{(1-p)n_i}{m}, & \text{if } i \neq j, \\ \frac{p+(1-p)n_i}{m}, & \text{if } i = j, \end{cases} \tag{4.6}$$

in which it is certain that e_{ij} sums up to 1. It is not difficult to find that the parameter p exactly corresponds to r, because we have

$$a_i \propto \frac{p + \sum_j (1-p)n_i}{m} = \frac{p + (1-p)mn_i}{m}, \tag{4.7}$$

where m is again the number of host types, and

$$b_j \propto \frac{p + \sum_i (1-p)n_i}{m} = \frac{1}{m}, \tag{4.8}$$

leading the assortativity coefficient p to be identical to r. This indicates that the interpretation of the assortativity coefficient in relation to its underlying contact mechanism can be as simple as that shown in the mixture model (4.5) in which only the proportionate mixing component is expected to explain between-group contact frequency. To be strict, the mixture model (4.5) is unlikely to hold in practice, and thus, rather than using the Kronecker delta-type assumption in (4.5) the use of distribution to describe the influence of preferential mixing has been proposed elsewhere [46].

4.2.2 Vulnerability of Kappa to Assortative Transmission

When mathematical models are applied to describing infectious disease epidemics, two different types of matrix should be explicitly distinguished. One is the contact matrix $\{c_{ij}\}$ describing the contact rates per unit time within and between groups of host. As described in model (4.5), the mixture type assumption may be employed to parameterize $\{c_{ij}\}$ in the simplest manner. For clarity, hereafter we refer to the assortativeness of $\{c_{ij}\}$ as "contact assortativity".

On the other hand, there is a different matrix $\mathbf{K} = \{k_{ij}\}$, which is more relevant to the transmission dynamics, gives the average number of secondary cases in host i generated by a single primary case of host j throughout its entire course of infectiousness in a fully susceptible population. The matrix is referred to as the next-generation matrix [28], mapping the distribution of secondary cases based on that of primary cases, describing the heterogeneous patterns of transmission in a single generation of transmission event. Each element k_{ij} is dimensionless. Other than the contact frequency, the frequency of infectious disease transmission is regulated by susceptibility of exposed individuals, infectiousness of primary cases and other factors (including biological and non-biological ones), and the next-generation matrix captures these features as well as the contact heterogeneity. Using the above-mentioned mixture type of contact, let α_i and β_j represent age-specific susceptibility and infectiousness of hosts of type i and j respectively, $\{k_{ij}\}$ may be parameterized as

$$k_{ij} \propto \begin{cases} \alpha_i\beta_j(1-p)n_i, & \text{if } i \neq j, \\ \alpha_i\beta_j p + \alpha_i\beta_j(1-p)n_i, & \text{if } i = j, \end{cases} \tag{4.9}$$

as was used in practical applications elsewhere [43, 73, 104]. Hereafter, we refer to the assortativeness of $\{k_{ij}\}$ as "transmission assortativity".

Here, the distinction of two different types of assortativity, i.e. contact and transmission, is made, because the transmission is not only characterized by contact but also by all other intrinsic and extrinsic factors including α_i and β_j in model (4.9). For example, when children are far more susceptible to influenza than adults (which is believed as the case based on empirical evidence [43]), the transmission assortativity would be the result of contact assortativity (with high frequency of child-to-child contacts) weighted by high relative susceptibility among children due to model (4.9). In such an instance, the transmission assortativity requires a particular attention in appropriately quantifying the propensity of within-group contacts that are made by chance.

Here we consider the chance adjusted agreement measure. Although not explicitly mentioned by Newman [95], the assortativity coefficient (4.3) is mathematically identical to the so-called Cohen's kappa statistic [20] which is known as the most commonly used chance-adjusted agreement measure for multiple ratings. In the case of infectious disease transmission, there are only two raters, i.e. contactor and contactee, with discrete grouping of choices such as age-groups. In other words, as long as the matrix captures

the transmission between a pair of individuals (i.e. one susceptible and one infectious host) over a single generation, the agreement statistic can be restricted to the case of two raters. Although Cohen's kappa is more robust measure than simple calculation of observed agreement, it is also known that there are situations in which the kappa yields unexpected results. The phenomenon is referred to as the paradoxes of kappa [19,41], and this is directly relevant to considering the transmission assortativity.

The paradoxes can be illustrated by considering the next-generation matrix adapted from Lam et al. [73] which employed the mixture type assumption for contact and also described the transmission dynamics of pandemic influenza (H1N1-2009) within and between populations of children and adults using model (4.9) (Table 1). We consider three different matrices, **A**, **B** and **C**. As for the baseline matrix **A**, we follow the parameterization of model (4.9), assuming that $n_c = 0.32$, $\alpha_c = 2.06$, $\alpha_a = \beta_c = \beta_a = 1$, and $p = 0.50$ [73] where subscripts c and a stand for children and adults, respectively. The basic reproduction number, the average number of secondary cases generated by a single primary case in a fully susceptible population, is calculated as the dominant eigenvalue of **K**, and in this example set at 1.5. Within-group transmission, which is measured by the observed agreement, is seen in 76.7% of all secondary transmissions, while the chance-adjusted measure, kappa is calculated as 0.517. In Matrix **B**, the frequency of child-to-child transmission

Table 4.1. The age-dependent next generation matrix and the corresponding agreement.

	A[b]		B[b]		C[b]	
	child	adult	child	adult	child	adult
child	1.34	0.32	1.61	0.32	1.34	0.02
adult	0.33	0.83	0.33	0.56	0.64	0.83
obs[a]	0.767		0.767		0.767	
kappa	0.517		0.459		0.540	
AC1	0.548		0.590		0.548	

[a]obs, observed agreement.

[b]Examples of the next-generation matrix. In matrix A, the parameters were fixed at $n_c = 0.32$, $\alpha_c = 2.06$, $\alpha_a = \beta_c = \beta_a = 1$, and $\theta = 0.50$ [73]. The basic reproduction number is given by the dominant eigenvalue and calculated as 1.5. Matrices B and C have identical observed agreement values with A, but matrix B increased the frequency of child-to-child transmission by 1.2 times as that in A and matrix C increased the frequency of adult-to-child transmission by 1.9 times as that in A.

is magnified by 1.2 times as compared to matrix **A**, and the increment of the secondary transmissions among children is reduced from adult-to-adult transmission (so that the total of within-group secondary transmissions is kept as identical to matrix **A**). Other two elements, between-group transmission frequencies are unaltered from matrix **A**. Of course, the observed agreement of matrix **B** remains the same as matrix **A**, because the sum of diagonal elements is unaltered. However, kappa is calculated as 0.459. Namely, by magnifying the within-group transmission in a specific single host type (i.e. children), the chance-adjusted agreement statistic was reduced without any sensible reason. This is referred to as the kappa's paradox I.

In Matrix **C**, the frequency of adult-to-child transmission is magnified by 1.9 times to that of matrix **A**. The sum of anti-diagonal elements is kept identical to matrices **A** and **B**, and the diagonal elements are unaltered from matrix **A**. Again, the observed agreement of matrix **C** is calculated as 76.7%, identical to those from matrices **A** and **B**. However, kappa is calculated as 0.540. By introducing the bias in between-group transmission, the kappa statistic was elevated. This increase in kappa owing to the bias in non-diagonal elements is referred to as the kappa's paradox II.

These paradoxes may be unlikely to matter a lot for contact assortativity, while the introduction of host-specific characteristics such as α_i and β_j in model (4.9) to describing the transmission assortativity can easily lead to observing the paradoxes (see below). In other words, the assortativity coefficient (4.3) (which is mathematically identical to kappa statistic) could be vulnerable as a measure of transmission assortativity, especially when the assortativity of transmission introduces the sources of paradoxes I and II to the contact matrix.

4.3 Results

4.3.1 Comparison between Kappa and AC1

As a paradox-resistant measure of agreement, Gwet has proposed the so-called AC1 statistic in which AC stands for "agreement coefficient" [53]. Let γ be the coefficient of transmission assortativity given by the AC1, and is written as:

$$\gamma = \frac{\sum_i e_{ii} - p_e}{1 - p_e}, \tag{4.10}$$

where p_e is the chance agreement probability. The right-hand side of (4.10 is conceptually the same as Cohen's kappa in which p_e was calculated as a summation of the product of two marginal sums. In the case of AC1 statistic, it is calculated as

$$p_e = \frac{1}{m-1} \sum_{k=1}^{m} \pi_k (1 - \pi_k), \tag{4.11}$$

where π_k is the average of marginal sum over row k and column k, i.e.,

$$\pi_k = \frac{\sum_j k_{kj} + \sum_i k_{ik}}{2 \sum_i \sum_j k_{ij}}. \tag{4.12}$$

The chance agreement for AC1 is calculated as shown in (4.11), because AC1 considers the chance agreement as the product of (i) the probability that two raters agree given that the subject being rated was assigned a nondeterministic score (i.e. the probability of simple chance agreement is $1/m$) and (ii) the propensity that a rater will assign a nondeterministic score, which is estimated by the ratio:$\sum_{k=1}^{m} \pi_k(1 - \pi_k)/(1 - 1/m)$.

Kappa statistic regards the chance agreement probability as if all observed ratings may yield an agreement by chance. However, Gwet pointed out that this may lead to

unpredictable results with agreement data that actually have a rather small propensity for chance agreement [52]. This may be in many instances the case for the transmission of infectious diseases. The AC1 statistic considers the chance agreement as proportional to the portion of ratings and conditional on the random rating. By appropriately accounting for the propensity of chance agreement, AC1 successfully reduces the chance agreement to the right magnitude. Further details, theoretical properties and examples related to the AC1 statistic are given elsewhere [52, 53].

Table 1 shows the estimates of AC1 corresponding to each of the matrices **A**, **B** and **A**. Using the baseline matrix **A**, AC1 is estimated at 0.548. When the within-child transmission is increased (matrix **B**), AC1 is calculated as 0.590. When the bias of between-group transmission is introduced (matrix **C**), AC1 remains to be 0.548. The variation of AC1 was within 10%, and perhaps more importantly, AC1 was not underestimated even when the matrix which induces paradox I is analyzed. As there is no perfect chance-adjusted agreement, AC1 is also not the perfect measure (i.e. not entirely free from conceptual error), but this statistic is regarded as far less vulnerable to known paradoxes of kappa statistic and can be strictly interpreted as the conditional probability that two randomly selected raters agree given that there is no agreement by chance [83]. As long as the measure of assortativity employs the chance-adjusted agreement coefficient, the biggest concern of the transmission assortativity is the possibility to appropriately account for chance agreement, which indicates that AC1 suits to measure the transmission assortativity.

As a numerical comparison between kappa and AC1, Figure 4.1 shows the sensitivities of these measures to the product of relative susceptibility and infectiousness in the formulation (4.9). As α and β among children are elevated, observed and actual within-group transmission would increase among the total of secondary transmissions. kappa is greatly influenced by paradoxes, especially paradox I due to a representation of child-to-child transmission. kappa even decreases with the increase in the product of α and β among children. Nevertheless, the increasing feature of within-group transmission is captured by AC1 in Figure 4.1, avoiding underestimation of chance-adjusted agreement due to paradox I. Similarly, Figure 4.2 examines the sensitivity of chance adjusted agreement coefficients to the proportion of children in the population. As the fraction of child population size increases, the chance agreement increases, and thus, kappa and AC1 decrease. However, as the child-to-child transmission increases with an increase in the fraction of children, the kappa experiences greater decline than AC1 does due to paradox I.

AC1 statistic is regarded as more valid measure than kappa to evaluate the transmission assortativity, and its usefulness in practice may extend to the contact assortativity, especially in the case we observe clusters of contact only among specific types of host (e.g. clustering only among school-age children). However, kappa (or the classical assortativity coefficient) may be preferred for measuring the contact assortativity, because kappa has been known to mechanistically correspond to p, i.e. the proportion of contacts that are spent for within-group mixing, in the simplest form of preferential mixing assumptions

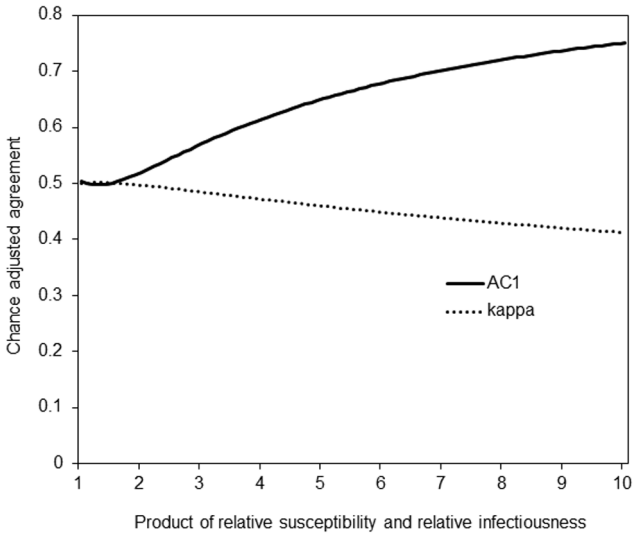

Figure 4.1. Comparison between kappa and AC1 statistics by the product of relative susceptibility and relative infectiousness among children. The chance-adjusted agreements of secondary transmissions, derived from the next-generation matrix, are shown as a function of the product of relative susceptibility and relative infectiousness among children (α_c and β_c). The solid line shows the AC1, whereas the Cohen's kappa is drawn in dashed line. Other parameters for the next-generation matrix were fixed at $n_c = 0.32$, $\alpha_a = 1$, $\beta_a = 1$ and $p = 0.5$ among which p refers to the proportion of contacts that are spent for within-group mixing [73]. It should be noted that the elements of the next-generation matrix are the frequencies of between- and within-group contacts weighted by relative susceptibility and relative infectiousness (and thus, the kappa value is different from 0.50) and here we examine the impact of kappa's paradox I (i.e. domination of child-to-child transmission) on the resulting chance-adjusted agreement coefficients.

(4.5). It is thus important to explore the relationship between p and computation of AC1 in the simplest model (4.5) of the contact assortativity.

In the case of m different types of host, AC1 is written as

$$\gamma = \frac{\sum_i e_{ii} - \frac{1}{m-1}\sum_{k=1}^{m}\pi_k(1-\pi_k)}{1 - \frac{1}{m-1}\sum_{k=1}^{m}\pi_k(1-\pi_k)}, \tag{4.13}$$

where

$$\sum_i e_{ii} \propto mp + (1-p), \tag{4.14}$$

and

$$\pi_k(1-\pi_k) \propto [p + m(1-p)n_k + 1]\left(1 - \frac{p + m(1-p)n_k + 1}{2}\right). \tag{4.15}$$

Although we cannot come up with further insightful analytical findings, one can notice that there are several special cases. If there is only a single type of host ($m = 1$) constituting a population, both γ and p are not practically relevant measures, but they agree

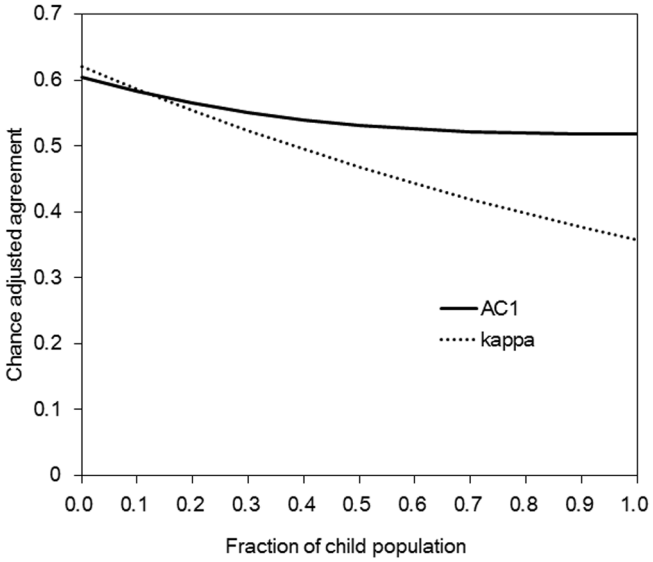

Figure 4.2. Comparison between kappa and AC1 statistics by the proportion of children in a population. The chance-adjusted agreement of secondary transmissions, derived from the next-generation matrix, are shown as a function of the fraction of children in the population (n_c). The solid line shows the AC1, whereas the Cohen's kappa is drawn in dashed line. Other parameters for the next-generation matrix were fixed at $\alpha_c = 1$, $\alpha_a = 1$, $\beta_c = 2.06$, $\beta_a = 1$ and $p = 0.5$ among which p refers to the proportion of contacts that are spent for within-group mixing [73]. It should be noted that the elements of the next-generation matrix are the frequencies of between- and within-group contacts weighted by relative susceptibility and relative infectiousness (and thus, the kappa value is different from 0.50) and here we examine the sensitivity of chance-adjusted agreement coefficients to differing proportion of the population.

to be 1. If all the contacts are spent for within-group mixing ($p = 1$), the corresponding AC1 statistic γ would also be 1.

When each subpopulation is equally distributed so that $n_i = 1/m$ for any i, this would greatly simplify the chance agreement (4.15). The trace of the contact matrix is given by (4.14), and the chance agreement would be zero. Since the sum of all the elements of contact matrix is m, the AC1 is calculated as

$$\gamma = \frac{\sum_i e_{ii}}{m} = p + \frac{1-p}{m}. \tag{4.16}$$

Two important messages from equation (4.16) are that (i) it indicates that γ is greater than p as long as the population is equally distributed. This may be regarded as consistent with the numerical results in Figures 4.1 and 4.2. (ii) When there are so many different types of host (so that $m \to \infty$), the difference between γ and p would be diminished and the two are approximated.

4.4 Discussion

The present study discussed the use of chance-adjusted agreement coefficients to measure the assortativity of contact and transmission of infectious diseases. We have demonstrated that p in the preferential mixing in infectious disease modeling has excellently corresponded to the Newman's assortativity coefficient (or Cohen's kappa). Subsequently, we have explicitly distinguished the transmission assortativity from contact assortativity, because the former captures not only the contact heterogeneity but also many other intrinsic and extrinsic factors characterizing the frequency of within- and between-group transmission. The distinction between the contact and the transmission was made, because kappa statistic is vulnerable to the paradoxes which are likely to be the case to assess the transmission assortativity. In such an instance, AC1 statistic, a relatively new chance-adjusted agreement coefficient, computed in similar way to kappa and not very computationally intensive measure, was shown to be paradox resistant. However, AC1 was shown to be less interpretable than kappa, and does not easily correspond to the mechanistically interpretable mixture model to describe the preferential mixing.

There is no doubt that each of the currently available agreement coefficients involves a variety of technical problems, and none has been regarded as perfect measure. In fact, it is well known that Cohen's kappa does not adjust for both chance agreement and misclassification errors. Although AC1 was shown to be paradox resistant, the statistic is not entirely free from the paradoxes, and moreover, our application has shown that it does not lead to useful mixing assumption in parameterizing the kinetics (i.e. mechanistic features) of transmission due to a difficulty in eliminating the relative population size in the chance agreement (4.15). In the future, it is likely that multiple measures will be required to assess different aspects of the assortative network. In the context of assortativity, the strength may be measured by chance adjusted agreement or correlation, and the propensity of contact (e.g. the distance between two different types of host) should also be measured by absolute disassortativeness [40]. The direction of the contact would also be an important issue in appropriately capturing the transmission dynamics on an explicit network [86]. The relevance of these topological aspects to mathematical formulation of the approximate heterogeneous transmission dynamics has yet to be explored [39, 67].

As quantified in social contact surveys [24, 90, 131], the actual heterogeneous mixing has been shown not to be well captured by classical model such as classical preferential mixing in model (4.5). As seen in an effort to capture the age-dependent heterogeneity using a contact surface [13], the model to be applied to empirically observed data needs to capture more realistic features than the mechanistic mixture model (4.9) does. As seen in an attempt by Glasser et al. [48], more mathematical formulations would be required to express the assortative mixing as a measurable quantity so that we can implement the statistical estimation. However, it is also true that one of the simplest models to be employed and fitted to the early outbreak data with a discrete group structure would be the

one-parameter preferential mixing model [43]. For this reason, we believe that this study has satisfied an essential need to emphasize the importance of measuring transmission assortativity using paradox-resistant change-adjusted agreement measure.

Chapter 5

The Impact of Model Building on the Transmission Dynamics

5.1 Introduction

There are two intriguing characteristics in quantitatively modeling infectious disease data. First, the risk of infection to an individual is dependent on the risks of other individuals in the same population unit. Second, the infection event is seldom directly observable. Among these two, the dependence has been addressed during the process of model building, e.g., a heterogeneous contact structure has been explicitly considered in various types of models [67] and sometimes by examining the conditional risk of infection at a confined setting (e.g. household). On the other hand, it has been common to address the unobservable nature of infection event by employing a convolution equation, i.e. the so-called "backcalculation method", to infer the time of infection based on the dataset of illness onset [13, 49, 106, 109]. However, the deconvolution procedure has been frequently dealt with as a statistical technique that is independent of the transmission model [97], and the process of model building tended to be separated from the unobservable character of infection event.

Ignoring the unobservable nature during model formulation would complicate the model fitting to empirical data. In many instances, a temporal distribution of infected individuals (i.e. an epidemic curve) is analyzed, and most frequently, the best available dataset is the daily counts of cases. The data are usually collected based on observable information only, e.g. counts of cases according to the date of diagnosis of clinically apparent illness. Only in the better case, epidemiologists are granted an access to the daily frequency of illness onset. Nevertheless, the data generating process of the empirical information is rather different from assumed transition mechanism within the so-called SIR (susceptible-infectious-removed) model. The SIR model is considered as inconsistent with the data, because the transition from S to I state is determined by the event of infection (which is unobservable) and the other transition from I to R state is determined by the loss of infectiousness (which is even more difficult to observe) [2]. In light of a need to construct a model that better adheres to the observable information, a previous study proposed a

novel modeling approach that classifies infected individuals into asymptomatic and symptomatic ones while still adopting a common multistate model structure [62]. In the case of the unobservable SEIR (susceptible-exposed-infectious-removed) model, the model handles unobservable information within the multistate structure, classifying infected individuals into pre-infectious (exposed) and infectious individuals [2, 62] that are not directly distinguishable from each other in empirical observation.

Although a previous study recognized the importance of asymptomatic transmission in considering the feasibility of non-pharmaceutical public health interventions (e.g. contact tracing and case isolation) [44], the impact of correctly and precisely capturing the natural course of "illness" on the effectiveness of interventions (e.g. vaccination) has yet to be discussed. In the past, the contribution of asymptomatic individuals to the transmission dynamics tended to be modeled by employing the widely adopted SEIR model while splitting infectious individuals (I-class) into symptomatic and asymptomatic cases (e.g. [79]). The underlying assumptions and any potential drawbacks for employing the SEIR model on this matter have not been clarified, and thus, we would like to examine if an epidemic threshold (which yields the critical vaccination coverage) is greatly influenced by the abovementioned difference in model building approaches.

Employing a mathematical modeling approach, the present study aims to assess the impact of model building strategy on the transmission dynamics of an infectious disease under vaccination practice. In particular, we investigate differential values of epidemic threshold between models that rest on observable and unobservable information.

5.2 Materials and Methods

5.2.1 Two Models

We consider two different types of mathematical models, one based on observable variables including symptom onset and recovery from clinical illness (hereafter referred to as the "observable model") and the other based on unobservable information including infection event and infectiousness (the "unobservable model"). Whereas the unobservable model in the following is a variant of the SEIR model [79], the observable model considers the transition of infected individuals based on illness onset and the disappearance of symptoms that are directly visible in the field data [2] (Figure 5.1A and 5.1B). The word "observable" is intended to reflect the presence of observable symptoms (i.e. not including those observed or detected by employing laboratory testing during the asymptomatic period). Thus, the observable model might also be referred to the "symptom-based" model. Similarly, the unobservable model may be referred to as the "contagiousness-dependent" model. Here we briefly describe the time-dependent growth of an epidemic based on the observable model, the compartments of which are drawn in Figure 5.1A. Let $J_S(t, \tau)$ and $J_S(t, \sigma)$ be

the numbers of asymptomatic and symptomatic cases at calendar time t, infection-age τ since infection and disease-age σ since illness onset. The growth of cases is described by:

$$\begin{aligned}\left(\frac{\partial}{\partial t}+\frac{\partial}{\partial \tau}\right) J_A(t,\tau) &= -\left(\eta(\tau)+\gamma_A(\tau)\right) J_A(t,\tau),\\ \left(\frac{\partial}{\partial t}+\frac{\partial}{\partial \sigma}\right) J_S(t,\tau) &= -\gamma_S(\sigma) J_S(t,\sigma),\end{aligned} \tag{5.1}$$

where $\eta(\tau)$ is the rate at which asymptomatic cases develop symptoms, and $\gamma_A(\tau)$ and $\gamma_S(\sigma)$ are the rates at which asymptomatic and symptomatic cases are fully recovered. We consider an initial growth phase of an epidemic at which the depletion of susceptible individuals S_0 is negligible. Let $\lambda(t)$ be the force of infection, or the rate at which susceptible individuals are infected. Two boundary conditions, i.e., the new infection and new illness onset, are written as

$$\begin{aligned}J_A(t,0) &= \lambda(t) S_0,\\ J_S(t,0) &= \textstyle\int_0^\infty \eta(\tau) J_A(t,\tau) d\tau,\end{aligned} \tag{5.2}$$

where $\lambda(t)$ is, by adopting a mass action principle, parameterized as:

$$\lambda(t) = \int_0^\infty \beta_A(\tau) J_A(t,\tau) d\tau + \int_0^\infty \beta_S(\sigma) J_S(t,\sigma) d\sigma, \tag{5.3}$$

where $\beta_A(\tau)$ and $\beta_S(\sigma)$ are the infection-age and disease-age dependent rates of secondary transmission, respectively. It should be noted that the recovered individuals in Figure 5.1A are assumed as no longer infectious. An advantage of this modeling approach is that a reasonable computation of epidemiological measurements (e.g. the reproduction number, the generation time and the serial interval) can be achieved, adhering to observed available information [62]. Moreover, transitions from the asymptomatic state to the symptomatic or recovered state are in line with the actual clinical course of infection, i.e., only a part of asymptomatic individuals develop symptoms and the rest of infected individuals recover from infection without symptoms. The basic reproduction number of this model is computed as follows [62]:

$$R_0 = R_1 + \alpha R_2, \tag{5.4}$$

where R_1, R_2 and α are the average number of secondary cases generated by a single asymptomatic case (only during the asymptomatic period), the average number of secondary cases generated by a single symptomatic case throughout the course of the symptomatic period, and the conditional probability of developing symptom given infection, respectively. The probability of symptomatic illness, α is multiplied to R_2 only, because all infected individuals experience asymptomatic class while only the fraction α of infected individuals result in symptomatic infection. The model (1) is a stage-structured model in which the reproduction number is calculated from the integral kernel of the specific class of host in its renewal equation [69]. R_1, R_2 and α are defined as

$$\begin{aligned} R_1 &= S_0 \int_0^\infty \beta_A(\tau) \exp\left(-\int_0^\tau (\eta(a) + \gamma_A(a))da\right) d\tau, \\ R_2 &= S_0 \int_0^\infty \beta_S(\sigma) \exp\left(-\int_0^\sigma \gamma_S(a)da\right) d\sigma, \\ \alpha &= \int_0^\infty \eta(x) \exp\left(-\int_0^x (\eta(s) + \gamma_A(s))ds\right) dx, \end{aligned} \tag{5.5}$$

which we will use in later discussion.

The other type of a model, i.e., the unobservable model, can be said to be the infection-age structured SEIR model that further classifies infectious individuals into symptomatic and asymptomatic cases [79] (Figure 5.1B). Let $E(t,\tau)$, $I_A(t,\tau,\sigma)$ and $I_S(t,\tau,\sigma)$ be the numbers of pre-infectious individuals, asymptomatic infectious individuals and symptomatic infectious individuals, respectively, at calendar time t, infection-age τ and disease-age σ. The dynamics is described by

$$\begin{aligned} \left(\tfrac{\partial}{\partial t} + \tfrac{\partial}{\partial \tau}\right) E(t,\tau) &= -\epsilon(\tau)E(t,\tau), \\ \left(\tfrac{\partial}{\partial t} + \tfrac{\partial}{\partial \tau}\right) I_S(t,\tau) &= -k\epsilon(\tau)E(t,\tau) - \kappa_S(\tau)I_S(t,\tau), \\ \left(\tfrac{\partial}{\partial t} + \tfrac{\partial}{\partial \tau}\right) I_A(t,\tau) &= (1-k)\epsilon(\tau)E(t,\tau) - \kappa_A(\tau)I_A(t,\tau), \end{aligned} \tag{5.6}$$

where $\epsilon(\tau)$, $\kappa_A(\tau)$ and $\kappa_S(\tau)$ represent the rate of acquiring infectiousness, and the recovery rates among asymptomatic and symptomatic infectious individuals, respectively. k is the weight ($0 \leq k \leq 1$) of the rate at which exposed individuals acquire infectiousness that determines the probability of developing symptom. A boundary condition for new infections is

$$E(t,0) = \lambda(t)S_0, \tag{5.7}$$

where the force of infection is

$$\lambda(t) = \int_0^\infty \beta(y)\left(mI_A(t,y) + I_S(t,y)\right) dy, \tag{5.8}$$

where $\beta(\tau)$ represents the rate of secondary transmission at infection-age τ, and m represents the relative infectiousness of asymptomatic cases as compared to symptomatic cases. The basic reproduction number, R_0, for this unobservable model is given by

$$R_0 = kR_3 + (1-k)R_4, \tag{5.9}$$

where R_3 and R_4 are the average numbers of secondary cases generated by a single asymptomatic case and a single symptomatic case throughout the course of infectiousness, respectively. In equation (5.9), k and $(1-k)$ are multiplied to R_3 and R_4, respectively, because the probabilities of an infected individual to experience symptomatic and asymptomatic infections are given by k and $(1-k)$, respectively. Again, the reproduction numbers, R_3 and R_4, are calculated from the integral kernel of the renewal process, i.e., we define

$$
\begin{aligned}
R_3 &= S_0 \int_0^\infty \beta(\tau) \int_0^\tau \epsilon(x) \exp\left(-\int_0^x \epsilon(y)dy - \int_x^\tau \kappa_S(y)dy\right) dxd\tau, \\
R_4 &= mS_0 \int_0^\infty \beta(\tau) \int_0^\tau \epsilon(x) \exp\left(-\int_0^x \epsilon(y)dy - \int_x^\tau \kappa_A(y)dy\right) dxd\tau.
\end{aligned} \tag{5.10}
$$

Using these two models under a homogeneously mixing assumption, we investigate the importance of appropriately capturing the observable natural course of infection in epidemiological models.

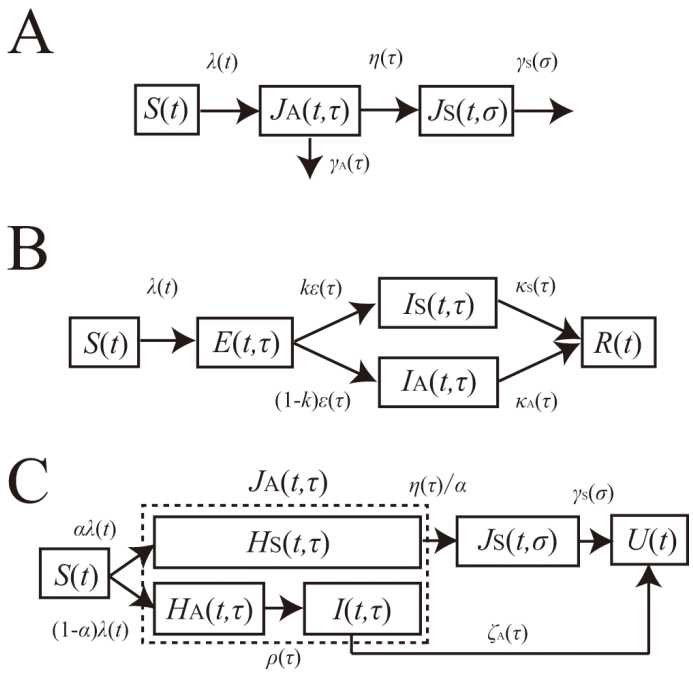

Figure 5.1. Compartments of observable and unobservable models. A. The compartment of an observable model. The model describes the transitions depending on illness onset and recovery from clinical symptoms. Once infected, all infected individuals experience asymptomatic period, J_A, some of which fully recover from infection without symptoms, and the remaining develop symptoms, J_S. B. The compartment of an unobservable model. The model describes the transitions depending on acquirement or disappearance of infectiousness. Upon infection, infected individuals experience the latent period (i.e. Exposed compartment (E)) after which each acquires infectiousness and is classified as either symptomatic (I_S) or asymptomatic (I_A) one. C. The compartment of the special case of the observable model. The model describes the transitions based on symptoms, but partially accounts for infectiousness too. To let it be similar to model B, we decomposed asymptomatic individuals, J_A of the observable model (panel A) into pre-symptomatic individuals, H_S and fully asymptomatic individuals with or without infectivity. U represents recovered individuals.

5.2.2 Analytical and Numerical Analyses

To explicitly account for the observable clinical course of infection, underlying assumptions of using a parameter k in the unobservable model as the probability of symptomatic

infection remain unclear (Figure 5.1B and system (5.6); because the transition from E to I state does not have anything to do with illness onset). Moreover, it is fruitful to identify different model assumptions between two models and their practical relevance to infectious disease control. Thus, here we take two different approaches to identify the structural differences and different assumptions between two models. First, we impose additional assumptions to the observable model, thereby permitting it to resemble the SEIR-like unobservable model. A simplistic analytical computation is performed to mathematically determine the difference between the two models. Second, we numerically compute the basic reproduction numbers based on the two models. It is clear, even intuitively, that the presence of pre-symptomatic transmission is a major difference between the observable model and the unobservable SEIR type model. Thus, we examine the sensitivity of the basic reproduction number to the proportion of pre-symptomatic secondary transmissions among the total of asymptomatic transmissions.

Subsequently, we investigate the differential impact of vaccination on the reproduction number (or, on the epidemic threshold) of the two models. In a published study, the next-generation matrix was employed to incorporate various different biological actions of vaccination into the transmission dynamics under vaccination [7]. However, the derivation of the next-generation matrix in the published study remained heuristic, and moreover, the computation rested only on the unobservable SEIR-like model. Thus, here we derive the next-generation matrix based on the linearized system of both (5.1) and (5.6), measuring the impact of differential model formulation on the reproduction number. When analytically computing the matrix, various different effects of vaccination are considered, including not only the reductions in susceptibility and infectiousness but also the reduction in the risk of symptomatic illness [55].

5.2.3 Parameter Values

For numerical illustration, we examine the plausible parameter space for four different viral infectious diseases. Table 5.1 shows the parameter values that are adopted to numerically calculate the threshold quantities and other associated variables of observable and unobservable models [6, 7, 11, 33, 43, 44, 62, 74, 77, 79, 80, 93, 99, 121, 126]. Smallpox is considered for the exposition of the similarity between two different models, because it involves very few asymptomatic transmissions [33, 87, 105]. HIV/AIDS is the opposite example of smallpox with respect to the proportion of asymptomatic transmissions among the total of secondary transmissions. Namely, the secondary transmission mostly occurs before the onset of AIDS [62]. Influenza and varicella are considered as examples that lie between smallpox and HIV/AIDS. In particular, influenza is considered, because (i) the unobservable model with asymptomatic and symptomatic infectious individuals was initially employed with an application to influenza [79] and (ii) a variety of vaccine effects have been quantified based on challenge and community-based studies [7], which offers a suitable condition to explore the impact of model formulation on the transmission

Description	Notation	Parameter values				References/
		Smallpox	Influenza	HIV	Varicella	Assumptions
The average number of secondary cases produced by an asymptomatic case	R_1	0.69	0.60	3.67	3.24	[33] & calculated
The average number of secondary cases produced by a symptomatic infection	R_2	6.18	1.20	0.00	3.24	[33] & calculated
The average number of secondary cases produced by a fully asymptomatic case	R_a	1.37	0.96	6.12	6.47	[33] & calculated
Probability of developing symptoms in the unobservable model	α (or k)	1.00	0.75	0.80	1.00	[79] & assumed
Basic reproduction number of the observable model	R_0	6.87	1.50	3.67	6.47	[6, 33, 43, 77, 99]
Proportion of asymptomatic transmissions among all secondary transmissions	θ	0.10	0.40	1.00	0.50	[11, 44, 62, 80]
Proportion of pre-symptomatic transmissions among all asymptomatic infection	g	1.00	0.60	0.67	1.00	[74] & calculated
Vaccine efficacy of reducing infectiousness	VE_I	0.80	0.15	0.60	0.80	[6, 7, 11, 80, 93, 121, 126]
Vaccine efficacy of reducing susceptibility	VE_S	0.95	0.41	0.40	0.50	[6, 7, 11, 80, 93, 121, 126]
Vaccine efficacy of preventing progression to symptomatic illness	VE_P	0.87	0.67	0.60	0.50	[6, 7, 11, 80, 93, 121, 126] & assumed

Table 5.1. Parameter values for observable and unobservable models of directly transmitted infectious diseases.

dynamics in the presence of vaccination. It should be noted that successful vaccine of HIV has yet to be offered [108] and the corresponding vaccine effect parameters were only hypothetically assumed.

5.3 Results

5.3.1 Using Observable Model to Mimic Unobservable Model

To analytically describe the difference between two modeling approaches, we consider the unobservable model as a special case of the abovementioned observable model. Figure 5.1C shows the compartments of a variant of the observable model that are intended to mimic the SEIR structure. To do this, we divide the asymptomatic infected individuals $J_A(t,\tau)$ in Figure 5.1A into three sub-populations, i.e., (i) pre-symptomatic individuals who are supposed to develop symptom after spending the incubation period, $H_S(t,\tau)$, (ii) asymptomatic non-infectious individuals who will not become symptomatic throughout the course of infection, $H_A(t,\tau)$, and (iii) asymptomatic infectious individuals, $I(t,\tau)$. The fate of experiencing symptomatic infection is determined upon infection with a probability α, similarly to that taking place when acquiring infectiousness in the SEIR model (Figure 5.1B). In the following, those who remain asymptomatic throughout the course of infection (i.e. $H_A + I$) is referred to as "fully" asymptomatic, while those who eventually develop symptoms, H_S is referred to as "pre-symptomatic" for clarity. Recovered individuals at calendar time t is denoted by $U(t)$. The transition rates from H_S to J_S, H_A to I, J_S to U, and I to U are $\frac{\eta(\tau)}{\alpha}$, $\rho(\tau)$, $\gamma_S(\sigma)$, and $\zeta_A(\tau)$, respectively, where τ and σ again represent the infection-age and the disease-age, respectively. For consistency between the observable and unobservable models, the transition from H_S to J_S is artificially scaled by α, because J_S in the observable model welcomes only the fraction α of infected individuals to symptomatic class, which occurs not only during the transition from H_S to J_S but also when infected individuals enter to H_S. The time-dependent growth of infected individuals is described by

$$\begin{aligned}
&\left(\tfrac{\partial}{\partial t} + \tfrac{\partial}{\partial \tau}\right) H_S(t,\tau) = -\tfrac{\eta(\tau)}{\alpha} H_S(t,\tau),\\
&\left(\tfrac{\partial}{\partial t} + \tfrac{\partial}{\partial \tau}\right) H_A(t,\tau) = -\rho(\tau) H_A(t,\tau),\\
&\left(\tfrac{\partial}{\partial t} + \tfrac{\partial}{\partial \tau}\right) J_S(t,\tau) = -\gamma_S(\sigma) J_S(t,\sigma),\\
&\left(\tfrac{\partial}{\partial t} + \tfrac{\partial}{\partial \tau}\right) I(t,\tau) = \rho(\tau) H_A(t,\tau) - \zeta_A(\tau) I(t,\tau),
\end{aligned} \tag{5.11}$$

with the following boundary conditions:

$$\begin{aligned}
&H_S(t,0) = \alpha\lambda(t) S_0,\\
&H_A(t,0) = (1-\alpha)\lambda(t) S_0,\\
&J_S(t,0) = \tfrac{1}{\alpha}\textstyle\int_0^t \eta(\tau) H_S(t,\tau) d\tau,
\end{aligned} \tag{5.12}$$

where the force of infection, $\lambda(t)$, is parameterized as

$$\lambda(t) = m\int_o^\infty \beta_S(\tau)I(t,\tau)d\tau + \int_0^\infty \beta_H(\tau)H_S(t,\tau)d\tau + \int_0^\infty \beta_S(\sigma)J_S(t,\sigma)d\sigma, \qquad (5.13)$$

where m is the relative infectiousness among those who remain asymptomatic, β_H and β_S are the rates of transmission caused by pre-symptomatic and symptomatic individuals, respectively. It should be noted that m is multiplied to only the first integral term, because m is defined as the infectiousness of "fully" asymptomatic individuals relative to that among those who experience symptomatic state in the observable model (Figure 5.1B), as was defined elsewhere [79]. This scaling was required to let the model in Figure 5.1A mimic the model in Figure 5.1B. It is evident from Figure 5.1C that for the unobservable model (Figure 5.1B) to agree with the observable one (Figure 5.1C), the incubation period and the latent period must be identical. Moreover, the recovery from an infectious state should also be identical to the recovery from symptomatic illness. Two models become consistent from each other if the following conditions are met:

(a) $\alpha = k$ (i.e. assumed probabilities of symptomatic infection in two models are identical),

(b) $\epsilon(\tau) = \eta(\tau)/\alpha = \rho(\tau)$ (i.e. the incubation period is identical to the latent period; or equivalently, $\beta_H(\tau) = 0$ for any τ),

(c) $\kappa_S(\tau) = \gamma_S(\sigma)$ and $\kappa_A(\tau) = \zeta_A(\sigma)$ (i.e., the recovery rates of both models are an identical constant).

Writing in the way we computed the observable model in (5.4), the basic reproduction number is computed as

$$R_0 = R_1^{'} + \alpha R_2^{'}, \qquad (5.14)$$

where

$$\begin{aligned} R_1^{'} &= (1-\alpha)mS_0\int_0^\infty \beta_S(\tau)\int_0^\tau \rho(x)\exp\left(-\int_0^x \rho(y)dy - \int_x^\tau \zeta_A(y)dy\right)dxd\tau \\ &\quad +\alpha S_0\int_o^\infty \beta_H(\tau)\exp\left(-\int_o^\tau \frac{\eta(x)}{\alpha}\right)d\tau, \\ R_2^{'} &= \frac{S_0}{\alpha}\int_0^\infty \beta_S(\sigma)\int_0^\sigma \eta(y)\exp\left(-\int_0^y \frac{\eta(x)}{\alpha}dx - \int_y^\sigma \gamma_S(z-y)dz\right)dyd\sigma. \end{aligned} \qquad (5.15)$$

In summary, two models are rather different and can be consistent only in the case that the model could be written by ordinary differential equations and only when the incubation period can be equated to the latent period.

5.3.2 Comparison of the Basic Reproduction Number

We continue to compare the special case of the observable model (Figure 5.1C) with the unobservable SEIR type model (Figure 5.1B). As was implicated from abovementioned conditions (a)-(c) to ensure consistency between the two models, it should be noted that there is no concept of pre-symptomatic transmission in the unobservable model. On the contrary, the special case (Figure 5.1C) can still account for pre-symptomatic transmission as long as we assume that $\beta_H(\tau) > 0$. Let g represent the proportion of pre-symptomatic transmissions among the total of asymptomatic transmissions, then the basic reproduction number of the special case model (5.14) is rewritten as follows:

$$R_0 = (1-\alpha)R_a + \alpha(R_{pre} + R_2^{'}). \tag{5.16}$$

The average number of secondary cases generated by a single fully asymptomatic case should be identical between (5.16) and (5.17), i.e.,

$$gR_1^{'} = \alpha R_{pre}. \tag{5.17}$$

Figure 5.2 examines the impact of g on the resulting estimate of the basic reproduction number, varying only g (and the corresponding α) in the model and using fixed values for all other parameters in equations (5.16) and (5.17) (see Table 5.1). Note that g=0 is the special case in which the observable model (Figure 5.1C) is fully consistent with the unobservable model. As g increases, R_0 for smallpox and influenza are elevated. However, R_0 for HIV and varicella are lowered as a function of g. Assuming that R_{pre} is proportional to R_a, the differential sensitivity is understood by considering the weighted average in (5.16) and (5.17). That is, we have

$$g = \frac{\alpha R_{pre}}{\alpha R_{pre} + (1-\alpha)R_a}, \tag{5.18}$$

or $\alpha = gR_a/(1-g)R_{pre} + gR_a$, indicating that the larger g, the larger α has to be. Consequently, if the number of fully asymptomatic transmissions is smaller than other transmissions (in the case of influenza and smallpox), R_0 is an increasing function of g. However, when there are substantial pre-symptomatic transmissions (e.g. HIV/AIDS), the relationship between R_0 and g is reversed.

5.3.3 Model Building and Vaccination

In the following, a comparison of the reproduction numbers under vaccination is made between the observable model (Figure 5.1A) and the unobservable model (Figure 5.1B). Because a randomly mixing population is divided into vaccinated and unvaccinated ones, we introduce the next-generation matrix. Let p, $1-q_S$, $1-q_I$, and $1-q_D$ be the vaccination coverage, vaccine efficacy in reducing susceptibility, infectiousness, and efficacy of preventing symptomatic illness, respectively. As heuristically derived elsewhere [7,55], the

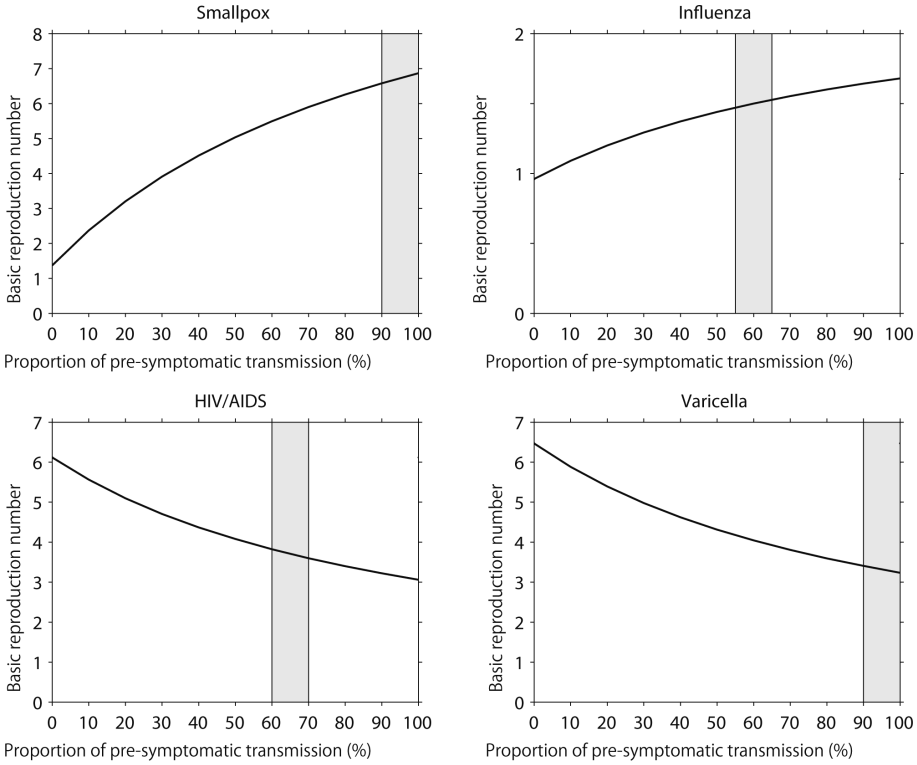

Figure 5.2. The basic reproduction number and the pre-symptomatic transmission. The impact of varying the proportion of pre-symptomatic transmissions among all asymptomatic transmissions (the horizontal axis; denoted by g in the main text) on the basic reproduction number, R_0. Only the value of g (and the corresponding α) in the model is varied. All other parameters are fixed (see Table 5.1). Shaded area represents the plausible parameter region of the proportion of pre-symptomatic transmissions among the total asymptomatic transmissions, g, for a specific disease.

next-generation matrix that describes secondary transmission between and among vaccinated and unvaccinated cases is employed. Let $\psi(\tau)$ be the so-called reproduction kernel of the renewal process of the observable model that describes the class-age dependent rate of secondary transmission per single infected individual [28], i.e.,

$$\psi(\tau) = S_0 \begin{pmatrix} (1-p)\left(\beta_A(\tau)L_1(\tau) + \beta_S(\tau)L_2(\tau)L_3(\tau)\right) & q_I(1-p)\left(\beta_A(\tau)L_1(\tau) + q_D\beta_S(\tau)L_2(\tau)L_3(\tau)\right) \\ q_S p\left(\beta_A(\tau)L_1(\tau) + \beta_S(\tau)L_2(\tau)L_3(\tau)\right) & q_S q_I p\left(\beta_A(\tau)L_1(\tau) + q_D\beta_S(\tau)L_2(\tau)L_3(\tau)\right) \end{pmatrix} \tag{5.19}$$

where the first row represents the exposure to unvaccinated susceptible individuals. It should be noted that q_D appears inside parenthesis in the second column (i.e. secondary transmissions caused by vaccinated cases). The survival rates $L_1(\tau)$, $L_2(\tau)$ and $L_3(\tau)$ in (21) are written as

$$\begin{aligned} L_1(\tau) &= \exp\left(-\int_0^\tau (\eta(a) + \gamma_A(a)da)\right), \\ L_2(\tau) &= \exp\left(-\int_0^\tau (\gamma_S(a)da)\right), \\ L_3(\tau) &= \eta(\tau)\exp\left(-\int_0^\tau (\eta(a) + \gamma_A(a)da)\right). \end{aligned} \tag{5.20}$$

The next-generation matrix of the observable model under vaccination is given by the integral of $\psi(\tau)$, i.e.,

$$\mathbf{K_1} = \int_0^\infty \psi(\tau)d\tau = \begin{pmatrix} (1-p)\left(R_1 + \alpha R_2\right) & q_I(1-p)\left(R_1 + \alpha q_D R_2\right) \\ q_S p\left(R_1 + \alpha R_2\right) & q_S q_I p\left(R_1 + \alpha q_D R_2\right) \end{pmatrix}. \tag{5.21}$$

Let $F(\sigma)$ and $L(\sigma)$ be matrices that describe the class-age dependent rate of the appearance of new infections and the proportion of those who remain infectious, respectively, i.e.,

$$F(\sigma) = S_0 \begin{pmatrix} (1-p)\left[k\beta(\sigma) + (1-k)m\beta(\sigma)\right] & q_I(1-p)\left[kq_D\beta(\sigma) + (1-kq_D)m\beta(\sigma)\right] \\ q_S p\left[k\beta(\sigma) + (1-k)m\beta(\sigma)\right] & q_S q_I p\left[kq_D\beta(\sigma) + (1-kq_D)m\beta(\sigma)\right] \end{pmatrix}, \tag{5.22}$$

$$L(\sigma) = \begin{pmatrix} \int_0^\sigma \epsilon(x)\exp\left(-\int_0^x \epsilon(y)dy - \int_x^\sigma \kappa_S(y)dy\right)dx & 0 \\ 0 & \int_0^\sigma \epsilon(x)\exp\left(-\int_0^x \epsilon(y)dy - \int_x^\sigma \kappa_A(y)dy\right)dx \end{pmatrix}. \tag{5.23}$$

The next-generation matrix of the unobservable model is obtained from [28]:

$$\begin{aligned} \mathbf{K_2} &= \int_0^\infty \psi(\tau)d\tau, \\ &= \int_0^\infty F(\sigma)L(\sigma)d\sigma, \\ &= R_3 \begin{pmatrix} (1-p)\left[k + w(1-k)\right] & q_I(1-p)\left[kq_D + w(1-kq_D)\right] \\ q_S p\left[k + w(1-k)\right] & q_S q_I p\left[kq_D + w(1-kq_D)\right] \end{pmatrix}, \end{aligned} \tag{5.24}$$

where w is the ratio of R_4 to R_3 and is identical to m if $\kappa_A = \kappa_B$. Note that q_D only changes the weight of R_3 (or R_4) inside the bracket of all elements. The effective reproduction number is the dominant eigenvalue of these matrices, i.e.,

$$\begin{aligned} R_{v,obs} &= (1-p)\left(R_1 + \alpha R_2\right)) + q_s q_I p\left(R_1 + \alpha q_D R_2\right), \\ R_{v,non} &= (1-p)R_3\left[k + w(1-k)\right] + q_S q_I p R_3\left[kq_D + w(1-kq_D)\right], \end{aligned} \tag{5.25}$$

where $R_{v,obs}$ and $R_{v,non}$ correspond to the reproduction numbers of the observable and unobservable models, respectively. It should be noted that only $R_{v,obs}$ is consistent with the data generating process of q_D, while this is not the case for $R_{v,non}$, because q_D in

the equation of $R_{v,non}$ is assumed to have had an impact on the transition rate from pre-infectious to infectious period (in addition to the impact on the probability of symptom development alone; Figure 5.1B).

To understand the extent of the different impact of q_D on the reproduction number between two models, Figure 5.3 compares the values of $R_{v,obs}$ and $R_{v,non}$ for selected four diseases as a function of vaccine-induced reduction in symptomatic illness, q_D. By varying q_D, different patterns of variation in the reproduction number are seen. For the examined three diseases, i.e., smallpox, influenza and varicella, $R_{v,non}$ was greater than $R_{v,obs}$. The relationship was reversed for HIV, and in particular, $R_{v,obs}$ of HIV was independent of q_D due to the assumed absence of secondary transmission following the onset of AIDS. Although the difference is subtle for smallpox and varicella, the critical level of influenza is clearly different between two models for influenza. Moreover, it should be noted that the critical coverage is an inverse function of the reproduction number, and a slightly greater reproduction number based on the unobservable model could incorrectly indicate us to vaccinate as many as additional 5-10% of the population as compared to the coverage calculated from the observable model. The difference in the critical coverage was most apparent for HIV/AIDS.

5.4 Discussion

The present study analyzed and compared observable and unobservable modeling approaches. Two major tasks have been completed. First, by rewriting the observable model as if it were an SEIR-type unobservable model, we aimed to clarify underlying assumptions of the unobservable model that involves asymptomatic transmission. For the two models to be identical, we have demonstrated that it is essential that the incubation period has to be identical to the latent period and also that no pre-symptomatic transmission occurs in both models. Only the observable model can directly incorporate vaccine-induced reduction in symptomatic illness (in the manner that the corresponding vaccine effect data is generated), and the probability of symptomatic infection in the unobservable model was shown to be multiplied to the transition rate from pre-infectious to infectious state without phenomenological justification. Second, we numerically solved both models and examined the sensitivity of R_0 to the frequency of pre-symptomatic transmission. We identified that the ignorance of pre-symptomatic transmission in the unobservable model can lead to an overestimate of R_0. Moreover, we have shown that the critical coverage of vaccination can be different between two models, because the vaccine efficacy of preventing symptomatic illness would influence the threshold in different mathematical manners.

The present study emphasizes that an appropriate model formulation would be essential to answer the corresponding scientific or public health question. As we have shown, an explicit formulation would also help clarify underlying assumptions that tend to be hidden

in common model structures. Considering a practical example of vaccination that influences the symptom onset, we have shown that the modeling approach to tackle this issue requires a model building approach that can explicitly account for the natural course of infection including asymptomatic and symptomatic states. Since the use of SEIR structure with two or more types of I-classes with different levels of symptom or clinical severity has also partially accounted for this matter of differential severity of symptom, and because the unobservable modeling approach to this issue has been proposed relatively early [79], the similar model structure has become widely adopted in a variety of settings in studying influenza and other directly transmitted infectious diseases [3–5, 34, 37, 59, 82]. However, we have shown that the unobservable model has to inherently adopt an assumption that there is no pre-symptomatic transmission, and in this model, vaccine-induced reduction in symptomatic illness has to influence the transition from pre-infectious to infectious state [7]. To explicitly and appropriately incorporate the vaccine effect in reducing the risk of a symptomatic disease into the model, it is fruitful to employ a model that directly accounts for disease progression.

Although our discussion might read as if we regard the observable model as always better than the unobservable one, this preference cannot always be true. In fact, the observable model is not perfect, largely missing the information of infectiousness in the model structure. However, if we handle the model fitting to the incidence of illness onset, the observable model must be most useful, because the renewal equation of only symptomatic cases can be computed and directly fitted to the data [62]. If our study objective was not to quantitatively measure model parameters based on observable empirical data (e.g. model fitting to real data), the unobservable model may be more useful in many other objectives (e.g. in considering the loss of infectiousness during the isolation period). Rather than emphasizing that we should regard the observable model as a default, we would like to emphasize that writing this particular issue from multiple angles would be useful for mathematical modeling studies; the present study was a single study that focused on symptom-based modeling approach in contrast to a classical one. Moreover, it should be noted that "theoretically" the best model in this context would be the one that accounts for both observable and unobservable information within a single model. Such a model can easily address the dependence structure between clinical illness and infectiousness [72], and indeed, the potential dependence and difference between the incubation period and the latent period are known as critical factors in determining the effectiveness of public health interventions including contact tracing and case isolation [14, 44, 71, 88]. As demonstrated by animal experiments for foot and mouth disease [14], an appropriate combination of well-designed experiments (or observations) and statistical inference could shed light on the scientific approach to (i) considering both illness and infectiousness and (ii) identifying ideal modeling strategy in the future [110].

Four limitations should be noted and described briefly. First, we conducted only univariate sensitivity analysis, ignoring any possible dependence between the frequency

of pre-symptomatic transmissions among the total asymptomatic transmissions and other epidemiological variables. Ignoring such dependence structure could sometimes lead to overestimating the effectiveness of public health interventions [35]. Second, we focused on the basic reproduction number, and did not extend epidemiological insights into other important quantities (e.g. growth rate of infections) [35,103]. Third, to keep the matter as simple as possible, our arguments rested on homogeneously mixing assumptions. Fourth, whereas our model rested on fixed compartment structures (Figure 5.1), the structure of model ultimately depends on specific diseases and study objectives [112].

Considering that we were successful in gaining useful epidemiological insights into future quantitative modeling by formulating the vaccination issue using an observable model, it is suggested that more studies based on observable epidemiological variables are conducted. Future studies can also tackle the issue of abovementioned dependence between clinical illness and infectiousness based on an explicit model with both pieces of information as variables and analyzing individual datasets with multiple dimensions.

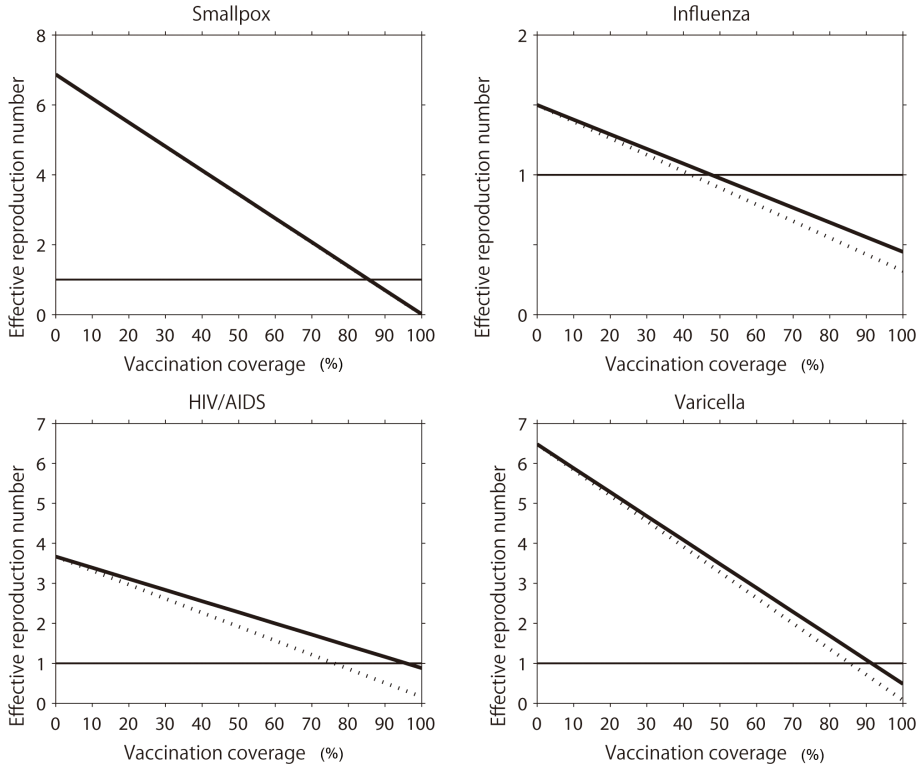

Figure 5.3. The effective reproduction number under vaccination practice. Effective reproduction numbers for the observable model and the unobservable model are compared as a function of vaccine-induced reduction in symptomatic illness. To permit comparison, in the absence of vaccination practice, the epidemic threshold values of the two models were assumed as identical. Vaccination coverage is fixed at 50%. The solid line shows the reproduction number of the unobservable model under vaccination. The dashed line shows the reproduction number of the observable model under vaccination. Except the vaccine-induced reduction in symptomatic illness, all parameters were fixed (see Table 5.1). For the unobservable model, relative infectiousness of asymptomatic individuals (compared to symptomatic individuals), m (or w), was arbitrarily fixed at 0.5 for three diseases other than varicella to which we assigned 0.7 (these particular values were arbitrarily chosen to visually demonstrate the difference between two models).

Chapter 6

Modeling the Obesity Epidemic

6.1 Introduction

6.1.1 Background

Obesity has become more and more widespread, increasingly recognized as one of the biggest global health problems. According to the estimate of the World Health Organization (WHO), the prevalence of obese individuals across the world was estimated at 9.8% in 2005 [138], and with a subsequent increase, an urgent preventive action has been deemed essential. The public health need for obesity control is evident, because obesity serves as one of the most important risk factors of various chronic diseases [136], including acute coronary heart disease and other circulatory diseases, diabetes and several types of cancer (e.g. colon cancer). Following the WHO's declaration of the global epidemic of obesity in 1997 [136], the World Health Assembly endorsed the Global Strategy on Diet, Physical Activity and Health (DPAS) in 2004 aiming to improve the situation by intervening diet and physical activity [137]. Accordingly, the member states of the WHO and other international partners have faced a need to construct and carry out obesity control programs. As part of the control effort, various epidemiological studies have been conducted to assess the effectiveness of each control program (i.e. through individual nutritional or physical exercise programs). However, there have been little attempt to qualitatively and quantitatively compare the effectiveness of different types of control programs and optimize obesity control program as a whole. In addition, very little epidemiological effort has been made to understand the entire epidemiological dynamics of obesity and its control using mathematical and theoretical approaches.

While actual interventions of dietary behaviours (e.g. avoiding excessive calorie intake) and those against insufficient physical activities are implemented, Christakis and Fowler [16] scientifically demonstrated that obesity can spread from person to person via a social contact network. The epoch-making finding of the spread of non-infectious disease through a social contact network was not only limited to obesity but also other health-related issues such as smoking [17]. Statistical review of social network analysis took place elsewhere [18], because the estimation problem of social network effects, including the use of dynamic

models and statistical control of confounders, has been discussed [21,22]. The underlying biological and social mechanisms of obesity epidemics have fascinated a broad range of scientific audience.

Provided that non-negligible fraction of obesity is caused by person-to-person transmission, the effectiveness of essential control programs against obesity epidemic would be characterized by nonlinear dynamics with a correlated risk structure. That is, estimating the risk of obesity involves the issue of dependence in which the risk of obesity in a single individual is determined not only by that particular individual but also by other individuals in the same population unit (i.e. the so-called "dependent happening"). In a positive sense, the dependence implies that one could expect herd effect (or herd immunity) by implementing public health interventions, which has been commonly seen in the epidemiology of infectious diseases [9]. However, it also implies that the contagious effect could lead to social problems including potential need to intervene friendship network and social discrimination.

The present study aims to describe an obesity epidemic by employing a simple mathematical model that accounts for both social contagion and non-contagious hazards of obesity, thereby comparing the effectiveness of different types of interventions. Using a simplistic model with randomly mixing assumption, we intend to explore the most effective intervention in a qualitative manner and identify epidemiological data gaps that have prevented us from explicitly evaluating and comparing the effectiveness of various obesity control programs.

6.2 Materials and Methods

6.2.1 A Model for the Social Contagion of Obesity

Considering that obesity is caused by both contagious and non-contagious routes, we describe the epidemiological process of becoming and recovering from obesity as a function of time. Despite the fact that the spread of obesity is believed to occur on a complex social network [16,18], here we exploit a model that describes the epidemiological process of obesity in a randomly mixing population, because the present study intends to clarify the implications of person-to-person transmission of obesity for public health control in a rudimentary fashion and identify fundamental data gaps that have to be urgently addressed in empirical observations. To describe the time-dependence of the risk of obesity, we use the ordinary differential equations (ODE) that capture the population dynamics of obesity. Referring to the simplest version of the most classical epidemiological model for directly-transmitted infectious diseases [2,68], we describe the time-evolution of susceptible (never-obese), infectious (obese) and recovered (ex-obese) individuals as a function of time t, namely, $S(t)$, $I(t)$ and $R(t)$ as follows:

$$\begin{aligned}
\frac{\mathbf{d}S}{\mathbf{d}t} &= \mu N - [\beta I(t) + \epsilon]S(t) - \mu S(t), \\
\frac{\mathbf{d}I}{\mathbf{d}t} &= [\beta I(t) + \epsilon]S(t) + \sigma[\beta I(t) + \epsilon]R(t) - (\mu + \gamma)S(t), \\
\frac{\mathbf{d}R}{\mathbf{d}t} &= \gamma I(t) - \sigma[\beta I(t) + \epsilon]R(t) - \mu R(t),
\end{aligned} \tag{6.1}$$

where N represents the total population size, assumed to be a constant over time for the sake of our exposition of epidemiological data gaps, that is, $N = S(t) + I(t) + R(t)$ for any t, μ is the birth and death rate of human host, β is the transmission coefficient, ϵ is the hazard of obesity due to non-contagious reasons, γ is the natural recovery rate, and σ is the relative risk of weight regain among ex-obese individuals which typically takes a value greater than 1 due to high risk of coming back to the obese state [134]. It should be noted that the system (6.1) assumes that ex-obese is not contagious. All of these three equations describe the background birth and death of the host using the rate, μ. Otherwise all terms are associated with acquirement of or recovery from obesity. Among never-obese individuals, $\lambda(t) = \beta I(t) + \epsilon$ is the hazard rate of obesity on a whole (or, is frequently referred to as the "force of infection" in infectious disease epidemiology) at which they experience obesity for the first time. Among ex-obese individuals, the hazard is σ times greater than that among never-obese individuals. The natural recovery of obesity occurs at the rate, γ. It should be noted that the force of infection, $\lambda(t)$ is modelled in an additive manner, i.e., expressed as a sum of two hazards, one through the contagious route $\lambda_1 = \beta I(t)$ and the other via the non-contagious route $\lambda_2 = \epsilon$, the latter of which is determined by many factors including genetics and lifestyle including dietary habit. For simplicity, we consider a situation in which λ_2 is constant. By employing the additive model for the force of infection, it is assumed that the contagious and non-contagious risks are independent from each other. However, considering that the social contagion should eventually influence dietary behaviour and physical activity to achieve a "transmission of obesity" in real life, it should be more natural to account for the dependence between β and ϵ (see Discussion). When we numerically solve the system (6.1), we consider an initial condition with $S(0) = N$. Solving equations, $\mathbf{d}(S, I, R)/\mathbf{d}t = 0$ and analysing the linearized equations, we find an asymptotically stable equilibrium point, (S^*, I^*, R^*) to which all the trajectories of the system converge so that the parameter sensitivity and the age-specific risk in the equilibrium can be examined.

6.2.2 Lifetime Risk of Obesity: Age-dependence

Although the present study focuses on temporal dynamics of obesity epidemic, here we consider the age-dependent dynamics rather than time-evolution, ignoring time-dependency and measuring only the age-specific risk of obesity in an endemic equilibrium. The age-dependency is specifically considered here, because (i) the most typical epidemiological measurement of obesity at an individual level may be the risk of obesity or associated disease by a certain age (or throughout the course of life), and (ii) we intend to understand

the fundamental epidemiological dynamics of obesity using the model (6.1) as it has direct implication for age-dependent risk of obesity [2].

For simplicity, here we consider an equilibrium state, (S^*, I^*, R^*) with some constant prevalence of obesity. To describe the age-specific risk in a stationary state, we consider variables $X(a)$ $Y(a)$ and $Z(a)$, representing the numbers of never-obese, obese and ex-obese individuals at age a, respectively. The dynamics is described as follows:

$$\begin{aligned} \frac{\mathrm{d}X}{\mathrm{d}a} &= -\lambda^* X(a), \\ \frac{\mathrm{d}Y}{\mathrm{d}a} &= \lambda X(a) + \sigma\lambda^* Z(a) - (\mu+\gamma)Y(a), \\ \frac{\mathrm{d}Z}{\mathrm{d}a} &= -(\sigma\lambda^* + \mu)Z(a) + \gamma Y(a), \end{aligned} \tag{6.2}$$

where λ^* represents the force of infection which combined both contagious and non-contagious hazards at an equilibrium. The total population size of age a is $N_c(a) = X(a) + Y(a) + Z(a)$. Due to exponentially distributed life-expectancy of human host, $N_c(a)$ is parameterized as

$$N_c(a) = N_c(0)\exp(-\mu a), \tag{6.3}$$

which has been conventionally employed in epidemiology for exploring the age distribution of infected individuals in an endemic equilibrium (Chapter 4 of [2]). Since the total population size remains constant over time, we have

$$N = \int_0^\infty N_c(0)\exp(-\mu a)da = \frac{N_c(0)}{\mu}. \tag{6.4}$$

In other words, $Nc(0)$ can be equated to μN. Since new-borns are assumed as never-obese, we have an initial condition $(X, Y, Z) = (Nc(0), 0, 0)$ and $X(a)$ is then written as

$$X(a) = N_c(0)\exp\{-(\lambda^* + \mu)a\}. \tag{6.5}$$

We define the life-time risk as a probability of not remaining in the never-obese state throughout the course of life, which is calculated by using the probability to remain never-obese by age a, $x(a) = X(a)/N_c(0)$. The cumulative risk by age a, $q(a)$, is computed as

$$q(a) = \int_0^a \lambda^* x(s)ds = \frac{\lambda^*}{\lambda^* + \mu}[1 - \exp\{-(\lambda^* + \mu)a\}]. \tag{6.6}$$

As $a \to \infty$, $q(a)$ takes $\lambda^*/(\lambda^* + \mu)$. This indicates that, the larger the prevalence, the larger the life-time risk to experience obesity at least once during the course of life. Accordingly, hereafter we use the equilibrium prevalence, calculated from time-dependent system (6.1), as an epidemiological outcome measure to assess and compare the effectiveness of different interventions.

Description	Notation	Baseline value	Reference
Population size	N	100,000	assumed
Average life expectancy at birth	$1/\mu$	69.4 (years)	[138]
Transmission coefficient of obesity	β	2.96×10^{-7} (per year)	[134]
Non-contagious hazard of obesity	ϵ	0.012 (per year)	[58]
Relative hazard of obesity among ex-obese	σ	8	[134]
Average duration of obesity	$1/\gamma$	35.8 (years)	[58]

Table 6.1. The parameters shown above were used for baseline scenario. During univariate sensitivity analysis, these parameters were also used except for a single parameter that was varied.

6.2.3 Parameter Setting

For the exposition of the epidemiological dynamics using time-dependent model, we parameterize model 6.1 referring to published empirical data. Table 6.1 summarizes the parameter values. We consider a hypothetical population with a population size N=100,000 which experiences random mixing, with the life expectancy at birth, $1/\mu$=69.4 years, calculated as the weighted average of country-specific life expectancies [138], which is broadly consistent with those in Southeast Asian countries (e.g. Laos at 62.8 years, Indonesia at 71.6 years and Vietnam at 72.4 years). The relative risk of weight regain among ex-obese individuals, σ is set at 8.0 according to literature [134]. The average duration of obesity, $1/\gamma$ and non-contagious hazard of obesity, ϵ are estimated at 35.8 years and 0.012 per year, respectively, based on the dataset from Framingham Heart Study [58]. The transmission coefficient, β is also explicitly estimated from an empirical dataset. Since our model in continuous time is not consistent with empirically observed risk on a static network [127], and because the other data from a social network were sampled from a non-stationary process with non-linear dynamics [58], the dataset for estimating β in the present study was derived from a confined household setting. The empirically observed household secondary attack proportion, SAP, has ranged from 0.14 to 0.28 for a short period of time as compared with the life expectancy at birth (e.g. for 4-28 years) [134]. Based on a generalized stochastic epidemic model in the confined setting [110, 127], the SAP with a single index case is translated to the basic reproduction number, R_0 by

$$SAP = \frac{R_0}{R_0 + m}, \tag{6.7}$$

where m represents the number of susceptible-and-exposed individuals in the household. In similar epidemic systems, R_0 is mathematically derived from a linearlized system (i.e. nearby disease-free equilibrium) as defined elsewhere [27], but unfortunately, disease-free equilibrium is always unstable for the system (6.1) except for ϵ=0 (i.e. except for the case without non-contagious hazard of obesity). Only for now, we use this special case, i.e., $R_0 = \beta N/(\gamma+\mu)$, that can only be true and theoretically derived when the non-contagious hazard of obesity is assumed as zero (which is a reasonable assumption for the empirical

data based on observation for a short period of time [134]). Assuming that m=3 and SAP ranged from 0.135 to 0.254, the transmission coefficient, β in our scenario analysis ranges from 1.99×10^{-7} to 4.33×10^{-7}. The mid-point of estimates, i.e., 2.96×10^{-7} is used as the baseline value.

6.2.4 Computational Scenarios

First, we solve the system (6.1) numerically to understand the time-dependent dynamics of never-obese, obese and ex-obese individuals. Second, we explore the impact of hazard parameters (i.e. hazards for contagious and non-contagious routes) and recovery parameters on the equilibrium prevalence of obesity. Third, to assess and compare the effectiveness of different control programs of obesity, we investigate the sensitivity of the equilibrium prevalence on the shift of parameters that determine the effectiveness of each program. When exploring the effectiveness of interventions, we use two different types of classification of control programs: (i) we consider varying only one parameter for each sensitivity analysis, and (ii) we consider varying a combination of parameters. For the latter, varying a combination of parameters that influence the risk of obesity among never-obese individuals is hereafter referred to as the primary prevention, and varying the other combination of interventions that influence the risk of obesity among obese and ex-obese individuals is referred to as the secondary prevention. It should be noted that the term "secondary prevention" is used here to represent the intervention that happens after experiencing illness (i.e. obesity) at least once. We measure the effectiveness of control programs by examining the impact of relative change in either (i) or (ii) on the equilibrium prevalence value.

6.3 Results

6.3.1 Baseline Dynamics of Obesity

Using aforementioned mathematical model (6.1), we consider the time evolution of prevalence (Figure 6.1A). As mentioned above, it should be noted that the initial condition $(S(0), I(0), R(0)) = (N, 0, 0)$ is set to demonstrate that obesity-free equilibrium is unstable and the dynamics surely causes an epidemic with an initial fuel from non-contagious hazard. As time goes by, the prevalence converges to a stationary value. According to the baseline setting in Table 6.1, it takes approximately 200 years to reach to an equilibrium state and the prevalence in our baseline setting is calculated at 60.8%. Although the prevalence estimate is higher than the empirically reported value, the obesity in real world is still growing, and on the technical side, the high value has resulted from exponentially distributed survival. Figure 6.1B shows the age distribution of S, I and R as a function of age a, using system (6.2) with the equilibrium prevalence and assuming that all new-borns are never-obese. The risk of obesity at a given age a (calculated as the "risk at birth") hits a peak at the age of 37.0 years, but subsequently decreases due to natural mortality.

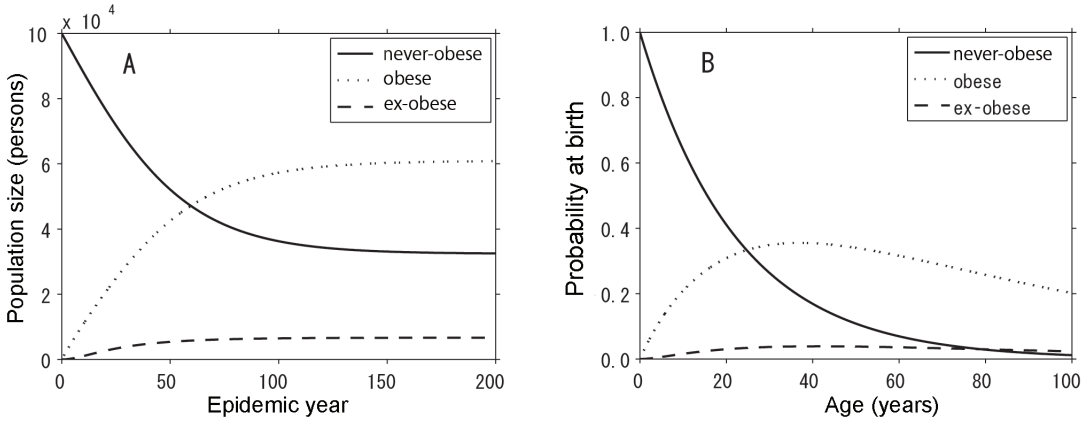

Figure 6.1. Baseline dynamics of an obesity epidemic. (A) Time-dependent and (B) age-dependent epidemiological trajectories are shown. A. The time evolution of the numbers of never-obese, obese and ex-obese individuals. As time goes by, the prevalence of obesity converges to an equilibrium level. B. Age-specific risk of obesity in a stationary state. The vertical axis represents the risk (or probability) of age a at birth (and thus, it should be noted that the proportions do not sum up to 1 due to natural mortality).

6.3.2 Hazard of and Recovery from Obesity

Obviously, the contents, subjects and objectives of many available interventions differ by control programs. Theoretically speaking, there are two types of interventions that belong to the primary prevention, i.e. the intervention on social contact and the preventing weight gain among never-obese individuals, each influencing the transmission coefficient β and non-contagious hazard ϵ, respectively. The intervention of social contact is intended to prevent person-to-person transmission by suppressing obesity contagion. The practical feasibility of such an intervention is subject to discussion, but in the present study the intervention is theoretically considered as resembling contact tracing of directly transmitted infectious diseases [71, 88]. Preventing weight gain among never-obese individuals is to control the diet and enhance physical activities, including the specification of nutrients and restriction of calorie intake [118]. Figure 6.2A shows the role of β and ϵ in regulating the prevalence of obesity. Overall, the lower the transmission coefficient ϵ is, the lower the prevalence would be. However, the equilibrium prevalence appears to be very sensitive to β, and abruptly varies at some value of β depending on the non-contagious hazard ϵ. For instance, when ϵ was set as equal to 0, one could theoretically expect an eventual eradication of obesity by controlling obesity contagion, and in such an instance, a disease-free equilibrium could occur. In this case, the model also appears to yield a backward bifurcation of prevalence, indicating the absence of simple threshold governed by β. That is, due to the presence of re-infection, the model can find an endemic equilibrium even for $R_0 < 1$, indicating a difficulty in controlling obesity in the presence of person-to-person

transmission. There are two types of interventions that belong to the secondary prevention, i.e. the dietary control program among obese individuals and the follow-up program of ex-obese individuals, each influencing on the duration of obesity $1/\gamma$ and the relative hazard among ex-obese σ, respectively. The dietary restriction in this context is targeted on obese individuals only [84], and the follow-up program is to encourage ex-obese individuals not to be overweight again [124]; ex-obese individuals are known to be more prone to obesity than never-obese individuals [36]. Figure 6.2B shows the role of $1/\gamma$ and σ in regulating the prevalence of obesity. Overall, the shorter the duration of obesity $1/\gamma$ is, the lower the equilibrium prevalence would be. Unlike Figure 6.2A, the prevalence does not abruptly vary with σ. Varying σ to lower or greater values led the prevalence of obesity to be less sensitive to $1/\gamma$.

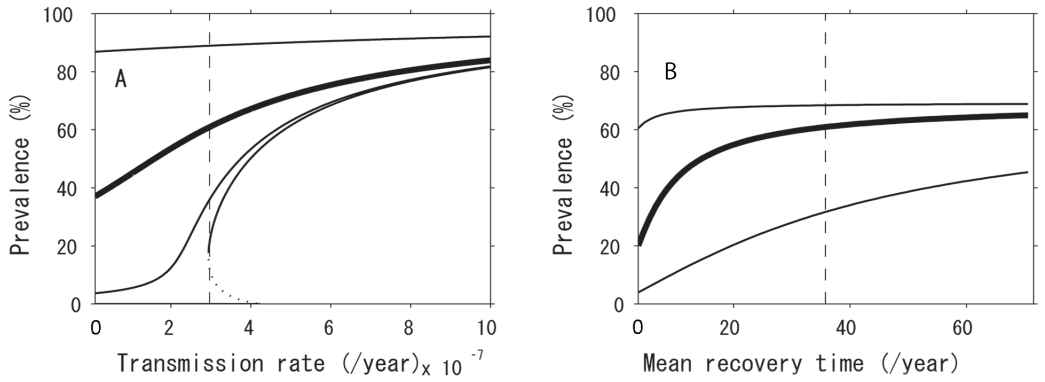

Figure 6.2. Sensitivity of the prevalence of obesity to the parameters determining the hazard and the recovery. Equilibrium prevalence is computed by varying a single parameter, i.e., the transmission rate for panel A and the mean recovery rate for panel B. A. The bold line shows the baseline result, varying only the transmission coefficient β. The other lines represent the scenarios in which ϵ is varied to the 0%, 10% and 1000% relative to the baseline value (from the horizontal axis to the top, the lines represent 0, 10 and 1000%, respectively). B. The bold line shows the equilibrium prevalence of obesity using baseline parameter values other than the average duration of obesity, $1/\gamma$. Two other lines represent the scenarios in which σ is varied to 10% (bottom) and 1000% (top), respectively, relative to the baseline value.

6.3.3 Comparison of Intervention Effectiveness

When we compare the effectiveness of multiple control programs, interventions that vary only a single parameter of model (1) are separately examined from those varying a combination of multiple parameters. For the combination of multiple parameters, the primary and secondary preventions are separately grouped for comparison due to practical consistency in the grouping. Since the system (6.1) focused on the intrinsic dynamics without any interventions, here we specifically show the way that extrinsic factors influence the

growth of obesity. As a parameter governing the primary prevention α, we assume that both contagious and non-contagious hazards are equally reduced by the factor α as follows:

$$\begin{aligned}
\frac{\mathrm{d}S}{\mathrm{d}t} &= \mu N - \alpha[\beta I(t) + \epsilon]S(t) - \mu S(t), \\
\frac{\mathrm{d}I}{\mathrm{d}t} &= \alpha[\beta I(t) + \epsilon]S(t) + \sigma[\beta I(t) + \epsilon]R(t) - (\mu + \gamma)S(t), \\
\frac{\mathrm{d}R}{\mathrm{d}t} &= \gamma I(t) - \sigma[\beta I(t) + \epsilon]R(t) - \mu R(t).
\end{aligned} \tag{6.8}$$

It should be noted that only the hazards among never-obese individuals are reduced. In addition, there is a possibility that an assumed marginal independence between β and ϵ could lead to an overestimation of the effectiveness of primary prevention (because the reduction of prevalence with an identical α in the presence of dependence can be greater than that we show here). Similarly, we consider the secondary prevention which includes the dietary restriction among obese individuals and the follow-up program among those experienced obesity at least once in combination. Supposing that the associated intervention programs are enhanced by a factor κ, we modelled the secondary prevention as follows:

$$\begin{aligned}
\frac{\mathrm{d}S}{\mathrm{d}t} &= \mu N - [\beta I(t) + \epsilon]S(t) - \mu S(t), \\
\frac{\mathrm{d}I}{\mathrm{d}t} &= [\beta I(t) + \epsilon]S(t) + \kappa\sigma[\beta I(t) + \epsilon]R(t) - (\mu + \tfrac{\gamma}{\kappa})S(t), \\
\frac{\mathrm{d}R}{\mathrm{d}t} &= \tfrac{\gamma}{\kappa} I(t) - \kappa\sigma[\beta I(t) + \epsilon]R(t) - \mu R(t).
\end{aligned} \tag{6.9}$$

It should be noted that the follow-up program reduced the overall hazard of re-infection (including those arising from social contagion and lifestyle), because the follow-up program does not specify the way of regaining weight among ex-obese individuals and is primarily intended to reduce susceptibility of ex-obese individuals toward re-infection.

Figure 6.3 shows the sensitivity of prevalence to independent variations in each parameter. While panels A and C show the results of univariate sensitivity, panels B and D are the results from varying two parameters in combination. Panels A and B employ 1.99×10^{-7} per year as the transmission coefficient β which is the lowest in range, while Panels C and D adopted the highest value 4.33×10^{-7} per year. When β is small, Figure 6.3A demonstrates that preventing weight gain among never-obese individuals, ϵ, is most effective and influential. Dietary restriction among obese individuals, $1/\gamma$, appeared to be the second most effective option. Namely, as long as β remains very small, and thus, the transmission of obesity cannot be maintained in the host population via person-to-person transmission routes, an intervention program that aims to reduce the non-contagious hazard would be the most effective strategy, and moreover, quickly removing obese individuals by the control program would be expected to reduce obesity effectively. Combined interventions are compared in Figure 6.3B. The effectiveness of reducing overall hazards of obesity among never-obese individuals would be similar to that of targeting obese and

ex-obese individuals. In addition, increasing α would be more influential to elevate the prevalence than increasing κ.

However, when the transmission coefficient is set to be very high so that the transmission of obesity can be maintained through social contagion, preventing weight gain among never-obese individuals, ϵ, appears to be the least effective. Rather, promoting the dietary restriction $(1/\gamma)$ and implementing the follow-up program (σ) would be more effective in reducing the prevalence of obesity. In a certain range, intervening β is the most influential parameter in reducing the prevalence, while in reality it might be difficult to directly reduce obesity contagion by a control program. When a combination of two control strategies can be selected, the primary and secondary preventions yielded similar population impacts and the superiority of the effectiveness depends on the strength of the interventions at an individual level.

6.4 Discussion

In the present study, we investigated epidemiological models that describe the obesity epidemic, spreading via social contact and acquired due to non-contagious reasons. We assessed and compared the effectiveness of different types of intervention programs which aim to reduce the risk of obesity. As the most important practical finding, we identified that the optimal choice of intervention programs considerably varies with the transmission coefficient of obesity, β. When β is small, the transmission cannot be maintained by social contagion alone. In such an instance, our model has suggested that preventing weight gain among never-obese individuals would be the most effective option, although it should be remembered that our approach adopted marginal independence between β and ϵ, and the effectiveness of primary prevention might have been overestimated. When β is large enough to sustain the transmission of obesity through the person-to-person route, dietary restriction among obese individuals could potentially be the most effective. In other words, depending on the transmissibility of obesity, the effectiveness of reducing obesity hazards would greatly vary, and thus, the population impact of each program would be dependent on the transmission dynamics of obesity. When a combination of interventions can be selected, the primary prevention is likely more influential than the secondary prevention for a small effect size, but on the whole primary and secondary preventions yielded similar population impacts. Despite the dependence of optimal interventions on β, it should be noted that the transmission potential of obesity in community setting has yet to be explicitly estimated.

Since WHO has addressed DPAS, emphasizing the importance of diet and physical activity as two main factors that determine the risk of obesity [137], the worldwide effort of obesity control has started, conducting and evaluating various programs. As we have shown using a simplistic model, the social contagion of obesity must be a key concern for public health for decision-making, because the design of effective control programs requires

us to capture and understand the population dynamics of obesity in an explicit manner, and moreover, empirically quantify the transmissibility of obesity. As the most important data gap, we have identified that the transmission potential of obesity contagion has to be estimated, as it drastically varies the optimal choice of interventions. To estimate the contagious hazard of obesity, household-based prospective cohort study of susceptible and recovered individuals is desirable, because not only the transmissibility within households but also the relevance of the transmission potential to the natural history of obesity can be measurable. Nevertheless, it should be noted that the threshold property, R_0 is unlikely to be maintained in the obesity model due to non-contagious risk and re-infection.

Whereas we have shown that primary and secondary preventions yielded similar reductions in the equilibrium prevalence of obesity in a certain parameter space, it should be remembered that the primary and secondary preventions require different types and amounts of effort, not sharing an identical effect size. Considering that the length of obese period could influence the risk of later health outcomes (e.g. diabetes), the primary prevention may better be more advantageous in reducing the devastating outcomes. Addressing the associated life-course issues including an assessment of economic impact is the subject for future studies.

Despite our key finding in identifying the transmissibility as the most influential component to determine the optimal interventions, there are five issues that are regarded as limitation or should be cautiously interpreted. First, while obesity contagion on a social contact network has been empirically studied in literature [36, 50, 66], we have employed a homogeneously mixing assumption for mathematical convenience and to identify key parameter of obesity dynamics without ambiguity [112]. Of course, using empirically observed network data would permit us to describe more realistic situations [58]. Considering that the threshold level of obesity epidemic likely differs in heterogeneous contact networks, future studies should quantify the transmissibility of obesity on an explicit contact network and identify the corresponding appropriate way of public health control. Second, the natural history of obesity, including the duration of obesity and frequency of recurrence, is largely unknown [117]. Due to shortage of information, we have had to ignore age-dependent heterogeneity, e.g. differential calorie consumptions by age [89]. Third, an equilibrium prevalence of our model is calculated as high as 60.8%, which is greater than currently observed prevalence [138]. However, the prevalence in the present day has yet to reach the stable level, and has been in increasing trend [58], and thus, we believe that our exercise has not been far from reality even by using a simplistic model. Fourth, we did not take into account the cost to be compared across different intervention programs. Identification of optimal programs would require an explicit analysis of cost-benefit and cost-effectiveness aspects. Lastly, on the technical side, further work could explore the use of alternative modelling approaches, e.g. conditional risk model with stochastic dependence structure, which could avoid overestimating the effectiveness of primary prevention.

Despite these limitations due mainly to simplifications of our modelling exercise, a number of advantages in our study should be noted. First, we took into account the relative hazard of obesity among ex-obese individuals, while an earlier study that shares a similar scopes with our study ignored the elevated risk of weight regain among ex-obese individuals [58]. Rather than focusing on network heterogeneity, our study has intended to examine the impact of nonlinear transmission with complex natural history on the optimal choice of interventions [50, 87]. Second, due to simple model structure, our model has remained to be analytically tractable, and thus, a variety of different epidemiological measures, including life-time risk of obesity-related diseases, can be additionally derived. For instance, one can easily extend our concept to account for the delay or a fraction of obese individuals in developing a chronic disease later in life. Using a convolution of the time delay function from obesity to a heart attack, $f(s)$ of length s and the risk of once becoming obese by age a, $1 - x(a)$, with a scaling factor (i.e. the overall risk) of heart attack p, one can describe the risk of heart attack as a function of age as

$$w(a) = p \int_0^\infty f(s)(1 - x(a - s))ds, \tag{6.10}$$

although the use of $1 - x(a)$ is subject to discussion (e.g. rather, one may prefer to use individual history of being obese). Such modelling exercise can potentially enable us to describe the long-term and secondary impact of obesity control in reducing closely associated diseases or deaths at a population level, while explicitly accounting for nonlinearity in the spread and control of obesity. Third, a little more complex natural history may better be incorporated into the model. For instance, non-contagious hazard was assumed as a fixed value in the present study, but in reality the hazard may depend on age which reflects not only the physiological age-dependence but also the history of escape from obesity. Not only obesity but also other behavioural contagion can be analysed using similar modelling approaches [57]. Despite numerous future tasks, we believe that we have successfully simplified the population dynamics of obesity, identifying the importance of quantifying the transmission potential to determine public health control programs in the future.

The optimal choice of interventions against obesity varies by the transmission potential of obesity from person to person. To attain appropriate assessment and comparison of different types of public health control programs of obesity, it is critical that the epidemiological dynamics of obesity, especially the transmission potential, is quantified in advance.

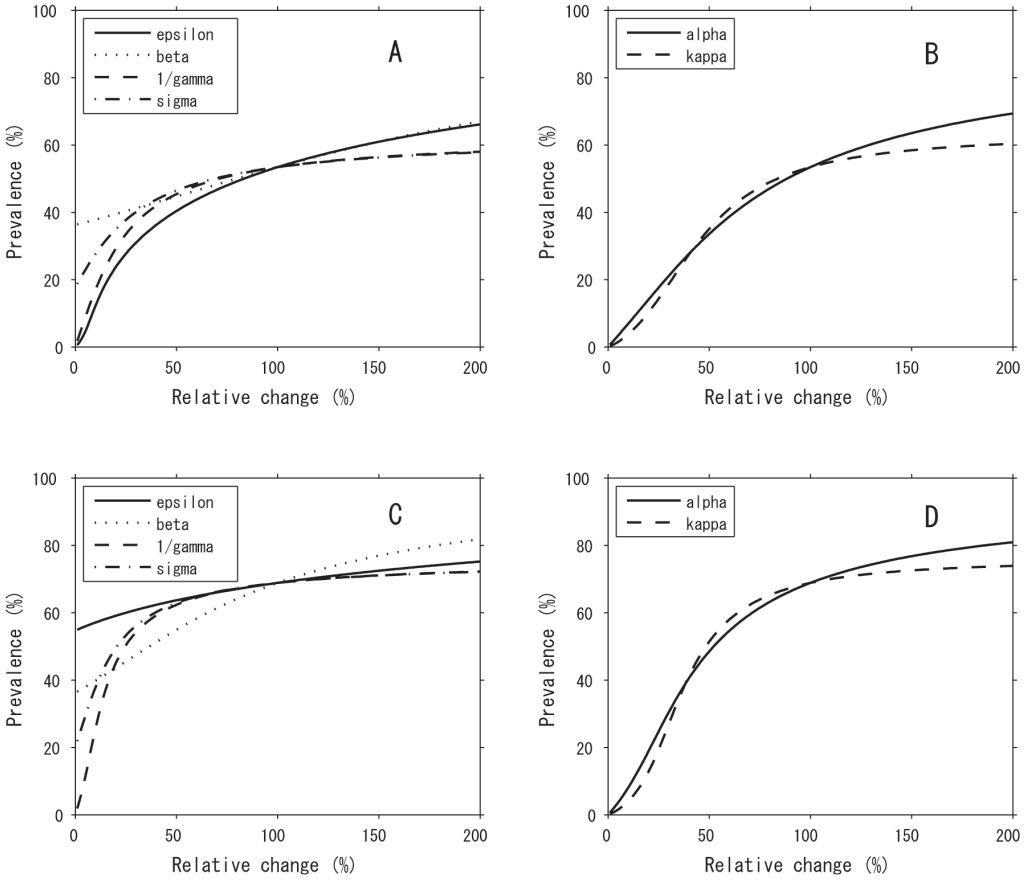

Figure 6.3. Sensitivity of the prevalence of obesity to different control programs. Effectiveness of interventions is measured by equilibrium prevalence as a function of relative reduction in certain parameters. A&C. The prevalence when single parameters (ϵ, β, $1/\gamma$ and σ) are independently varied. B&D. Comparison between the primary prevention (reducing α) and the secondary prevention (reducing κ). The baseline value of β is set to be low in panels A and B (1.99×10^{-7} per year), while panels C and D shows the case when β is set at high (4.33×10^{-7} per year).

Chapter 7

Conclusion

In this thesis, I have attempted to resolve several issues in public health by focusing on the data generating process to explain observations obtained from limited data.

In Chapter 1, I demonstrated the importance of the mathematical modeling in the context of infectious disease epidemiology, while giving a brief account of the recent progress made in the development of modeling techniques. The data generating process that explains observations from passive data collection can be roughly divided into two parts: the transmission process and the observation process. Therefore, to address public health issues surrounding infectious disease, this process must be captured precisely in the model.

In Chapters 2 and 3, I attempted to address public health issues using only limited passive data by constructing a model reflecting the data generating process. In Chapter 2, I proposed an estimation method to jointly infer the CFR and the exponential growth rate in the early phase of an influenza epidemic, in which we can only determine the number of confirmed cases and deaths at most. I then constructed the corresponding epidemic and observational models. In a realistic setting, 2-3 months is required to compare the estimated CFR with the pre-specified CFR value, as defined by the US Pandemic Severity Index, for example.

In Chapter 3, I proposed a modeling method to estimate vaccine efficacy against measles by jointly quantifying the parameters governing the temporal dynamics of a measles outbreak, such as R_0. This proposed method is based solely on epidemiological surveillance data with partial information on vaccination history. The results suggest that it is necessary to undertake (re-)vaccination of the population aged 519 years to prevent any further measles outbreaks in Japan.

In Chapters 4 and 5, I attempted to show the importance of the model building to describe the data generating process. In Chapter 4, I focused on factors influencing the transmission process; assortativity in particular. I discussed the use of chance-adjusted agreement coefficients to measure the assortativity of contacts and transmission of infectious diseases. I have shown that p, as expressed in the preferential mixing formulation, corresponds closely to Newman's assortativity coefficient (or Cohen's kappa). I explicitly distinguished transmission assortativity from contact assortativity, given that the former

captures not only the heterogeneity of contacts, but also many other intrinsic and extrinsic factors characterizing the frequency of within- and between-group transmission. In Chapter 5, in which I compared models for observable (symptom-based) and unobservable (contagiousness-dependent) outcomes, I emphasized that it is essential to use a model formulation appropriate to the public health issue in question—including those relating to vaccination interventions. My evaluation of the validity of incorporating the effect of a vaccine against clinical disease in epidemiological models has shown that an explicit model formulation would also aid in clarifying the underlying assumptions that tend to be hidden in commonly encountered model structures.

Finally, I applied this infectious disease model to other non-communicable health conditions. In Chapter 6, I investigated epidemiological models to describe the obesity epidemic, which can be considered to spread via social contacts while being acquired non-communicably. I demonstrated that the optimal choice of intervention is highly sensitive to the intensity of infection.

Unfortunately, it was not within the scope of this thesis to cover all the issues surrounding infectious disease modeling. However, I believe this thesis contributes to our understanding of infectious disease and its results are of significant value for informing public health policymaking and practice for preventing the emergence, or re-emergence, of infectious disease.

Acknowledgments

First of all, I would like to express my deepest gratitude to my adviser, Prof. Kazuyuki Aihara, for his invaluable support and advice throughout my master's course and doctoral course. I have learnt much from his attitude toward researches and others. Moreover, I would like to thank Prof. Satoru Iwata, Prof. Hideyuki Suzuki, Prof. Naoki Masuda, and Prof. Tetsuya Kobayashi for kindly participating in the thesis committee.

I would also like to thank Prof. Hiroshi Nishiura. He invited me to the School of Public Health, the University of Hong Kong as a visiting student and helped me to precede my research. I really could concentrate on my research throughout my stay in Hong Kong. Furthermore, it was very exciting experience to collaborate with the researchers in public health. I realized that in order to fight against the infectious disease, the mathematical modelers including me have to work with the specialists in the corresponding fields, such as doctors, epidemiologists, and civil servants.

I would like to express my deep gratitude to all the members of the Laboratories for Mathematics, Lifesciences, and Informatics, all the members of First Aihara Innovative Mathematical Modelling Project. I am afraid I cannot name all here, but I really appreciate their kind support, fruitful suggestions, and stimulating my interest. I would also like to thank the secretary staffs of the laboratories for their generous support. Finally, I would like to thank my family for their kind understanding and generous support.

Bibliography

[1] Aichi Prefectural Institute of Public Health . National Epidemiological Surveillance of Vaccine-Preventable Diseases (NESVPD). Aichi Prefectural Institute of Public Health: Aichi, 2007.

[2] Anderson R. M. and May R. M. *Infectious Diseases of Humans: Dynamics and Control*. Oxford University Press, 1992.

[3] Arino J., Brauer F., van den Driessche P., Watmough J., and Wu J. Simple models for containment of a pandemic. *Journal of the Royal Society, Interface / the Royal Society*, 3(8):453–457, June 2006.

[4] Arino J., Brauer F., van den Driessche P., Watmough J., and Wu J. A final size relation for epidemic models. *Mathematical biosciences and engineering*, 4(2):159–175, Apr. 2007.

[5] Balcan D., Hu H., Goncalves B., Bajardi P., Poletto C., Ramasco J. J., Paolotti D., Perra N., Tizzoni M., van den Broeck W., Colizza V., and Vespignani A. Seasonal transmission potential and activity peaks of the new influenza A(H1N1): a Monte Carlo likelihood analysis based on human mobility. *BMC medicine*, 7:45, Jan. 2009.

[6] Basta N. E., Chao D. L., Halloran M. E., Matrajt L., and Longini I. M. Strategies for pandemic and seasonal influenza vaccination of schoolchildren in the United States. *American journal of epidemiology*, 170(6):679–686, Sept. 2009.

[7] Basta N. E., Halloran M. E., Matrajt L., and Longini I. M. Estimating influenza vaccine efficacy from challenge and community-based study data. *American journal of epidemiology*, 168(12):1343–1352, Dec. 2008.

[8] Bjørnstad O. N., Finkenstädt B. F., and Grenfell B. T. Dynamics of measles epidemics: Estimating scaling of transmission rates using a Time series SIR model. *Ecological Monographs*, 72(2):169–184, May 2002.

[9] Blok D. J., van Empelen P., van Lenthe F. J., Richardus J. H., and de Vlas S. J. Unhealthy behaviour is contagious: an invitation to exploit models for infectious diseases. *Epidemiology and Infection*, pages 1–3, May 2012.

[10] Boëlle P.-Y., Ansart S., Cori A., and Valleron A.-J. Transmission parameters of the A/H1N1 (2009) influenza virus pandemic: a review. *Influenza and other respiratory viruses*, 5(5):306–316, Sept. 2011.

[11] Brisson M., Edmunds W., and Gay N. Varicella vaccination: Impact of vaccine efficacy on the epidemiology of vzv. *Journal of Medical Virology*, 70(S1):S31–S37, 2003.

[12] Britton T. Stochastic epidemic models: a survey. *Mathematical biosciences*, 225(1):24–35, May 2010.

[13] Brookmeyer R. and Gail M. H. *AIDS Epidemiology: A Quantitative Approach (Monographs in Epidemiology and Biostatistics)*. Oxford University Press, 1994.

[14] Charleston B., Bankowski B. M., Gubbins S., Chase-Topping M. E., Schley D., Howey R., Barnett P. V., Gibson D., Juleff N. D., and Woolhouse M. E. J. Relationship between clinical signs and transmission of an infectious disease and the implications for control. *Science*, 332(6030):726–729, May 2011.

[15] Chowell G., Bettencourt L. M. A., Johnson N., Alonso W. J., and Viboud C. The 1918-1919 influenza pandemic in England and Wales: spatial patterns in transmissibility and mortality impact. *Proceedings. Biological sciences*, 275(1634):501–509, Mar. 2008.

[16] Christakis N. A. and Fowler J. H. The spread of obesity in a large social network over 32 years. *The New England Journal of Medicine*, 357(4):370–379, July 2007.

[17] Christakis N. A. and Fowler J. H. The collective dynamics of smoking in a large social network. *The New England Journal of Medicine*, 358(21):2249–2258, May 2008.

[18] Christakis N. A. and Fowler J. H. Social contagion theory: examining dynamic social networks and human behavior. *Statistics in Medicine*, 32(4):556–577, Feb. 2013.

[19] Cicchetti D. V. and Feinstein A. R. High agreement but low kappa: II. Resolving the paradoxes. *Journal of clinical epidemiology*, 43(6):551–558, Jan. 1990.

[20] Cohen J. A Coefficient of Agreement for Nominal Scales. *Educational and Psychological Measurement*, 20(1):37–46, Apr. 1960.

[21] Cohen-Cole E. and Fletcher J. M. Detecting implausible social network effects in acne, height, and headaches: longitudinal analysis. *BMJ*, 337:a2533, 12 2008.

[22] Cohen-Cole E. and Fletcher J. M. Is obesity contagious? Social networks vs. environmental factors in the obesity epidemic. *Journal of health economics*, 27(5):1382–1387, Sept. 2008.

[23] Cowling B. J., Ng S., Ma E. S. K., Cheng C. K. Y., Wai W., Fang V. J., Chan K.-H., Ip D. K. M., Chiu S. S., Peiris J. S. M., and Leung G. M. Protective efficacy of seasonal influenza vaccination against seasonal and pandemic influenza virus infection during 2009 in Hong Kong. *Clinical infectious diseases : an official publication of the Infectious Diseases Society of America*, 51(12):1370–1379, Dec. 2010.

[24] Del Valle S., Hyman J., Hethcote H., and Eubank S. Mixing patterns between age groups in social networks. *Social Networks*, 29(4):539–554, Oct. 2007.

[25] Department of Health & Human Services . *Interim Pre-Pandemic Planning Guidance: Community Strategy for Pandemic Influenza Mitigation in the United States-Early, Targeted, Layered Use of Nonpharmaceutical Interventions*. Centers for Disease Control, Atlanta, GA, USA, 2007.

[26] Diekmann O. Limiting behaviour in an epidemic model. *Nonlinear Analysis: Theory, Methods & Applications*, 1(5):459–470, Aug. 1977.

[27] Diekmann O., Heesterbeek H., and Britton T. *Mathematical Tools for Understanding Infectious Disease Dynamics: (Princeton Series in Theoretical and Computational Biology)*. Princeton University Press.

[28] Diekmann O., Heesterbeek J. A. P., and Roberts M. G. The construction of next-generation matrices for compartmental epidemic models. *Journal of the Royal Society, Interface*, 7(47):873–885, June 2010.

[29] Division of Welfare and Health, Tokyo Metropolitan Government . Manual for the control of measles among junior high school and high school students. Tokyo Metropolitan Government: Tokyo, 2011.

[30] Echevarría-Zuno S., Mejía-Aranguré J. M., Mar-Obeso A. J., Grajales-Muñiz C., Robles-Pérez E., González-León M., Ortega-Alvarez M. C., Gonzalez-Bonilla C., Rascón-Pacheco R. A., and Borja-Aburto V. H. Infection and death from influenza A H1N1 virus in Mexico: a retrospective analysis. *Lancet*, 374(9707):2072–2079, Dec. 2009.

[31] Edmunds W. J., Gay N. J., Kretzschmar M., Pebody R. G., and Wachmann H. The pre-vaccination epidemiology of measles, mumps and rubella in Europe: implications for modelling studies. *Epidemiology and Infection*, 125(3):635–650, Dec. 2000.

[32] Eichner M., Diebner H. H., Schubert C., Kreth H. W., and Dietz K. Estimation of the time-dependent vaccine efficacy from a measles epidemic. *Statistics in Medicine*, 21(16):2355–2368, Aug. 2002.

[33] Eichner M. and Dietz K. Transmission potential of smallpox: estimates based on detailed data from an outbreak. *American journal of epidemiology*, 158(2):110–117, July 2003.

[34] Eichner M., Schwehm M., Duerr H.-P., and Brockmann S. O. The influenza pandemic preparedness planning tool InfluSim. *BMC infectious diseases*, 7:17, Jan. 2007.

[35] Ejima K., Aihara K., and Nishiura H. Modeling the obesity epidemic: social contagion and its implications for control. *Theoretical biology & medical modelling*, 10:17, Jan. 2013.

[36] El-Sayed A. M., Scarborough P., Seemann L., and Galea S. Social network analysis and agent-based modeling in social epidemiology. *Epidemiologic perspectives & innovations*, 9(1):1, Jan. 2012.

[37] Farrington C. On vaccine efficacy and reproduction numbers. *Mathematical Biosciences*, 185(1):89–109, 2003.

[38] Farrington C. P., Kanaan M. N., and Gay N. J. Branching process models for surveillance of infectious diseases controlled by mass vaccination. *Biostatistics*, 4(2):279–295, Apr. 2003.

[39] Farrington C. P. and Whitaker H. J. Contact Surface Models for Infectious Diseases. *Journal of the American Statistical Association*, 100(470):370–379, June 2005.

[40] Farrington C. P., Whitaker H. J., Wallinga J., and Manfredi P. Measures of disassortativeness and their application to directly transmitted infections. *Biometrical journal. Biometrische Zeitschrift*, 51(3):387–407, June 2009.

[41] Feinstein A. R. and Cicchetti D. V. High agreement but low kappa: I. The problems of two paradoxes. *Journal of clinical epidemiology*, 43(6):543–549, Jan. 1990.

[42] Finkenstädt B. F. and Grenfell B. T. Time series modelling of childhood diseases: a dynamical systems approach. *Journal of the Royal Statistical Society: Series C (Applied Statistics)*, 49(2):187–205, 2000.

[43] Fraser C., Donnelly C. A., Cauchemez S., Hanage W. P., Van Kerkhove M. D., Hollingsworth T. D., Griffin J., Baggaley R. F., Jenkins H. E., Lyons E. J., Jombart T., Hinsley W. R., Grassly N. C., Balloux F., Ghani A. C., Ferguson N. M., Rambaut A., Pybus O. G., Lopez-Gatell H., Alpuche-Aranda C. M., Chapela I. B., Zavala E. P., Guevara D. M. E., Checchi F., Garcia E., Hugonnet S., and Roth C. Pandemic potential of a strain of influenza A (H1N1): early findings. *Science*, 324(5934):1557–1561, June 2009.

[44] Fraser C., Riley S., Anderson R. M., and Ferguson N. M. Factors that make an infectious disease outbreak controllable. *Proceedings of the National Academy of Sciences of the United States of America*, 101(16):6146–51, Apr. 2004.

[45] Garske T., Legrand J., Donnelly C. A., Ward H., Cauchemez S., Fraser C., Ferguson N. M., and Ghani A. C. Assessing the severity of the novel influenza a/h1n1 pandemic. *BMJ*, 339:b2840, 7 2009.

[46] Ghani A. C., Donnelly C. A., Cox D. R., Griffin J. T., Fraser C., Lam T. H., Ho L. M., Chan W. S., Anderson R. M., Hedley A. J., and Leung G. M. Methods for estimating the case fatality ratio for a novel, emerging infectious disease. *American journal of epidemiology*, 162(5):479–486, Sept. 2005.

[47] Glass K. and Grenfell B. T. Waning immunity and subclinical measles infections in England. *Vaccine*, 22(29-30):4110–4116, Sept. 2004.

[48] Glasser J., Feng Z., Moylan A., Del Valle S., and Castillo-Chavez C. Mixing in age-structured population models of infectious diseases. *Mathematical biosciences*, 235(1):1–7, Jan. 2012.

[49] Goldstein E., Dushoff J., Ma J., Plotkin J. B., Earn D. J. D., and Lipsitch M. Reconstructing influenza incidence by deconvolution of daily mortality time series. *Proceedings of the National Academy of Sciences of the United States of America*, 106(51):21825–21829, Dec. 2009.

[50] González-Parra G., Acedo L., Villanueva Micó R.-J., and Arenas A. J. Modeling the social obesity epidemic with stochastic networks. *Physica A: Statistical Mechanics and its Applications*, 389(17):3692–3701, 2010.

[51] Gupta S., Anderson R. M., and May R. M. Networks of sexual contacts: implications for the pattern of spread of HIV. *AIDS*, 3(12):807–818, Dec. 1989.

[52] Gwet K. L. Computing inter-rater reliability and its variance in the presence of high agreement. *The British journal of mathematical and statistical psychology*, 61(1):29–48, May 2008.

[53] Gwet K. L. *Handbook of Inter-Rater Reliability: The Definitive Guide to Measuring the Extent of Agreement Among Multiple Raters, 3rd Edition.* Advanced Analytics, LLC, 2012.

[54] Haber M., Longini I. M., and Halloran M. E. Measures of the effects of vaccination in a randomly mixing population. *International journal of epidemiology*, 20(1):300–310, Mar. 1991.

[55] Halloran M. E., Longini I. M., and Struchiner C. J. *Design and Analysis of Vaccine Studies (Statistics for Biology and Health)*. Springer, 2010.

[56] Hethcote H. W. Qualitative analyses of communicable disease models. *Mathematical Biosciences*, 28(3):335–356, 1976.

[57] Hill A. L., Rand D. G., Nowak M. A., and Christakis N. A. Emotions as infectious diseases in a large social network: the SISa model. *Proceedings. Biological sciences*, 277(1701):3827–35, Dec. 2010.

[58] Hill A. L., Rand D. G., Nowak M. A., and Christakis N. A. Infectious disease modeling of social contagion in networks. *PLoS computational biology*, 6(11):e1000968, Jan. 2010.

[59] Hsieh Y.-H., Wang Y.-S., de Arazoza H., and Lounes R. Modeling secondary level of HIV contact tracing: its impact on HIV intervention in Cuba. *BMC infectious diseases*, 10:194, Jan. 2010.

[60] Iannelli M. *Mathematical theory of age-structured population dynamics*. Giardini Editori e Stampatori in Pisa, 1995.

[61] Inaba H. Weak ergodicity of population evolution processes. *Mathematical Biosciences*, 96(2):195–219, 1989.

[62] Inaba H. and Nishiura H. The state-reproduction number for a multistate class age structured epidemic system and its application to the asymptomatic transmission model. *Mathematical biosciences*, 216(1):77–89, Nov. 2008.

[63] Iwami S., Holder B. P., Beauchemin C. A. A., Morita S., Tada T., Sato K., Igarashi T., and Miura T. Quantification system for the viral dynamics of a highly pathogenic simian/human immunodeficiency virus based on an in vitro experiment and a mathematical model. *Retrovirology*, 9(1):18, Jan. 2012.

[64] Jacquez J. A., Simon C. P., Koopman J., Sattenspiel L., and Perry T. Modeling and analyzing HIV transmission: the effect of contact patterns. *Mathematical Biosciences*, 92(2):119–199, 1988.

[65] Jewell N. P., Lei X., Ghani A. C., Donnelly C. A., Leung G. M., Ho L.-M., Cowling B. J., and Hedley A. J. Non-parametric estimation of the case fatality ratio with competing risks data: an application to Severe Acute Respiratory Syndrome (SARS). *Statistics in Medicine*, 26(9):1982–1998, Apr. 2007.

[66] Jódar L., Acedo L., Villanueva R., Jódar L., Santonja F. J., and González-Parra G. Modeling dynamics of infant obesity in the region of Valencia, Spain. *Computers & Mathematics with Applications*, 56(3):679–689, 2008.

[67] Keeling M. J. and Rohani P. *Modeling Infectious Diseases in Humans and Animals*. Princeton University Press, 2007.

[68] Kermack W. O. and McKendrick A. G. A Contribution to the Mathematical Theory of Epidemics. *Proceedings of the Royal Society A: Mathematical, Physical and Engineering Sciences*, 115(772):700–721, Aug. 1927.

[69] Keyfitz B. and Keyfitz N. The McKendrick partial differential equation and its uses in epidemiology and population study. *Mathematical and Computer Modelling*, 26(6):1–9, 1997.

[70] Kiss I. Z., Simon P. L., and Kao R. R. A contact-network-based formulation of a preferential mixing model. *Bulletin of mathematical biology*, 71(4):888–905, May 2009.

[71] Klinkenberg D., Fraser C., and Heesterbeek H. The effectiveness of contact tracing in emerging epidemics. *PLoS One*, 1:e12, Jan. 2006.

[72] Klinkenberg D. and Nishiura H. The correlation between infectivity and incubation period of measles, estimated from households with two cases. *Journal of theoretical biology*, 284(1):52–60, Oct. 2011.

[73] Lam E. H. Y., Cowling B. J., Cook A. R., Wong J. Y. T., Lau M. S. Y., and Nishiura H. The feasibility of age-specific travel restrictions during influenza pandemics. *Theoretical biology & medical modelling*, 8:44, Jan. 2011.

[74] Lau L. L. H., Nishiura H., Kelly H., Ip D. K. M., Leung G. M., and Cowling B. J. Household transmission of 2009 pandemic influenza A (H1N1): a systematic review and meta-analysis. *Epidemiology (Cambridge, Mass.)*, 23(4):531–542, July 2012.

[75] Lessler J., Reich N. G., Cummings D. A. T., Nair H. P., Jordan H. T., and Thompson N. Outbreak of 2009 pandemic influenza A (H1N1) at a New York City school. *The New England Journal of Medicine*, 361(27):2628–2636, Dec. 2009.

[76] Li F. C. K., Choi B. C. K., Sly T., and Pak A. W. P. Finding the real case-fatality rate of H5N1 avian influenza. *Journal of epidemiology and community health*, 62(6):555–559, June 2008.

[77] Liao C. M., Chen S. C., and Chang C. F. Modelling respiratory infection control measure effects. *Epidemiology and Infection*, 136(3):299–308, Mar. 2008.

[78] Lipsitch M., Riley S., Cauchemez S., Ghani A. C., and Ferguson N. M. Managing and reducing uncertainty in an emerging influenza pandemic. *The New England Journal of Medicine*, 361(2):112–115, July 2009.

[79] Longini I. M., Halloran M. E., Nizam A., and Yang Y. Containing pandemic influenza with antiviral agents. *American journal of epidemiology*, 159(7):623–633, Apr. 2004.

[80] Longini I. M., Hudgens M. G., Halloran M. E., and Sagatelian K. A Markov model for measuring vaccine efficacy for both susceptibility to infection and reduction in infectiousness for prophylactic HIV vaccines. *Statistics in Medicine*, 18(1):53–68, Jan. 1999.

[81] Ma J. and van den Driessche P. Case fatality proportion. *Bulletin of mathematical biology*, 70(1):118–133, Jan. 2008.

[82] Matrajt L. and Longini I. M. Critical immune and vaccination thresholds for determining multiple influenza epidemic waves. *Epidemics*, 4(1):22–32, Mar. 2012.

[83] McBryde E., Bergeri I., van Gemert C., Rotty J., Headley E., Simpson K., Lester R., Hellard M., and Fielding J. Early transmission characteristics of influenza A(H1N1)v in Australia: Victorian state, 16 May - 3 June 2009. *Euro Surveillance*, 14(42), Jan. 2009.

[84] Merino J., Megias-Rangil I., Ferré R., Plana N., Girona J., Rabasa A., Aragonés G., Cabré A., Bonada A., Heras M., and Masana L. Body weight loss by very-low-calorie diet program improves small artery reactive hyperemia in severely obese patients. *Obesity surgery*, 23(1):17–23, Jan. 2013.

[85] Metz J. A. J. and Diekmann O. *The Dynamics of Physiologically Structured Populations*. Springer-Verlag, 1986.

[86] Meyers L. A., Newman M. E. J., and Pourbohloul B. Predicting epidemics on directed contact networks. *Journal of theoretical biology*, 240(3):400–418, June 2006.

[87] Mizumoto K., Ejima K., Yamamoto T., and Nishiura H. Vaccination and clinical severity: is the effectiveness of contact tracing and case isolation hampered by past vaccination? *International journal of environmental research and public health*, 10(3):816–829, Mar. 2013.

[88] Mizumoto K., Nishiura H., and Yamamoto T. Effectiveness of antiviral prophylaxis coupled with contact tracing in reducing the transmission of the influenza A (H1N1-2009): a systematic review. *Theoretical biology & medical modelling*, 10:4, Jan. 2013.

[89] Mizumoto K., Yamamoto T., and Nishiura H. Age-dependent estimates of the epidemiological impact of pandemic influenza (H1N1-2009) in Japan. *Computational and mathematical methods in medicine*, 2013:637064, Jan. 2013.

[90] Mossong J., Hens N., Jit M., Beutels P., Auranen K., Mikolajczyk R., Massari M., Salmaso S., Tomba G. S., Wallinga J., Heijne J., Sadkowska-Todys M., Rosinska M., and Edmunds W. J. Social contacts and mixing patterns relevant to the spread of infectious diseases. *PLoS Medicine*, 5(3):e74, Mar. 2008.

[91] Mossong J. and Muller C. P. Estimation of the basic reproduction number of measles during an outbreak in a partially vaccinated population. *Epidemiology and Infection*, 124(2):273–278, Apr. 2000.

[92] Mossong J., Nokes D. J., Edmunds W. J., Cox M. J., Ratnam S., and Muller C. P. Modeling the impact of subclinical measles transmission in vaccinated populations with waning immunity. *American journal of epidemiology*, 150(11):1238–1249, Dec. 1999.

[93] Nardone A., de Ory F., Carton M., Cohen D., van Damme P., Davidkin I., Rota M. C., de Melker H., Mossong J., Slacikova M., Tischer a., Andrews N., Berbers G., Gabutti G., Gay N., Jones L., Jokinen S., Kafatos G., de Aragón M. V. M., Schneider F., Smetana Z., Vargova B., Vranckx R., and Miller E. The comparative sero-epidemiology of varicella zoster virus in 11 countries in the European region. *Vaccine*, 25(45):7866–7872, Nov. 2007.

[94] Newman M. Assortative Mixing in Networks. *Physical Review Letters*, 89(20):208701, Oct. 2002.

[95] Newman M. Mixing patterns in networks. *Physical Review E*, 67(2):026126, Feb. 2003.

[96] Nicholson K. G., Webster R. G., and Hay A. J. *Textbook of influenza.* Blackwell Science Ltd, 1998.

[97] Nishiura H. Early efforts in modeling the incubation period of infectious diseases with an acute course of illness. *Emerging themes in epidemiology*, 4:2, Jan. 2007.

[98] Nishiura H. Case fatality ratio of pandemic influenza. *The Lancet infectious diseases*, 10(7):443–444, July 2010.

[99] Nishiura H. Correcting the actual reproduction number: a simple method to estimate $R(0)$ from early epidemic growth data. *International journal of environmental research and public health*, 7(1):291–302, Jan. 2010.

[100] Nishiura H. The relationship between the cumulative numbers of cases and deaths reveals the confirmed case fatality ratio of a novel influenza A (H1N1) virus. *Japanese journal of infectious diseases*, 63(2):154–156, Mar. 2010.

[101] Nishiura H. The virulence of pandemic influenza A (H1N1) 2009: an epidemiological perspective on the case-fatality ratio. *Expert review of respiratory medicine*, 4(3):329–338, June 2010.

[102] Nishiura H., Castillo-Chavez C., Safan M., and Chowell G. Transmission potential of the new influenza A(H1N1) virus and its age-specificity in Japan. *Euro Surveillance*, 14(22), June 2009.

[103] Nishiura H., Chowell G., Safan M., and Castillo-Chavez C. Pros and cons of estimating the reproduction number from early epidemic growth rate of influenza A (H1N1) 2009. *Theoretical biology & medical modelling*, 7:1, Jan. 2010.

[104] Nishiura H., Cook A. R., and Cowling B. J. Assortativity and the Probability of Epidemic Extinction: A Case Study of Pandemic Influenza A (H1N1-2009). *Interdisciplinary perspectives on infectious diseases*, 2011:194507, Jan. 2011.

[105] Nishiura H. and Eichner M. Infectiousness of smallpox relative to disease age: estimates based on transmission network and incubation period. *Epidemiology and Infection*, 135(7):1145–1150, Oct. 2007.

[106] Nishiura H. and Inaba H. Estimation of the incubation period of influenza A (H1N1-2009) among imported cases: addressing censoring using outbreak data at the origin of importation. *Journal of theoretical biology*, 272(1):123–130, Mar. 2011.

[107] Nishiura H., Klinkenberg D., Roberts M., and Heesterbeek J. A. P. Early epidemiological assessment of the virulence of emerging infectious diseases: a case study of an influenza pandemic. *PLoS One*, 4(8):e6852, Jan. 2009.

[108] Nishiura H. and Mizumoto K. Epidemiological determinants of successful vaccine development. *International journal of medical sciences*, 10(4):382–384, Jan. 2013.

[109] Nishiura H., Mizumoto K., Ejima K., Zhong Y., Cowling B., and Omori R. Incubation period as part of the case definition of severe respiratory illness caused by a novel coronavirus. *Euro Surveillance*, 17(42), Jan. 2012.

[110] Nishiura H., Yen H.-L., and Cowling B. J. Sample size considerations for one-to-one animal transmission studies of the influenza A viruses. *PLoS One*, 8(1):e55358, Jan. 2013.

[111] Nold A. Heterogeneity in disease-transmission modeling. *Mathematical Biosciences*, 240:227–240, 1980.

[112] Omori R., Cowling B. J., and Nishiura H. How is vaccine effectiveness scaled by the transmission dynamics of interacting pathogen strains with cross-protective immunity? *PLoS One*, 7(11):e50751, Jan. 2012.

[113] Orenstein W. A., Bernier R. H., and Hinman A. R. Assessing vaccine efficacy in the field. Further observations. *Epidemiologic reviews*, 10:212–241, Jan. 1988.

[114] Papenburg J., Baz M., Hamelin M.-E., Rhéaume C., Carbonneau J., Ouakki M., Rouleau I., Hardy I., Skowronski D., Roger M., Charest H., De Serres G., and Boivin G. Household transmission of the 2009 pandemic A/H1N1 influenza virus: elevated laboratory - confirmed secondary attack rates and evidence of asymptomatic infections. *Clinical Infectious Diseases*, 51(9):1033–1041, Nov. 2010.

[115] Perelson A. S., Kirschner D. E., and de Boer R. Dynamics of HIV infection of CD4+ T cells. *Mathematical biosciences*, 114(1):81–125, Mar. 1993.

[116] Presanis A. M., De Angelis D., Hagy A., Reed C., Riley S., Cooper B. S., Finelli L., Biedrzycki P., and Lipsitch M. The severity of pandemic H1N1 influenza in the United States, from April to July 2009: a Bayesian analysis. *PLoS Medicine*, 6(12):e1000207, Dec. 2009.

[117] Preston S. H., Mehta N. K., and Stokes A. Modeling obesity histories in cohort analyses of health and mortality. *Epidemiology*, 24(1):158–166, Jan. 2013.

[118] Reilly J. J., Kelly L., Montgomery C., Williamson A., Fisher A., McColl J. H., Lo Conte R., Paton J. Y., and Grant S. Physical activity to prevent obesity in young children: cluster randomised controlled trial. *BMJ*, 333(7577):1041, Nov. 2006.

[119] Richard S. A., Sugaya N., Simonsen L., Miller M. A., and Viboud C. A comparative study of the 1918-1920 influenza pandemic in Japan, USA and UK: mortality impact and implications for pandemic planning. *Epidemiology and Infection*, 137(8):1062–1072, Aug. 2009.

[120] Riley S., Kwok K. O., Wu K. M., Ning D. Y., Cowling B. J., Wu J. T., Ho L.-M., Tsang T., Lo S.-V., Chu D. K. W., Ma E. S. K., and Peiris J. S. M. Epidemiological characteristics of 2009 (H1N1) pandemic influenza based on paired sera from a longitudinal community cohort study. *PLoS Medicine*, 8(6):e1000442, June 2011.

[121] Schuette M. C. and Hethcote H. W. Modeling the effects of varicella vaccination programs on the incidence of chickenpox and shingles. *Bulletin of Mathematical Biology*, 61(6):1031–1064, Nov. 1999.

[122] Statistics Division, Aichi Prefectural Government . The residents living in Aichi prefecture. Population in Aichi prefecture. Aichi Prefecture: Aichi, 2012.

[123] Taubenberger J. K. and Morens D. M. 1918 Influenza: the mother of all pandemics. *Emerging Infectious Diseases*, 12(1):15–22, Jan. 2006.

[124] Taylor R. W., McAuley K. A., Barbezat W., Farmer V. L., Williams S. M., and Mann J. I. Two-year follow-up of an obesity prevention initiative in children: the APPLE project. *The American Journal of Clinical Nutrition*, 88(5):1371–1377, Nov. 2008.

[125] van Boven M., Kretzschmar M., Wallinga J., O'Neill P. D., Wichmann O., and Hahné S. Estimation of measles vaccine efficacy and critical vaccination coverage in a highly vaccinated population. *Journal of the Royal Society, Interface*, 7(52):1537–1544, Nov. 2010.

[126] Vázquez M., LaRussa P. S., Gershon A. A., Steinberg S. P., Freudigman K., and Shapiro E. D. The effectiveness of the varicella vaccine in clinical practice. *The New England Journal of Medicine*, 344(13):955–960, Mar. 2001.

[127] Velthuis A. G. J., Bouma A., Katsma W. E. A., Nodelijk G., and De Jong M. C. M. Design and analysis of small-scale transmission experiments with animals. *Epidemiology and Infection*, 135(2):202–217, Mar. 2007.

[128] Wallinga J., Heijne J. C. M., and Kretzschmar M. A measles epidemic threshold in a highly vaccinated population. *PLoS Medicine*, 2(11):e316, Nov. 2005.

[129] Wallinga J., Lévy-Bruhl D., Gay N. J., and Wachmann C. H. Estimation of measles reproduction ratios and prospects for elimination of measles by vaccination in some Western European countries. *Epidemiology and Infection*, 127(2):281–295, Oct. 2001.

[130] Wallinga J., Teunis P., and Kretzschmar M. Reconstruction of measles dynamics in a vaccinated population. *Vaccine*, 21(19-20):2643–2650, June 2003.

[131] Wallinga J., Teunis P., and Kretzschmar M. Using data on social contacts to estimate age-specific transmission parameters for respiratory-spread infectious agents. *American journal of epidemiology*, 164(10):936–944, Nov. 2006.

[132] Webb G. F. *Theory of Nonlinear Age-Dependent Population Dynamics (Chapman & Hall Pure and Applied Mathematics)*. CRC Press, 1985.

[133] Whitaker H. J. and Farrington C. P. Estimation of infectious disease parameters from serological survey data: the impact of regular epidemics. *Statistics in Medicine*, 23(15):2429–2443, Aug. 2004.

[134] Whitaker R. C., Wright J. A., Pepe M. S., Seidel K. D., and Dietz W. H. Predicting obesity in young adulthood from childhood and parental obesity. *The New England Journal of Medicine*, 337(13):869–873, Sept. 1997.

[135] Williams B. G., Cutts F. T., and Dye C. Measles vaccination policy. *Epidemiology and Infection*, 115(3):603–621, Dec. 1995.

[136] World Health Organization (WHO) . Obesity: Preventing and Managing the Global Epidemic. Report of a WHO Consultation. WHO Technical Report Series no. 894. WHO: Geneva, Switzerland, 2000.

[137] World Health Organization (WHO) . The Global Strategy on Diet, Physical Activity and Health (DPAS). WHO: Geneva, Switzerland, 2004.

[138] World Health Organization (WHO) . Global Health Observatory Data Repository. WHO: Geneva, Switzerland, 2011.

[139] Wu J. T., Ho A., Ma E. S. K., Lee C. K., Chu D. K. W., Ho P.-L., Hung I. F. N., Ho L. M., Lin C. K., Tsang T., Lo S.-V., Lau Y.-L., Leung G. M., Cowling B. J., and Peiris J. S. M. Estimating infection attack rates and severity in real time during an influenza pandemic: analysis of serial cross-sectional serologic surveillance data. *PLoS Medicine*, 8(10):e1001103, Oct. 2011.

[140] Wu J. T., Ma E. S. K., Lee C. K., Chu D. K. W., Ho P.-L., Shen A. L., Ho A., Hung I. F. N., Riley S., Ho L. M., Lin C. K., Tsang T., Lo S.-V., Lau Y.-L., Leung G. M., Cowling B. J., and Malik Peiris J. S. The infection attack rate and severity of 2009 pandemic H1N1 influenza in Hong Kong. *Clinical Infectious Diseases*, 51(10):1184–1191, Dec. 2010.

[141] Yang Y., Sugimoto J. D., Halloran M. E., Basta N. E., Chao D. L., Matrajt L., Potter G., Kenah E., and Longini I. M. The transmissibility and control of pandemic influenza A (H1N1) virus. *Science*, 326(5953):729–733, Oct. 2009.